

ISSN 0973-8916

# Current Trends in Biotechnology and Pharmacy

Volume- 17

Supplementary issue 3A

2023



[www.abap.co.in](http://www.abap.co.in)

## Current Trends in Biotechnology and Pharmacy

ISSN 0973-8916 (Print), 2230-7303 (Online)

### Editors

Prof.K.R.S. Sambasiva Rao, India  
krssrao@abap.co.in

Prof.Karnam S. Murthy, USA  
skarnam@vcu.edu

### Editorial Board

Prof. Anil Kumar, India  
Prof. P.Appa Rao, India  
Prof. Bhaskara R.Jasti, USA  
Prof. Chellu S. Chetty, USA  
Dr. S.J.S. Flora, India  
Prof. H.M. Heise, Germany  
Prof. Jian-Jiang Zhong, China  
Prof. Kanyaratt Supaibulwatana, Thailand  
Prof. Jamila K. Adam, South Africa  
Prof. P.Kondaiah, India  
Prof. Madhavan P.N. Nair, USA  
Prof. Mohammed Alzoghaibi, Saudi Arabia  
Prof. Milan Franek, Czech Republic  
Prof. Nelson Duran, Brazil  
Prof. Mulchand S. Patel, USA  
Dr. R.K. Patel, India  
Prof. G.Raja Rami Reddy, India  
Dr. Ramanjulu Sunkar, USA  
Prof. B.J. Rao, India  
Prof. Roman R. Ganta, USA  
Prof. Sham S. Kakar, USA  
Dr. N.Sreenivasulu, Germany  
Prof.Sung Soo Kim, Korea  
Prof. N. Udupa, India

Dr.P. Ananda Kumar, India  
Prof. Aswani Kumar, India  
Prof. Carola Severi, Italy  
Prof. K.P.R. Chowdary, India  
Dr. Govinder S. Flora, USA  
Prof. Huangxian Ju, China  
Dr. K.S.Jagannatha Rao, Panama  
Prof.Juergen Backhaus, Germany  
Prof. P.B.Kavi Kishor, India  
Prof. M.Krishnan, India  
Prof. M.Lakshmi Narasu, India  
Prof.Mahendra Rai, India  
Prof.T.V.Narayana, India  
Dr. Prasada Rao S.Kodavanti, USA  
Dr. C.N.Ramchand, India  
Prof. P.Reddanna, India  
Dr. Samuel J.K. Abraham, Japan  
Dr. Shaji T. George, USA  
Prof. Sehamuddin Galadari, UAE  
Prof. B.Srinivasulu, India  
Prof. B. Suresh, India  
Prof. Swami Mruthinti, USA  
Prof. Urmila Kodavanti, USA

### Assistant Editors

Dr.Giridhar Mudduluru, Germany

Dr. Sridhar Kilaru, UK

Prof. Mohamed Ahmed El-Nabarawi, Egypt

Prof. Chitta Suresh Kumar, India

[www.abap.co.in](http://www.abap.co.in)

ISSN 0973-8916

# Current Trends in Biotechnology and Pharmacy

(An International Scientific Journal)

**Volume- 17    Supplementary issue 3A**

**2023**



[www.abap.co.in](http://www.abap.co.in)

Indexed in Chemical Abstracts, EMBASE, ProQuest, Academic SearchTM, DOAJ, CAB Abstracts, Index Copernicus, Ulrich's Periodicals Directory, Open J-Gate Pharmoinfonet.in Indianjournals.com and Indian Science Abstracts.

## **Association of Biotechnology and Pharmacy (Regn. No. 28 OF 2007)**

The Association of Biotechnology and Pharmacy (ABAP) was established for promoting the science of Biotechnology and Pharmacy. The objective of the Association is to advance and disseminate the knowledge and information in the areas of Biotechnology and Pharmacy by organising annual scientific meetings, seminars and symposia.

### **Members**

The persons involved in research, teaching and work can become members of Association by paying membership fees to Association.

The members of the Association are allowed to write the title MABAP (Member of the Association of Biotechnology and Pharmacy) with their names.

### **Fellows**

Every year, the Association will award Fellowships to the limited number of members of the Association with a distinguished academic and scientific career to be as Fellows of the Association during annual convention. The fellows can write the title FABAP (Fellow of the Association of Biotechnology and Pharmacy) with their names.

### **Membership details**

(Membership and Journal)		India	SAARC	Others
Individuals	– 1 year	Rs. 600	Rs. 1000	\$100
LifeMember		Rs. 4000	Rs. 6000	\$500
Institutions	– 1 year	Rs. 1500	Rs. 2000	\$200
(Journal only)	Life member	Rs.10000	Rs.12000	\$1200

Individuals can pay in two instalments, however the membership certificate will be issued on payment of full amount. All the members and Fellows will receive a copy of the journal free.

## **Association of Biotechnology and Pharmacy**

(Regn. No. 28 OF 2007)

#5-69-64; 6/19, Brodipet

Guntur – 522 002, Andhra Pradesh, India



# Current Trends in Biotechnology and Pharmacy

ISSN 0973-8916

Volume 17 (Supplementary issue - 3A)	CONTENTS	2023
Invitro-Invivo Simulation Studies On Capecitabine Loaded Niosomes Intended for Brain Targeting <i>Abburi Ramarao, Guttikonda Venkata Rao, Satya Vani Chinnamaneni, Pallavi Kurra, Veenadevi Avani gadda, Komati Navya Sr , Mandava Bhagya Tej, Mandava Venkata Basaveswara Rao</i> 10.5530/ctbp.2023.3s.45		1074-1078
Studies on Phytochemical Screening, GC-MS Analysis and their Antibacterial Property Against <i>Vibrio cholerae</i> <i>Guru Prasad V., Gouthami Kuruvalli, Lavanya L., Suresh Babu Naidu Krishna, Khalid Imran and Vaddi Damodara Reddy</i> 10.5530/ctbp.2023.3s.46		1079-1089
Resistance of Antibiotic against <i>E. coli</i> isolated from city of Lake Bhopal, Madhya Pradesh- <i>Jitendra Malviya</i> 10.5530/ctbp.2023.3s.47		1090-1096
Phytochemical Screening and GCMS Analysis of Three Indian Traditional Medicinal Plants <i>B. K. Neethu* and Sitavi Yathiender</i> 10.5530/ctbp.2023.3s.48		1097-1105
In-silico screening of some isolated compounds of <i>Hemidesmus indicus</i> and evaluation of its antidiabetic potential <i>Sudip Pratihar, Robina Khatun, Prosun Ganguly, Barsan Banerjee, Md Nasiruddin Khan, Satya Narayan Dey, Basanta Sourav Sk, Tofajul Mirza, Sm Sohel Aktar, Tabasum Parvin, Suddhasattya Dey, *Priyanka Chandra, *Arijit Mondal</i> 10.5530/ctbp.2023.3s.49		1106-1115
Synthesis, Characterization and Antimicrobial Studies of Gabapentin Schiff Base Metal Complexes Containing Heterocyclic Ligand via Microwave-assisted Method <i>Jyoti C Ajbani, D Smita Revankar, M. Revanasiddappa, Suresh Babu Naidu Krishna, S Shankara</i> 10.5530/ctbp.2023.3s.50		1116-1128
<i>Antioxidant Potential of Zephyranthes citrina Seed Extract in Saccharomyces cerevisiae's Oxidative Stress Response System</i> <i>Sharangouda J. Patil, Renuka Jyothi S., Sadashiv S.O., Vishwantaha T., Jamila Khatoon Adam, and Suresh Babu Naidu Krishna</i> 10.5530/ctbp.2023.3s.51		1129-1140
<i>Bioactive Indole Heterocycles and their Synthetic Routes: A Comprehensive Review</i> <i>Shivangi Sharma, Amlan Kumar Das and Shivendra Singh</i> 10.5530/ctbp.2023.3s.52		1141-1158

---

*Differential approach of Bioremediation by Sclerotium rolfsii towards textile dye* Anthony Samuel , Vasantha Veerappa Lakshmaiah , Priyanjali Dias, Praveen N, Cannon Antony Fernandes, Aatika Nizam, Suresh Babu Naidu Krishna  
10.5530/ctbp.2023.3s.53 1159-1169

*Antimicrobial Study of Chitosan-Based Crosslinked Hydrogel Against Staphylococcus Aureus, Porphyromonas Gingivalis, Pseudomonas Aeruginosa, and Streptococcus Mutans* Arvind. S. Parmar,Aakash. S. Panwar,  
10.5530/ctbp.2023.3s.54 1170-1183

---

## Information to Authors

The Current Trends in Biotechnology and Pharmacy is an official international journal of Association of Biotechnology and Pharmacy. It is a peer reviewed quarterly journal dedicated to publish high quality original research articles in biotechnology and pharmacy. The journal will accept contributions from all areas of biotechnology and pharmacy including plant, animal, industrial, microbial, medical, pharmaceutical and analytical biotechnologies, immunology, proteomics, genomics, metabolomics, bioinformatics and different areas in pharmacy such as, pharmaceuticals, pharmacology, pharmaceutical chemistry, pharma analysis and pharmacognosy. In addition to the original research papers, review articles in the above mentioned fields will also be considered.

### Call for papers

The Association is inviting original research or review papers and short communications in any of the above mentioned research areas for publication in Current Trends in Biotechnology and Pharmacy. The manuscripts should be concise, typed in double space in a general format containing a title page with a short running title and the names and addresses of the authors for correspondence followed by Abstract (350 words), 3 – 5 key words, Introduction, Materials and Methods, Results and Discussion, Conclusion, References, followed by the tables, figures and graphs on separate sheets. For quoting references in the text one has to follow the numbering of references in parentheses and full references with appropriate numbers at the end of the text in the same order. References have to be cited in the format below.

Mahavadi, S., Rao, R.S.S.K. and Murthy, K.S. (2007). Cross-regulation of VAPC2 receptor internalization by m2 receptors via c-Src-mediated phosphorylation of GRK2. *Regulatory Peptides*, 139: 109-114.

Lehninger, A.L., Nelson, D.L. and Cox, M.M. (2004). *Lehninger Principles of Biochemistry*, (4th edition), W.H. Freeman & Co., New York, USA, pp. 73-111.

Authors have to submit the figures, graphs and tables of the related research paper/article in Adobe Photoshop of the latest version for good illumination and alignment.

Authors can submit their papers and articles either to the editor or any of the editorial board members for onward transmission to the editorial office. Members of the editorial board are authorized to accept papers and can recommend for publication after the peer reviewing process. The email address of editorial board members are available in website [www.abap.in](http://www.abap.in). For submission of the articles directly, the authors are advised to submit by email to [krssrao@abap.co.in](mailto:krssrao@abap.co.in) or [krssrao@yahoo.com](mailto:krssrao@yahoo.com).

Authors are solely responsible for the data, presentation and conclusions made in their articles/research papers. It is the responsibility of the advertisers for the statements made in the advertisements. No part of the journal can be reproduced without the permission of the editorial office.

## ***In vitro-in vivo* Simulation Studies on Capecitabine Loaded Niosomes Intended for Brain Targeting**

**Abburi Ramarao<sup>1</sup>, Guttikonda Venkata Rao<sup>2</sup>, Satya Vani Chinnamaneni<sup>3</sup>, Pal-lavi Kurra<sup>4</sup>, Veenadevi Avanigadda<sup>4</sup>, Komati Navya Sri<sup>5</sup>, Mandava Bhagya Tej<sup>5</sup>, Mandava Venkata Basaveswara Rao<sup>1</sup>**

<sup>1</sup>Department of Chemistry, Krishna University, Andhra Pradesh, India

<sup>2</sup>Department of Chemistry, SRR & CRR Govt. Degree College, Vijayawada, India

<sup>3</sup>Principal QC Lab Tech, Waters Corporation, Massachusetts, USA

<sup>4</sup>Vignan Pharmacy College, Vadlamudi, Guntur, AP, India

<sup>5</sup>Department of MBBS, NRI Academy of Medical Sciences, Chinakakani, Guntur, Andhra Pradesh, India

Corresponding author : [professormandava@gmail.com](mailto:professormandava@gmail.com)

### **Abstract**

*In silico* modelling are renowned for their potential to extend the *in vitro* data logically into *in vivo* data. In the current study pk- sim simulation software by open systems pharmacology (osp) was utilized to extract *in vivo* data of in-house developed capecitabine (cptb) niosomes formulation intended for brain targeting. The selected software allowed to consider brain as a compartment and thus estimated the correlation between simulated values and theoretical values of cptb. Various pharmacokinetic parameters of cptb namely molecular weight, solubility in water,  $p_{ka}$ ,  $\log p$ , intestinal permeability, unbound plasma fraction were provided as input parameters. Essential pharmacokinetic parameters namely  $c_{max}$ ,  $t_{max}$  auc and plasma half life ( $t_{1/2}$ ) were derived from the pk-sim software. Comparative plasma concentration time profile of experimental values vs simulated values ear-marked that there exists point to point correlation between *in vitro* parameters and *in vivo* parameters. It was also proved that the simulated values obtained were inline with the standard bibliographic pharmacokinetic parameter values of capecitabine indicating the scope for utilization of the pk sim software various other drug molecules and formulations.

**Keywords:** simulation studies, brain targeting, *in silico*, pk-sim software

### **Introduction**

In-silico model tools are accomplished to recognize the critical parameters that comprise drug physicochemical properties, dosage form related factors that affect the drug *in vivo* performance thus predicting the drug absorption built on the selected data set of input factors. The benefits of *in silico* simulation tools required less investment in resources and time compared to *in vivo* studies and also to suggest potential to screen virtual compounds. *In silico* model similarly reduced the number of experiments, simultaneous cost, and time mandatory for compound selection and development. *In silico* simulations have been recommended to decrease time and effort in developing generic drug products. (1) Physiologically based pharmacokinetic and pharmacodynamic (pbpk/pd) modeling has developed a extensively implemented tool in the industry to get a quantitative description of concentration–time profiles in dissimilar organ and tissues across human populations. A current survey exhibited that nearly 70% of medical company's use pre-clinical pbpk/pd modeling in all therapeutic areas (2).

Various commercial pbpk modeling simulation software comprising of gastroplus™, pk-sim, simcyp, adme works ddi simulator, chloepk etc. These software packages offer considerably flexibility to the pbpk model developer, nevertheless more innovative modeling and programming skills and experience are essential; thus, they are less appropriate for beginners. These packages are expert pbpk modeling software packages, offer less flexibility in model development, but they also involve less mathematical and modeling experience. (3) Pk-sim® is a comprehensive software tool for whole body simulation by using pbpk modeling. It permits rapid access to all significant anatomical and physiological parameters for humans and the supreme collective laboratory animals such as a mouse, rats, minipig, dog, monkey, beagle, and rabbit that are confined in the integrated database. Pbpk modeling has been used for decades in the field of toxicological risk assessment and has in current years been extended toward the application in the drug research and development area. Software tools frequently focus on isolated characteristics of drug action, such as pharmacokinetics at the organism scale or pharmacodynamic interaction on the molecular level. Pk-sim offers altered model structures for significant alterations between small and large molecules. (4) Pk-sim is a freeware which is widely available for utilization and easily understandable, compared to other software's used for pk parameter estimation.

In the current study capecitabine loaded niosomes intended for brain targeting through intranasal route was taken as input formulation in pk-sim software. Capecitabine is a chemotherapeutic agent with antineoplastic action consumed orally for the treatment of colorectal & metastatic breast cancer. It has a clinically proven efficacy against brain metastases. However, the role of capecitabine in treating CNS disorders is unexplored. Hence, an attempt was made to develop a niosomal formulation which can target brain effectively when administered through intranasal route. (5)

Pk-sim software is used as an alternate and animal less approach for determination of pharmacokinetic parameters of capecitabine. The formulation tested was intended to target the brain. Pk-sim software allows to consider brain as a compartment and thus estimate the correlation between simulated values and theoretical values of capecitabine.

## Materials and Methods

### *Insilico software*

Open systems pharmacology (osp) is an open science community converging on systems pharmacology with a robust prominence on the pbpk modeling. Osp makes previously profitable software implements pk-sim and mobi freely presented as osp suite under the gplv2 license where all source code and all content are public. The osp suite comprises different software tools and has a modular design to permit efficient multiscale modeling and simulation. (6)

### *Method*

Simulation studies were carried out by using pk sim® version 9. Generally, this software consists of 2 type's blocks i.e. Building blocks & simulation.

### *Building blocks*

A building block of the current study consist of the following elements:

### *Selection of individual*

European male species was selected for study with their age limit of 30 years, 75 kg body weight, height 176 cm, bmi of 23.57 Kg/m<sup>2</sup>.

### *Population*

about 100 population consisting of both male & female can be selected. Currently we are studying the simulation parameters at an individual level (each individual considered as one group).

### **Generating compound template**

Existing compound template, was regenerated as capecitabine basic template. Various physicochemical properties were given as inputs i.E. Log p value of 0.83nlog units was given as input, albumin was selected as binding site for capecitabine & the amount of unbound fraction was given as 65% in human & effective molecular weight of 359.35 G/mol was loaded as input using theoretical reference data (7 & 8). Further, pka value of capecitabine i.E., 8.30 & Solubility of capecitabine in water i.E., 26 Mg/ml was given as input based on theoretical reference data (9).

Adme parameters like permeability of drug was given as 0.15cm/sec. Metabolizing enzymes like cyp1a2 and cyp 3a4 were mentioned as input, since those enzymes play a major role in drug metabolism as per the literature. (10) Renal clearance of gfr fraction was given as 0.21 According to literature. (11) After loading necessary input values in accordance with the established literature, advanced parameters are auto-generated by the software.

### **Generation of formulation template**

Formulation templates are generated by selecting the options which corresponds to the type of selected drug release kinetics. Capecitabine niosomes formulation followed first order kinetics which is affirmed using the *in-vitro* drug release studies. Hence, the input was selected as first order. Further, as per the input requirements of software capecitabine half-life i.E., 45 Min was given as input to the generated formulation template. (12)

### **Administration protocol generation**

Administration protocol was generated with the following basic elements. Among the available elements for administration type (intravenous bolus, intravenous infusion, oral or user defined), user defined template was selected since our test formulation (capecitabine niosomes) was formulated as intranasal drug

delivery system. Various input parameters in the user defined template namely, dose of capecitabine was given as 150 mg, dosing intervals as single dose, targeted organ like brain, targeting compartment as a plasma were given to the software.

### **Addition of some events**

Some events like meal energy content of selected individuals (100 k. Cal), meal volume of 0.591, Meal fraction solid of 0.60, Gall bladder emptying lag time of 30 minutes were auto generated as inputs by the software.

### **Attachment of observed experimental data**

Excel sheet was generated by exporting the data from the graph obtained in the earlier step i.E., Formulation template generation. Alternatively, dissolution data for the selected drug can be given as input if table option was selected in the formulation template generation step.

Excel sheet containing time and fraction dose released was attached for performing simulation in the further step.

### **Simulation studies**

After completion of the above-mentioned building block steps then the stimulation step can be performed using a simple protocol for the simulation of small molecules or advanced protocol for the simulation of proteins or large molecules. In the current study we have followed a protocol for small molecules. In this process, the building block previously generated was added to the simulation icon for human individuals for a small molecule to facilitate simulation. Simulation was initiated by clicking on the define setting & run option to get simulated *in vivo* data generated by the software in the form of time profile graph containing both simulated & observed curves. Further simulation can be performed to obtain the parameter identification and sensitivity analysis.



**Results and Discussion**

**Simulation studies**

Simulation studies were performed using pk sim® with the construction of physiological based pharmacokinetic models of both population & human individuals as well as large animal species. In the current study, building blocks were generated using standard european humans as a selected individual. Input in terms of physicochemical properties i.E. Molecular weight of 359.35 G/mole, the solubility of water 26 mg/ml, fraction unbound to albumin of 65%, pka value of 8.3, Log p value of 0.83 Present in the literature for capecitabine were given to simulation software. The same values were represented in table no:1 further, generation of formulation & administration protocol for simple molecule into simulation study of individual humans yielded a comparative profile of simulat-

ed & experimental data as illustrated in figure no:1 the results conclude that the simulated pk parameter values were in correlation with bibliographic values as tabulated in table no:2.(13) The obtained pk parameter values which were within the acceptable bibliographic ranges indicate that the simulation model was significant.

Table no: 1 capecitabine parameters included in the software as input

Input parameters	Values
Molecular weight	359.35 g/mole
Solubility (water)	26 mg/ml
Pka (acid)	8.3
Log p	0.83 Log
Intestinal permeability	3.44 × 10 <sup>-7</sup> cm/min
Unbound plasma fraction (fup)	0.0065

Table no: 2 pharmacokinetic parameters with simulated data in comparison with bibliographic values.

Pharmacokinetic Parameters	PBPK simulation model	Bibliographic values
AUC	0.58 mg*h/l	0.461 – 0.698 mg*h/l
Cmax	5.98 µ mol/l	0.64 - 15.4 µ mol/l
Tmax	1.15 h	1 - 3 h
t1/2	0.75 h	0.55 to 0.89 h

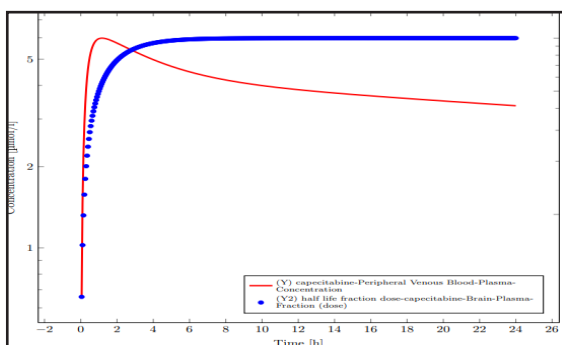


Figure no: 1 comparative plasma concentration time profile of experimental and simulated data.

**Conclusion**

Pk-sim® is a novel whole-body pbpk in silico model that can be used throughout all stages of the drug r&d process. It was developed, tested and evaluated in real-life projects within the pharmaceutical industry. Comparison of simulation results with experimental data provides a valuable method of interpreting rather than simply describing pk results. This particularly helps the researcher to identify specific effects (e.G. The relevance of active transport processes) very early on and, thus, can guide the experimental efforts, saving time and money.(14)

Simulation studies performed using pbpk modeling of pk sim software aided in extrapolating the *invitro* drug release data to *invivo* healthy human volunteer data and the obtained pk parameters were in simulation with the bibliographic values. Hence, the study finds the scope of the optimized formulation in delivering the drug incorporated at the brain region when incorporated intranasally. The study also portrays the scope of exploring the potential of optimized formulation in treating various cns disorders.

### References

1. Sandra g., Jelena p., And zorica d. (2013). Computer-aided biopharmaceutical characterization: gastrointestinal absorption simulation. ( 2<sup>nd</sup> edition), woodhead publishing limited., Pp- 177-232.
2. Janet, p., Laura i.F., Ferran .S. (2018). *In silico* models in drug development: where we are. Current opinions in pharmacology, 42:111-121.
3. Feras, k., And stephanie, i. (2011). Physiologically based pharmacokinetic modeling: methodology, applications, and limitations with a focus on its role in pediatric drug development. Journal of biomedicine and biotechnology, 1: 1-13.
4. Thomas e., Lars, k., Becker,c., Michiael, b., Katrin,c., Thomas gaub etal. (2011). A computational systems biology software platform for multiscale modeling and simulation: integrating whole body physiology, disease biology, and molecular reaction network. Frontiers in physiology, 2: 1-10.
5. Daniel, r., Budman. (2000). Capecitabine. Investigational new drugs. 18: 355–363.
6. Lippert j., Burghaus r., Edginton etal. (2019). Open systems pharmacology community-an open access, open source, open science approach to modeling and simulation in pharmaceutical sciences. Cpt pharmacometrics syst pharmacol, 8(12):878-882.
7. National center for biotechnology information (2023). Pubchem compound summary for cid 60953, capecitabine. Retrieved march 15, 2023 from <https://pubchem.ncbi.nlm.nih.gov/compound/capecitabine>.
8. Fda approved drug products: xeloda® (capecitabine) tablets, for oral use (2023 ) [link]
9. Miwa, m., Ura, m., Nishida, m., Sawada, n., Ishikawa, t., Mori, k., Shimma, n., And umeda, i., Ishitsuka h.(1998). Design of a novel oral fluoropyrimidine carbamate, capecitabine, which generates 5-fluorouracil selectively in tumors by enzymes concentrated in human liver and cancer tissue. Eur j cancer. 34(8):1274-81.
10. Jurgen, k., And franz, b. (2018). Pharmacokinetic enhancers (boosters)—escort for drugs against degrading enzymes and beyond, sci. Pharm, 86 (43):1-28.
11. Alquahtani, s., Alzaidi, r., Alsultan, a., Asiri , y., Alsaleh, k. (2022). Clinical pharmacokinetics of capecitabine and its metabolites in colorectal cancer patients. Saudi pharm. J, 30(5): 527-531.
12. Anbarasan, b., Rekha, s., Elango, k., Shriya, b., & Ramaprabhu, s. (2013). Optimization of the formulation and in-vitro evaluation of capecitabine niosomes for the treatment of colon cancer. Ijpsr, 4(4): 1504-1513.
13. Walko c. M., Lindley, c. (2005). Capecitabine: a review. Clin ther, 27 (1): 23-44.
14. Willmann, s., Jorge, l., Michael, s., Solodenko, j., Franco, f., And walter, s. (2003). Pk-sim®: a physiologically based pharmacokinetic 'whole-body' model. Bio-silico,1(4):121-124.

## Studies on Phytochemical Screening, GC-MS Analysis and their Antibacterial Property Against *Vibrio cholerae*

Guru Prasad V.<sup>1</sup>, Gouthami Kuruvalli<sup>2</sup>, Lavanya L.<sup>2</sup>, Suresh Babu Naidu Krishna<sup>3</sup>, Khalid Imran<sup>4</sup> and Vaddi Damodara Reddy<sup>5\*</sup>

<sup>1</sup>Department of Microbiology, <sup>2</sup>Department of Biochemistry, <sup>5</sup>Department of Biotechnology, School of Applied Sciences, REVA University, Bengaluru-560064, India

<sup>3</sup>Department of Biomedical and Clinical Technology, Durban University of Technology, Durban-4000, South Africa

<sup>4</sup>Department of Microbiology, Krupanidhi Degree College, Bengaluru-560035, India

Corresponding author: [damodara.reddyv@reva.edu.in](mailto:damodara.reddyv@reva.edu.in)

### Abstract

In the current study, two different MTCC strains of *Vibrio cholerae*, 3904 and 3906, were used to determine the anti-bacterial properties of *Cinnamomum verum* (*C. verum*) leaves (Family: Lauraceae). This was done through qualitative phytochemical compound screening and quantitative identification of volatile compounds using gas chromatography and mass spectrometry (GC-MS). Methanolic extract was subjected to phytochemical screening in order to determine the active components. Through qualitative examination revealed that the substance contained alkaloids, total carbohydrates, cardiac glycosides, flavonoids, glycosides, phenols, saponins, and tannins. Due to the abundance of phytochemical agents in the extract, GC-MS experiments were conducted. Based on their retention times and coverage percentages in mass spectra, these studies identified 42 volatile chemicals. The maximum zone of inhibition for the antibacterial activity of methanol extract were 15.9 mm for the *V. cholerae* MTCC 3904 strain and 16.3 mm for the *V. cholerae* MTCC 3906 strain, respectively, at concentrations of 100 $\mu$ L, Azithromycin showed 22.30 mm, a positive control, at a dosage of 30 $\mu$ g. Total antibacterial activity was determined to be 15.05  $\pm$  1.15 mm and 15.10  $\pm$  1.15 mm, respectively, in the

examined bacterial strains. These values are equivalent to conventional azithromycin. In conclusion, *C. verum* can be a potential therapeutic agent against *V. cholerae* strains, this is due to strong antibacterial nature of active biomolecules present in the medicinal plant.

**Keywords:** *Cinnamomum verum*, Phytochemicals, GC-MS analysis, *V. cholerae*, Azithromycin

### Introduction

The investigation of novel anti-microbial compounds from plant origin is gained lot of interest in researchers; also, it is inevitable due to multi drug resistance of microorganism, regardless of molecular mechanisms involved in the antibiotics and to combat any level of infection. For the centuries, in order to find the novel antibiotic and resistance of epidemic spreads, scientists and medical practitioners have developed the appropriate application of antibiotics (1). Efficient application of any antibiotics in humans depends upon the problem level and scenario of infection, which was always better under physician prescription established in their regulation against the infection and the responsibility of patient's during the therapeutic time. In anti-microbial findings, bacteria are major fo-

cus to face with fierce struggle which were developed the several molecular mechanisms as multidrug resistance against synthetic anti-microbial drugs whose function mainly involved in enzymatic inactivation (2, 3), changing the drug route, and utilization of lower concentration of drug in cells as per the membrane permeability or cell specific overexpression at the efflux pumps (4). During the reaction of efflux pumps antibiotics segregated in self-defense mode which are removed actively from the cell. For any new antibacterial developments, lethality of drug concentration in active sites of cells results into predispose of pathogenic organism which is under the threat of over resistance (5). Knowing such scenario of pathogens, efflux pump reaction is inevitable to target the organisms and this major challenge is to tackle by the research by developing newer drugs, which is less toxic and higher rate of efficacy of potent molecules, in single or in synergistic approach with other usual antibiotic drugs combating effectively against any infections of multidrug-resistance. Medicinal plants are the treasure for fighting any infective agents and it has been used in all the countries from centuries to various diseases. In today's context, there is an extreme revival of medicinal plant interest and almost exploited the sources for identification of novel drugs (6) which shown pharmacological significance in various approach (7). The present investigation is to explore the *C. verum* phytochemicals qualitatively, identification of volatile compounds by GC-MS analysis and their biological action against *V. cholera* strains under *in vitro* conditions.

## Materials and Methods

### Plant material

The University of Trans-disciplinary Health Sciences and Technology in Bengaluru, Karnataka, India, certified the *Cinnamomum verum*, or Daalchini, leaves that were obtained from the botanical garden of the Agriculture University in Bengaluru.

### Preparation of plant extracts

The leaves of *C. verum* were collected, cleaned thoroughly in double distilled water, chopped into small pieces and for the removal of moisture shade dried in room temperature. Around 200 g of leaves material was accurately weighed, crushed, powdered and Soxhlet extraction in methanol at 50°C were carried out. Buchi's rotary vacuum was used to obtain the concentrated extract and the resulted extract was preserved in refrigerator until use of experimental studies (8-10).

### Screening of phytochemicals

Qualitative screening of phytochemicals was conducted in order to investigate the primary metabolites present in the methanol extract of *C. verum* leaves. This further aimed to identify the volatile compounds by GC-MS analysis.

The *C. verum* extract was screened for phytochemical analysis by following modified method of Sharangouda and Patil, (9), with the comparison of standard method of Harnborne, (10) and Fransworth, (11) to investigate the secondary metabolites such as alkaloids, total carbohydrates, cardiac glycosides, flavonoids, glycosides, phenols, saponins, tannins, terpenoids and total proteins. For the preparation of phytochemical reagents for the tests followed standard method of Harnborne (12). To make the concentration to obtain the proper solution of methanol extract further dissolve in water (Milli-Q ultra-pure distilled water) and filtered for removal of residues.

### Gas chromatography and mass spectroscopy (gc-ms) analysis

#### Preparation of extract

Filtered 10mg/ml of aromatic medicinal plant extract of *C. verum* leaves (methanol) was prepared further in methanol due to high polarity of the solvent and for which 1µl plant extract was employed to quantify the volatile compounds by GC-MS analysis.

### **Instruments and chromatographic conditions**

GC-MS analysis of *C. verum* extract was performed using a Thermo GC-MS Clarus 500 (Perkin Elmer). For MS detection, the MS DSQ II electron ionization mode with an ionization energy of 70 eV was used, with a mass range at m/z 50-650. Zebron capillary column 2B-XLB. The analysis was conducted using a column with the following specifications: 30 meters in length, 0.25mm (I.D), and 0.25 film thickness (m). The initial column temperature was set to 60°C for five minutes. Temperatures of 280°C and 290°C, respectively, were established for the GC injector and MS transfer line. The GC was carried out in spitless mode. As the carrier gas, helium (1.0 ml/min flow rate) was employed. There was an injection volume of 1.0 µL. The plant extract was diluted in methanol, passed through a polymeric solid phase extraction (SPE) column, and then subjected to GC-MS analysis to determine its constituent parts. Compounds in the plant sample were found using computer searches on the NIST REFPROP Version 9.1 database and comparisons of the GCMS spectrum.

### **Bioactive constituents' identification**

The National Institute of Standard and Technology's (NIST's) database, which contains more than 62,000 patterns were used for the interpretation of the Mass Spectrum GC-MS. A comparison was made between the spectra of the unknown components and the spectrum of known components kept in the NIST collection. The test materials' constituent parts' names, molecular formulas, weights, and chemical structures were determined.

### **Anti-bacterial activity**

The extract of *C. verum* applied to anti-bacterial activity by disk diffusion using Agar plate method (Muller-Hinton (MH)) using the standard azithromycin for control (positive) and methanol (negative) for the comparison. The strains used in the present investigations are *Vibrio cholera* MTCC 3904 and *V. cholera* MTCC 3906. Test strains are allowed to grow in around 14 hours in Luria Broth (LB) froth medi-

um at around 30 °C. The incubated culture was then placed in MH medium. Each strain swabbed in MH Agar plates by sterile lab grade cotton swabs. Wells were made 6mm diameter on each plate by using standard lab grade gel puncture tool. The methanol extract of *C. verum* leaves of different concentrations 10, 20, 30, 40, 50, 60, 70, 80, 90 and 100 µl were poured on each well by using calibrated micropipette. Results of antibacterial activity were measured by zone of inhibition which obtained clearly around the well, where extract loaded and incubated at 37 °C constantly for 24hrs.

### **Statistical analysis**

All experiments were performed in triplicates and the mean difference was statistically calculated. The values are expressed as mean ± SEM. Students "t" test was used and  $p < 0.01$  was considered as statistically significant.

### **Results and Discussion**

#### **Phytochemicals screening of cinnamomum verum methanol extract of leaves**

The phytochemical screening of *C. verum* methanol extract of leaves exhibited good results for alkaloids, total carbohydrates, cardiac glycosides, flavonoids, glycosides, phenols, saponins, and tannins but negative results for terpenoids and total proteins (Table 1). Many researchers in the field of medicinal plants have reported similar findings employing various types of plant parts and extracts (13-15).

Table.1 Screening of phytochemicals qualitatively in leaves of methanolic extract of *C. verum*

Screening of Qualitative Phytochemical Analysis	
Tests	<i>C. verum</i>
Total Carbohydrates	+ ve
Cardiac glycosides	+ ve
Flavonoids	+ ve
Terpenoids	- ve



Glycosides	+ve
Tannins	+ve
Alkaloids	+ve
Phenols	+ve
Saponins	+ve
Total Proteins	-ve

**Gc-ms analysis of methanolic extract of *c. Verum* leaves**

The GC-MS analysis of the methanolic extract results were shown in figure 2 and it has eluted 42 different active compounds. Identification of volatile compounds were assessed with the comparison of standards of NIST and Wiley 9.1. Most of the phytochemical were characterized by their respective area (%) depends on the availability and elution on particular retention time. The obtained peaks of the chromatograms, shown highest % of area by 10-Nonadecanone (11.84), Apiol (7.02), Pentadecanoic acid (6.26), 3,7,11,15-Tetramethyl-2-hexadecen-1-ol (5.02),  $\alpha$ -Tocopherol- $\beta$ -D-mannoside (4.78), Hexadecanoic acid, methyl ester (2.53), Diisooctyl phthalate(2.44), 9,12,15-Octadecatrienoic acid, (Z,Z,Z)- (1.87), 9,12,15-Octadecatrienoic acid, methyl ester, (Z,Z,Z)- (1.66), Phytol (1.77), 8,11-Octadecadienoic acid, methyl ester (1.47), 1,2-Bis (trimethylsilyl) benzene(1.40), Tricyclo (4.3.1.1(3,8))undecan-1-amine(1.37), 3 $\beta$ ,6 $\alpha$ ,20 $\beta$ -Trihydroxy-5  $\alpha$ -pregnane (1.20), 1,3-Dioxane-5-methanol, 5-ethyl- (1.13), Androst-11-en-17-one, 3-formyloxy-, (3. $\alpha$ , 5. $\alpha$ .)- (1.09), 3,7,11,15-Tetramethyl-2-hexadecen-1-ol (1.01), Hydrazine, N-(N-methyl-1-azacyclotridecan-2-ylidene)-N'-(di(methylthio)methylidene)- (1.00), and rest other 27 volatile compounds shown less than 1 % of area as per the elution on particular retention time. As per the literature many of the volatile compounds which were present in the plant shown potent cytotoxicity activities and also several researchers reported for various pharmacological applications on these compounds in different plants, hence these volatile compounds listed with various

characters to understand their biological action in table 2.

**Table.2** Quantification of volatile compounds by GC-MS analysis of methanolic extract of *C. verum* leaves based on retention time, peak area (%) and their names

Sl. No.	Compound Name	Retention Time	M/Z	Peak Area (%)
1	cis-Aconitic anhydride	4.03	40	0.258605
2	3-tert-Bu-tyl-5-chloro-2-hydroxy-benzophenone	4.226	40	0.458313
3	5-Nitro-3-cyano-2(1H)-pyridone	4.29	44	0.286222
4	4-Carbamoyl-5-methylhexanoic acid, methyl ester	4.729	40	0.25252
5	2-Deoxy-D-galactose	6.735	57	0.36625
6	1,3-Dioxane-5-methanol, 5-ethyl-	6.79	57	1.13271
7	1,1-Difluorocyclohexan-3-ol	6.815	57	0.98037
8	Apiol	8.26	222	7.02984
9	3,7,11,15-Tetramethyl-2-hexadecen-1-ol	10.64	68	5.02365
10	3,7,11,15-Tetramethyl-2-hexadecen-1-ol	11.04	95	0.41302
1	2-Cyclopenten-1-one, 4-hydroxy-3-methyl-2-(2,4-pentadienyl)-, (Z)-(+)-	11.313	40	0.166978
12	3,7,11,15-Tetramethyl-2-hexadecen-1-ol	11.379	81	1.01896
13	1,2-Benzenedicarboxylic acid, 2-butoxyethyl butyl ester	11.592	149	0.77162
14	Hexadecanoic acid, methyl ester	12.357	74	2.53206
15	Pentadecanoic acid	13.126	73	6.26521
16	8,11-Octadecadienoic acid, methyl ester	15.405	81	1.47058
17	9,12,15-Octadecatrienoic acid, methyl ester, (Z,Z,Z)-	15.545	79	1.66363
18	Phytol	15.629	71	1.78180
19	9,12,15-Octadecatrienoic acid, (Z,Z,Z)-	16.351	79	1.87666



20	Tricyclo(4.3.1.1(3,8)) undecan-1-amine	21.665	44	1.38974
21	Diisooctyl phthalate	22.282	149	2.446947
22	3.beta.-Acetoxy-bis-nor-5-cholenamide	24.25	73	0.66110
23	6-Isopropenyl-4,8a-dimethyl-1,2,3,5,6,7,8,8a-octahydro-naphthalen-2-ol	24.651	159	0.39112
24	8-Pregnene, 3-acetoxy-20-hydroxymethyl-4,4,14-trimethyl-	24.802	341	0.34201
25	1,3-Dioxolane, 4-((octadecyloxy)methyl)-2-phenyl-	25.925	149	0.14055
26	Silanamine, N-(2,6-dimethyl-4-((trimethylsilyloxy)phenyl)-1,1,1-trimethyl-	25.965	73	0.96934
27	.3beta.,6.alpha.,20.beta.-Trihydroxy-5.alpha.-pregnane	26.103	73	1.20526
28	Hydrazine, N-(N-methyl-1-azacyclo-tridecan-2-ylidene)-N'-(di(methylthio)methylidene)-	26.475	44	1.00675
29	7-Hydroxy-6,9a-dimethyl-3-methylene-decahydro-azuleno(4,5-b) furan-2,9-dione	27.03	107	0.25691
30	Haloxazolam	27.26	281	0.98480
31	Pregnane-3,11,20,21-tetrol, cyclic 20,21-(methylboronate), (3.alpha.,5.alpha.,11.beta.,20R)-	27.329	93	0.35701
32	T-2 Tetraol	28.798	67	0.32008
33	10-Nonadecanone	29.189	71	11.84532
34	Silane, diphenylisobutoxy(5-methoxy-3-methylpentyl)-	29.575	281	0.94791
35	Ethanethioic acid, S-(8-(diethylphosphono)octyl) ester	30.143	281	0.92556

36	2,4-Di-tert-butyl-6-(tert-butylamino) phenol	30.289	208	0.52400
37	.alpha.-Tocopherol-beta.-D-mannoside	30.384	165	4.78939
38	Androst-11-en-17-one, 3-formyloxy-, (3.alpha.,5.alpha.)-	30.478	207	1.09485
39	Kauran-18-oic acid, 7-(acetyloxy)-15,16-epoxy-, methyl ester, (4.alpha.,7.beta.,15.alpha.)-	30.632	159	0.30512
40	1,2-Bis(trimethylsilyl) benzene	31.94	207	1.40814
41	Acrylophenone, 3,3-diphenyl-, semicarbazone	32.338	44	0.58697
42	5-Chloropentanoic acid, 2-butyl ester	32.373	55	0.30752
43	2,3-Diphenylquinoxaline 1-oxide	32.499	282	0.56888
44	Cyclooctasiloxane, hexadecamethyl-	33.668	147	0.84829

GC-MS analysis of *C. verum* leaves methanolic extract (Figure 2) revealed a total of 42 volatile compounds based on peak detection and retention time on each compound, indicating the presence of forty-four different volatile compounds with various biological properties. These compounds were discovered by their characterization in GC-MS analysis by differentiating retention duration in each compound as well as their peak (%) in the examined plant extract. These features are characterized based on the retention period of each concentration of the peak area in percent area in the entire spectrum (Table 2). The characterized results represented as per the peak and percent area of the volatile compounds, i.e., 10-Nonadecanone (11.84), Apiol (7.02), Pentadecanoic acid (6.26), 3,7,11,15-Tetramethyl-2-hexadecen-1-ol (5.02),  $\alpha$ -Tocopherol- $\beta$ -D-mannoside (4.78), Hexadecanoic acid, methyl ester (2.53), Diisooctyl phthalate (2.44), 9,12,15-Octadecatrienoic acid, (Z,Z,Z)- (1.87), 9,12,15-Octadecatrienoic acid, methyl ester, (Z,Z,Z)- (1.66), Phytol (1.77),

8,11-Octadecadienoic acid, methyl ester (1.47), 1,2-Bis (trimethylsilyl)benzene (1.40), Tricyclo (4.3.1.1(3,8))undecan-1-amine(1.37), 3 $\beta$ ,6 $\alpha$ ,20 $\beta$ -Trihydroxy-5  $\alpha$ -pregnane (1.20), 1,3-Dioxane-5-methanol, 5-ethyl- (1.13), Androst-11-en-17-one, 3-formyloxy-, (3. $\alpha$ , 5. $\alpha$ -) (1.09), 3,7,11,15-Tetramethyl-2-hexadecen-1-ol (1.01), Hydrazine, N-(N-methyl-1-azacyclotridecan-2-ylidene)-N'-(di(methylthio)methylidene)- (1.00) and remaining 27 volatile compounds shown less than 1 % with respect retention time and peak area. Patil *et al.*, revealed the active principal compounds of petroleum ether of *Citrus medica* seeds and their biological action on *in vivo* models (16). Eramma and Patil, (17) revealed 41 distinct volatile compounds from crude

and TLC fractions in *Flacourtia indica* root extract of methanol, GC-MS analysis indicated the presence of, including Heneicosane (25.945), Squalene (20.51), Cholesterol (33.525), Cycloheptasiloxane, tetradecamethyl-(14.864), 2, 4-Di-tert-butylphenol-(16.032), Cycloheptasiloxane hexadecamethyl (16.848), Cyclononasiloxane octadecamethyl (20.733), and n-Hexadecanoic acid (22.092). Kolgi *et al.*, reported alkaloid and flavonoid present in *Leucas aspera* leaves of chloroform and ethanol extracts revealed antioxidant and anticancer property (18, 19). Similar compounds present in *Simarouba glauca* seed petroleum and ethanol extracts reported for antioxidant property (20, 21).

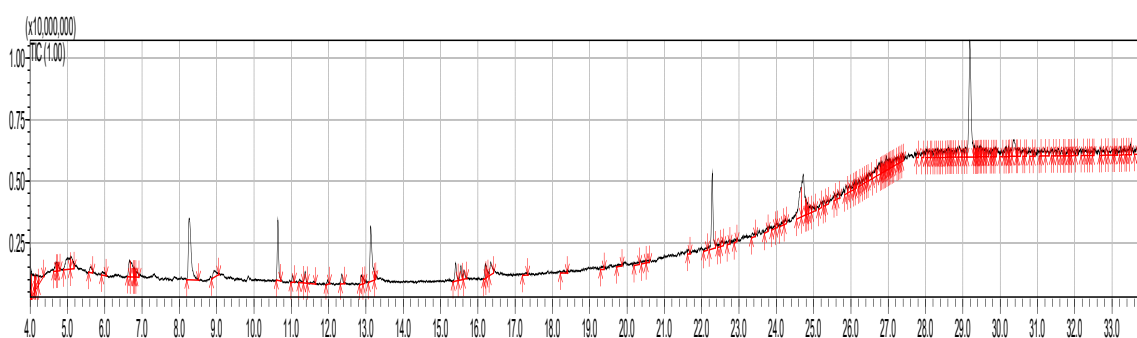


Figure 1: GC-MS analysis spectrum of *C. verum* leaves of methanolic extract.

#### **Antimicrobial activity of *C. verum* leaves methanolic extract**

The antibacterial activity was tested *in vitro* against the 24 h *V. cholera* two strains of bacteria utilising the disc diffusion plate method of Muller-Hinton (MH) agar, with conventional azithromycin and methanol serving as positive and negative controls, respectively. The disc diffusion method was used to test the antibacterial susceptibility of *C. verum* leaves extract against *V. cholera* MTCC-3904 and 3906 strains. The maximum inhibitory zone observed on higher concentrations at 100% methanol extract was 15.8 mm and 16.5 mm, respectively, while the minimum at 60% methanol extract was 10.5 mm and 11.8 mm. The positive control azithromycin

(30 g) demonstrated the greatest inhibitory zone on *V.cholera* strains MTCC-3904 and 3906 at 40% concentration (Figure 2). Srivastava *et al.*, (22) discovered that several spices have extremely strong antibacterial efficacy against *Vibrio* bacterium species isolated from pond water, with Black pepper having the highest zone of inhibition at 100% ethanol extract and 70% activity on methanol extract. Coriander had the greatest zone of inhibition at 85% extract and the lowest activity at 70% on ethanol extract. Cinnamon showed the greatest zone of inhibition at 85% acetone extract and the least at 70% action on ethanol extract. Green cardamom was discovered to have a strong potential against isolated *Vibrio* species (Table 3).

Table 3: Total antibacterial activity and zone of inhibition of methanol extract of *C. verum* leaves

Organisms	Zone of Inhibition (mm)											Total Antibacterial Activity
	Concentration of Methanol extract of <i>C. verum</i> leaves										Zone of Inhibition (mm)	
	10	20	30	40	50	60	70	80	90	100	100 Conc.	
V. cholera 3904	-	-	-	-	-	-	10.5	10.8	12.4	13.8	15.8	15.05±1.15 mm
	-	-	-	-	-	10.5	12.5	12.8	14.5	15.9		
V. cholera 3906	-	-	-	-	-	-	12.4	12.8	13.5	13.8	16.8	15.10±1.15 mm
	-	-	-	-	-	11.5	11.2	14.5	13.8	16.2		
Positive Control (Azithromycin)	V. cholera 3904	22.5	22.8	22.4	22.9							13.22±0.05 mm
	V. cholera 3906	22.8	22.6	22.8	22.7							14.44±1.15 mm
Negative Control (Methanol)	V. cholera 3904	-	-	-	-							
	V. cholera 3906	-	-	-	-							

Based on the minimum inhibitory concentration at higher zone of inhibition on 100% methanol extract, total antimicrobial activity was tested in triplicates on the same organisms and found zone of inhibition 15.05±1.15 mm and 15.10±1.15 mm in *Vibrio cholera* MTCC-3904 and 3906 strains, respectively, whereas positive control showed 13.22±0.05 mm and 14.44±1.15 mm and it was significant increase in the methanol extract of *C. verum* the data was presented in Table 3. Previous research has clearly shown that active components such as camphene, limonene, caryophyllene, and others have excellent bactericidal activities (23). Ragasa et al., (24) demonstrated antibacterial activity of sapwood extract (*Dracontomelon dao*) against *Staphylococcus typhimurium*, *Klebsiella pneumoniae*, *Staphylococcus aureus*, *Bacillus subtilis*, *Candida albicans*, and *Aspergillus niger* us-

ing ethanolic extract, and they revealed these activities were due to the of 54 compounds which were analysed through GC-MS of the extract, among GCMS analyses of *Rhus semialata* chloroform extract of seeds identified active ingredients such as Tridecane, Decane, Anethole, (Z)6, (Z)9-Pentadecadein-1-ol, and Squalene as a more volatile molecule, as well as antibacterial capabilities in diverse species (25). Several other studies on the pharmacological properties of the plant *Dracontomelon dao* revealed potent antimicrobial activity with various organisms, antioxidant activity with various scavenging potential, anti-inflammatory in quantitative method, anti-diabetic in in vitro studies, and anti-trypanosomal activities (26-29). On the same plant, isolation and characterisation of other plant components proposed for medicinal and therapeutic activities (30, 31).

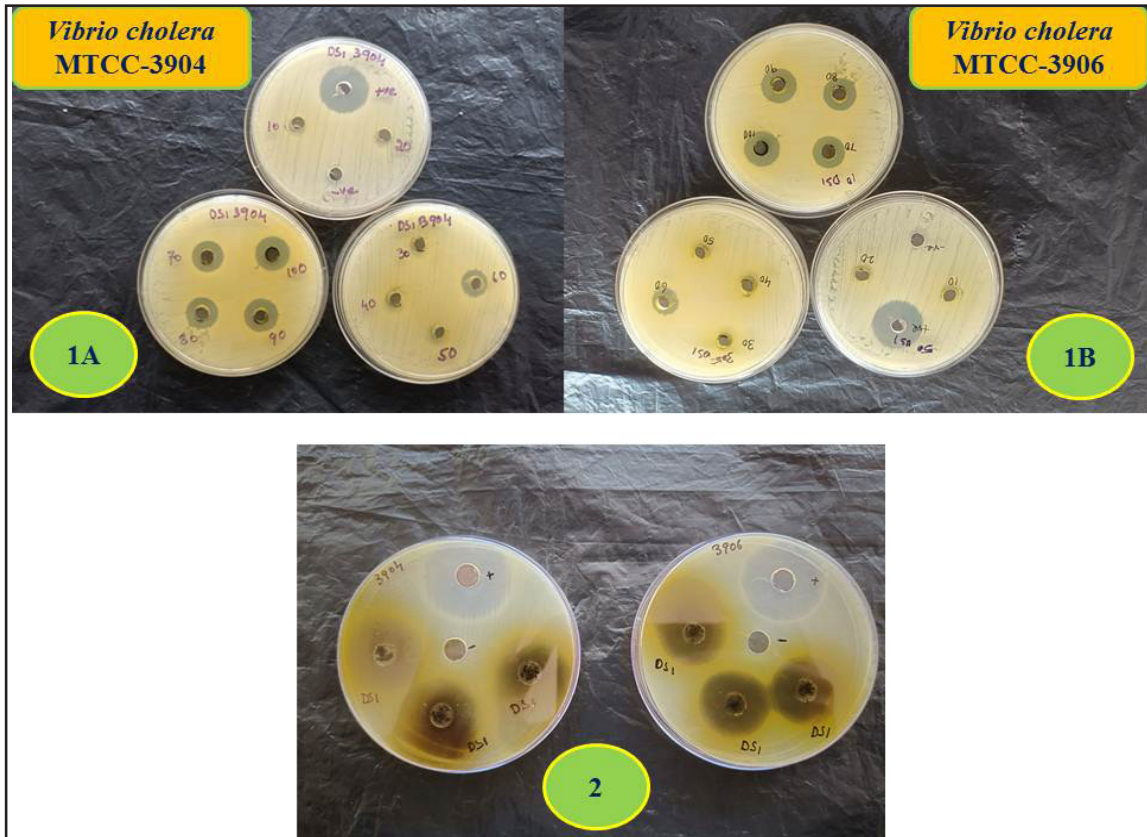


Figure 2: Antibacterial activity of methanol extract of *C. verum* leaves resulted zone of inhibition (mm) of bacterial strains 1A) *V. cholera* MTCC-3904, 1B) *V. cholera* MTCC-3906 2) *V. cholera* MTCC-3904 & 3906 showing total antibacterial activity with the comparison of azithromycin positive control and methanol negative control

### Conclusion

The experimental research of *C. verum* leaves extract revealed significant secondary metabolites and antibacterial activity against two different strains of *V. cholera*, employing ten different doses of the methanol extract (10, 20, 30, 40, 50, 60, 70, 80, 90, and 100  $\mu$ l). In a qualitative analysis of phytochemicals, screening study results showed that alkaloids, total carbohydrates, cardiac glycosides, flavonoids, glycosides, phenols, saponins, and tannins had antimicrobial properties against *V. cholerae* strains at grade dependent concentrations in disc diffusion method. GCMS analysis revealed 42 volatile chemicals in the methanol extract, with higher concentrations of the 15 compounds

exhibiting antibacterial capabilities and maybe other biological actions. Other substances in the literature exhibit antioxidant, anti-inflammatory, anticarcinogenic, antifertility, and antisteroidogenic activities in addition to antimicrobial. These findings point to *Cinnamomum verum* leaves having powerful natural antibacterial properties.

### Acknowledgements

The authors are thankful to REVA University, Bengaluru-560064, Karnataka, India for providing financial assistance in the form of JRF and also providing all necessary facilities to carried out research work. KSBNU would like to thank Durban University of Technology for research fellowship



### Conflict of Interest

The authors declare no conflict of interest.

### References

1. Llor, C. and Bjerrum, L. (2014). Antimicrobial resistance: risk associated with antibiotic overuse and initiatives to reduce the problem. *Therapeutic Advances and Drug Safety*, 5(6): 229-241.
2. Prestinaci, F., Pezzotti, P. and Pantosti, A. (2015). Antimicrobial resistance: a global multifaceted phenomenon. *Pathogen and GlobL Health*, 109(7): 309-318.
3. Malathi, V., Revathi, K. and Devaraj S.N. (2020), Antimicrobial resistance an interface between animal and human diseases. *Indian Journal of Veterinary and Animal Science Research*, 43(2): 113–124.
4. Li, X.Z. and Nikaido, H. (2009). Efflux-mediated drug resistance in bacteria: an update. *Drugs*. 69(12): 1555-1623.
5. Terreni, M., Taccani, M. and Pregnolato, M. (2021). New antibiotics for multidrug-resistant bacterial strains: latest research developments and future perspectives. *Molecules*, 26(9): 2671.
6. Salmerón-Manzano, E., Garrido-Cardenas, J.A. and Manzano-Agugliaro, F. (2020). Worldwide research trends on medicinal plants. *Interantional Journal of Environmental Research and Public Health*, 17(10): 3376.
7. Thileepan, T., Thevanesams V. and Kathirgamanathars S. (2017). Antimicrobial activity of seeds and leaves of myristica fragrans against multi-resistant microorganisms. *Journal of Agricultural Science and Technology*, A7: 302-308.
8. Bhat, S.G. (2021). Medicinal plants and its pharmacological values. In: *Natural medicinal plants*. El-Shemy, H.A. editor. IntechOpen: London
9. Sharangouda and Patil, S.B. (2007). Phytochemical screening and antifertility activity of various extracts of *Citrus medica* (Lemon) seeds in albino rats. *Advances in Pharmacology and Toxicology*, 8(2):71-4.
10. Harborne, J.B. (1998). *Phytochemical Methods*. Chapman & Hall, London, pp. 60-63.
11. Farnsworth, N.R. (1966). Biological and phytochemical screening of plants. 55(3): 225-276.
12. Harborne, J.B. (1973). *Phytochemical Methods: A Guide to Modern Techniques of Plant Analysis*, Chapman and Hall, London, UK.
13. Pant, D.R., Pant, N.D., Saru, D.B., Yadav, U.N. and Khanal, DP. (2017). Phytochemical screening and study of antioxidant, antimicrobial, antidiabetic, anti-inflammatory and analgesic activities of extracts from stem wood of *Pterocarpus marsupium* Roxburgh. *Journal of Intercultural Ethnopharmacology*, 6(2): 170-176.
14. Rahman, G., Syed, U.J., Syed, F., Samiullah, S. and Nusrat, J. (2017). preliminary phytochemical screening, quantitative analysis of alkaloids, and antioxidant activity of crude plant extracts from *Ephedra intermedia* indigenous to Balochistan. *The Scientific World Journal*, Article ID: 5873648, 7 pages.
15. Fatemeh, R., Maryam, S.M., Rahele, D., Roya, K., Elahe, E. (2022). Phytochemical classification of medicinal plants used in the treatment of kidney disease based on traditional Persian medicine. *Evidence-Based Complementary and Alternative Medicine*, Article ID: 8022599, 13 pages.

16. Patil, S.J., Venkatesh, S., Vishwanatha, T., Banagar, S.R., Banagar, R.J. and Patil, S.B. (2014). GCMS analysis of bioactive constituents from the petroleum ether extracts of *Citrus medica* seeds. *World Pharmacy and Pharmaceutical Sciences*, 3: 1239-1249.
17. Eramma, N. and Patil, S.J. (2023). Exploration of the biomolecules in roots of *Flacourtia indica* (Burm. F) Merr. methanol extract by chromatography approach. *Letters in Applied NanoBioscience*, 12(4): 166-177.
18. Kolgi, R.R., Haleshappa, R., Sajeeda, N., Keshamma, E., Karigar, C.S. and Patil S.J. (2021). Antioxidant studies, *in vitro* cytotoxic and cell viability assay of flavonoids and alkaloids of *Leucas aspera* (Wild.) Linn leaves. *Asian Journal of Biological and Life Sciences*, 10(1): 165-171.
19. Kolgi, R.R., Patil, S.J. and Karigar, C.S. (2020). Antioxidant and anticancer properties of chloroform extract of *Leucas aspera* from Tumkur district. *Proceedings of National Conference National Web Conference on Sustainability in the Commerce, Scientific, Technological, Linguistic and Environmental Sectors*. pp.106-107.
20. Haleshappa, R., Patil, S.J., Usha, T. and Murthy SM. (2020). Phytochemicals, antioxidant profile and GCMS analysis of ethanol extract of *Simarouba glauca* seeds. *Asian Journal of Biological and Life Sciences*, 9(3): 379-385.
21. Haleshappa, R., Keshamma, E., Girija, C.R., Thanmayi, M., Nagesh, C.G., Fahmeen, L.G.H. et al., (2020). Phytochemical Study and Antioxidant Properties of Ethanolic Extracts of *Euphorbia milii*. *Asian Journal of Biological Sciences*, 13(1): 77-82.
22. Srivastava, A., Singh, A.N. and Singh M. (2016). Antibacterial activity of spices against *Vibrio* species isolated from pond water. *European Journal of Experimental Biology*, 6(2):21-25.
23. Rahaman, A., S.A. Siddiqui, F.O. Altuntas, S.Okay, F. Gul and I. Demirtas, 2019. Phenolic profile, essential oil composition and bioactivity of *Lasia spinosa* (L.) Thwaites. *Brazilian Archives of Biology and Technology*. Vol.62: e19170757.
24. Ragasa, C.Y., T.C. Batarra, J.L.A. Vivar, M.M. De Los Reyes and C.C. Shen, 2017. Chemical constituents of *Dracontomelon dao* (Blanco) Merr. et Rolfe. *Pharmacogn. J.*, 9: 654-656.
25. Shruthy, S., Gothe, A., Aier, K, Kirankumar, S., Kalva P.K. and Patil S.J. (2019). Bioactive molecules and antimicrobial studies of Indian traditional medicinal plant *Rhus semialata* seeds. *Research Journal of Medicinal Plants*, 13: 10-17.
26. Dela Pena, J.F., Dapar, M.L.G., Aranas, A.T., Mindo, R.A.R. Cabrido, C.K., et al., (2019). Assessment of antimicrobial, antioxidant and cytotoxic properties of the ethanolic extract from *Dracontomelon dao* (Blanco) Merr. & Rolfe. *Pharmacophore*, 10: 18-29.
27. Khan, M.R. and Omoloso, A.D. (2002). Antibacterial and antifungal activities of *Dracontomelon dao*. *Fitoterapia*, 73: 327-330.
28. Mazura, M.P., M.H.S.N. Aisyah and B. Idayu, 2016. Assessing Malaysian forest species for lipogenase inhibitory activity. *Proceedings of the 14th Seminar on Medicinal and Aromatic Plants*, October 11-12, 2016, Malaysia, pp: 236-239
29. Yusro, F., Ohtani, K. and Kubota, S. (2016). Inhibition of  $\alpha$ -glucosidase by methanol extracts from wood bark of *Anac-*



- ardiaceae*, *Fabaceae*, *Malvaceae* and *Phyllanthaceae* plants family in West Kalimantan, Indonesia. *Kuroshio Science*, 9: 108-122.
30. Norhayati, I., Getha, K., Murni, Y.N., Ling, S.K., Sahira S.K., *et al.*, (2016). *In vitro* anti-trypanosomal activity of selected forest plant species. Proceedings of the 14<sup>th</sup> Seminar on Medicinal and Aromatic Plants, October 11-12, 2016, Malaysia, pp: 269-272.
31. Su, X.F., Liang, Z.Y. and Zhang, Y.X. (2008). Study on the chemical constituents of essential oil from the skins of stem of *Dracontomelon dao* (Blanco) Merr. et Rolfe. *Lishizhen Med. Materia Medica Research*, 19: 1640-1641.

# Antibiotic Resistance against *E. coli* Isolated from City of Lake Bhopal, Madhya Pradesh

Jitendra Malviya

Department of Life Sciences and Biological Sciences, IES University, Bhopal

Corresponding Author: jitmalviya123@gmail.com

## Abstract

*E. coli* samples from Upper Lake Bhopal were examined in this investigation for different antibiotic resistances. Different integrons and genes were employed to describe MDR isolates. The diffusion method has been utilized to scrutinize 150 *E. coli* by Kirby Bauer disc detaches from nine sample locations in Upper Lake Bhopal (UPB) for phylogenetic relationships and antibiotic susceptibility. The level of resistance was significantly higher in vancomycin (74%) as compared to cefazolin (88%). Out of 150 isolates, 37 (25%) were found to be resistant to ten or more drugs. Additionally, a high prevalence of polymyxin-B and azithromycin predisposition was observed in 90% of *E. Coli* isolates. All the collected test samples exhibited resistance to fluoroquinolones, tetracyclines, chloramphenicol, and beta-lactam antibiotics. It was higher in middle-lake Bhopal *E. coli* isolates than in the upper and lower reaches. *E. coli* samples from Upper Lake Bhopal showed rising trimethoprim/sulphonamide resistance. MDR isolates were present in all samples. MAR scores greater than 0.25 indicated contamination in the upper, middle, and lower Upper Lake. The animal isolates showed resistance to lactams and aminoglycosides, with 80.9% of all isolates being multidrug-resistant. Integrons were

found in 85 MDR isolates resistant to at least six chemicals and four antimicrobial types of classes.

**Keywords:** Upper Lake, *Strain E.coli*, MDR, Antibiotics Resistance, Antimicrobial activity

## Introduction

Bhopal heart of Madhya Pradesh and city of Lake famously Known for two artificial lakes that are situated in the central of Bhopal. Surface area of 1.30 km<sup>2</sup> and a catchment area of 9.7 km<sup>2</sup>, and a combined catchment area of 363 km<sup>2</sup>, is smaller than the main lake i.e., Upper-Lake is a significant resource of drinking water, meeting over 40% of Bhopal's residents' average daily water needs while rerouting was mainly carried out in the Lower Lake. However, the ecological environment of Lake Bhopal has deteriorated in recent years due to the inflow of point and non-point source toxins from the metropolitan area, including sewage, solid waste, as well as dregs and improvements as of the national catchments. This is also a result of lakeshore encroachment. The lake's biological health and water quality have declined as a result of these circumstances.

*E. coli* is an enteric- bacteria that is often discovered in untreated sewage and huma

n gastrointestinal tracts. It also poses a serious threat to human health since it may cause a number of extra-intestinal diseases such pneumonia, meningitis, urinary tract infections, and bacteremia. Antibiotics are often used to treat these infections effectively. Antibiotic overuse, on the other hand, has resulted in a substantial rise in bacterial resistance. Because of the significant frequency of antibiotic resistance in *E. coli*, the efficacy of treatments such as penicillin, sulfa medicines, fourth-generation cephalosporins, and fluoroquinolones has been greatly reduced over the last several decades. The placement of carbapenem-resistant Enterobacteriaceae, particularly *E. coli*, to (WHO) as global pathogen list of priorities demonstrates that the issue of antibiotic resistance has worsened and necessitates a comprehensive response. According to prior study (1, 2) the rise of multidrug-resistant *E. coli* makes antibiotic therapy ineffective, resulting in a rise in mortality and morbidity around the world.

*Escherichia coli* is a kind of bacterium found in human as well as in animal intestines even though almost all of *E. coli* strains are safe, a small number may trigger mild to severe illness. (8) When present in high concentrations, *E. coli* can significantly alter the microbial composition of water. (3, 4) It might cause harmful algal blooms and other issues for aquatic ecosystems by changing how other bacteria and microorganisms in the water are balanced. To stop the spread of disease and safeguard the health of people and wildlife, it's critical to keep an eye on *E. coli* levels in water sources, especially those used for recreational pursuits like swimming or fishing. *E. coli* levels in water systems can be decreased with routine testing and proper waste disposal. (5) This is due to the fact that *E. coli* may act as a food source for other microorganisms, increasing their diversity and population in the water. It can also result in a decline in overall microbial diversity and an increase in dangerous bacteria if the amount of *E. coli* is too high. Certain species that can thrive on *E. coli* may find a more hospitable en-

vironment in areas with higher concentrations of the pathogen, increasing their diversity and population. (5) If the ecosystem's delicate balance is upset, this could also result in competition for resources and potentially hazardous changes. *E. coli* density has an impact on the microbial composition of water. To ensure that it stays within safe ranges and does not upset the balance of microbial diversity, it is crucial to regularly check the mass of *E. coli* in water systems. (6) This can be accomplished by conducting routine testing and putting policies in place to stop contamination from sources like sewage discharge or agricultural runoff. (7)

The current study beheld on the antibiotic's resistance trends of *E. coli* strains recovered from the Upper Lake in Bhopal, Madhya Pradesh. The primary goal of this investigation was to evaluate the incidence of antibiotic-resistant *E. coli* bacteria in lake water and their resistance patterns to routinely used antibiotics. (9) The findings of this study could provide crucial insights into the potential dangers connected with drinking Upper Lake water and aid in the development of effective ways to prevent the bacterial growth that are resistant to antibiotics.

## Materials and Methods

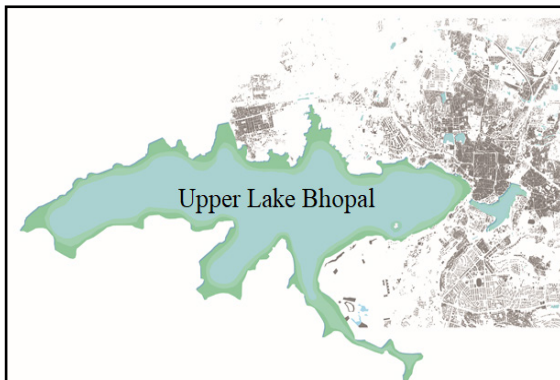
### Study site

### Isolated bacteria

The study includes looking at 150 *Escherichia coli* samples taken from Upper Lake water as well as 16 isolates previously acquired from faces and sewage. The aquatic *E. coli* samples were collected from several locations in the Upper Lake area of Bhopal, including Kamla Park, Wetland Lake View, Kohe-Fiza, Kaliasot, Kerwa Dam, Bharvan Park, Lake View Point, VIP Road, Van Vihar National Park, Bhadbhada.

This was done using a direct inoculation in enrichment broths was previously used to isolate direct sewage isolates from fecal samples of several types of sewage from Bhopal. These

*E. coli* isolates were all identified using the *E. coli* TM Identification Kit's standard strains. Periodically, the isolates' purity was examined on EMB agar, a selective medium. These isolates' glycerol stocks were created and kept at 4°C. The strain named "*E. coli* ATCC 25922" was obtained from IMTECH, Chandigarh for reference. Utilizing the Kirby Bauer method, antimicrobial



susceptibility profiling was carried out on all 150 *E. coli* isolates using 19 different antibiotics. (10, 11)

Figure 1. Upper Lake Bhopal, India (GPS Coordinates 23°14'41.532"N , 77°22'37.488 E)

### Studies supporting the use of antibiotics

The antibiotic resistance member of enterobacteriaceae family *E. coli* samples were evaluated using the "Kirby Bauer disc diffusion" approach against 19 different drugs (4). To perform the test, medication discs were obtained from HiMedia in Mumbai, India, including Aminoglycosides such as Gentamicin-10 mcg, "Tobramycin and lactams Imepenem-10 mcg, Ceftriaxone-30 mcg, Cefotaxime-30 mcg, Cefazolin-30 mcg, and Cefuroxime-30 mcg nitrofurantoin, linezolid, glycopeptides, polymyxin-B, macrolides, chloramphenicol, tetracycline, fluoroquinolones, and rifampicin. (21) A 0.06 McFarland turbidity average were arranged by mingling 0.6 ml of 1% ( $H_2SO_4$ ) 99.5 ccs of 1%  $H_2SO_4$ , and  $BaCl_2$ . Then, 6 millilitres of this solution were distributed to bacterial culture tubes for testing, and the turbidity was evaluated

using spectrophotometry at 625 nm to ensure an OD between 0.08 and 0.13. The McFarland standard was stored at 4 °C while being wrapped in foil. (11)

The MAR (Multiple Antibiotic Resistance) was used to calculate the total resistance to antibiotics score for the Upper Lake testing sites (New Bhopal). The entire antibiotics confirmed was divided the whole quantity of isolates at that location to arrive at this score. If the resultant index is larger than 0.25, there is a substantial probability of contamination.

### Results and Discussion

In this study, sampling sites covering a total area of 372.35 square kilometres were used, including Kamla Park, Wetland Lake View, Kohe-Fiza, Kaliasot, Kerwa Dam, Bharvan Park, Lake View Point, VIP Road, Van Vihar National Park, Bhadbhada. The maximum height of the tank was 508.65 centimeter. The study also included nine *E. coli* samples from a sewage source. Nineteen different antibiotics were tested against fifty different *E. coli* strains in all.

### Phenotypes of antimicrobial resistance

Susceptibility testing was performed on 155 *E. coli* isolates across 19 different antibiotics from 12 different classes. The evaluation of antibiotic susceptibility was based on the guidelines of CLSI. The resistance, intermediate, or susceptibility status of each isolate against each antibiotic was determined. Out of 124 water *E.*

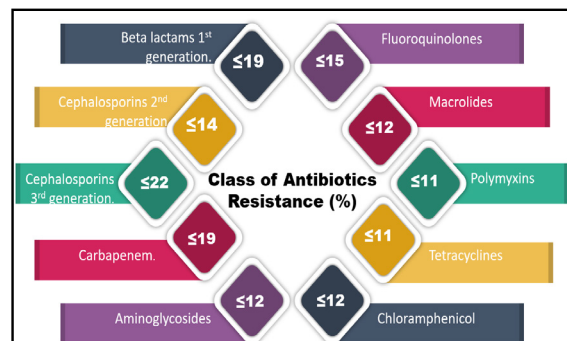


Figure 2. Classes of Antibiotics Resistance

*coli* isolates, 80.9% were classified as multi-drug-resistant due to their positive test results for resistance to three different antibiotic classes. Similarly, 26 *E. coli* isolates obtained from direct sewage samples were also found to have MDR features.(23)

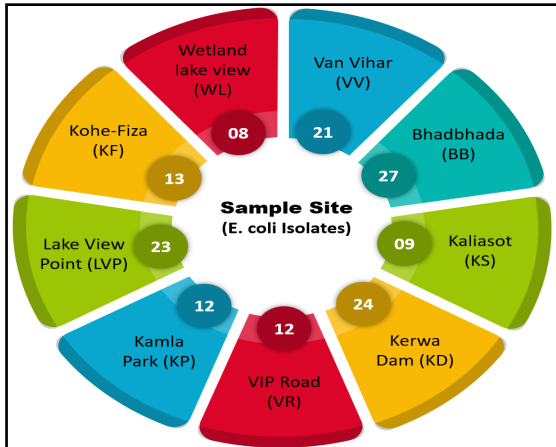


Figure 3. Sampling Sites of *E. coli*

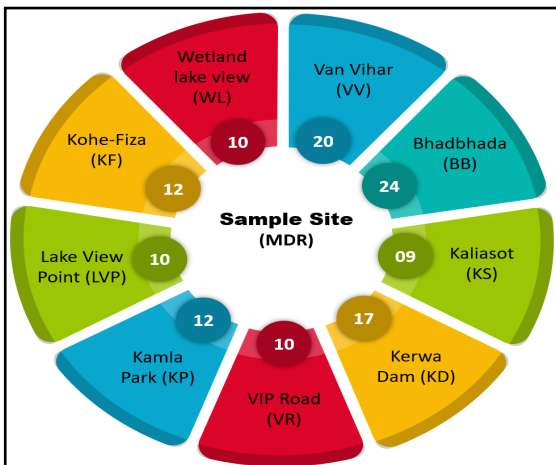


Figure 4. Different location of Upper Lake Bhopal with MDR isolates

Among these various antibiotics tested, cefazolin (88%) and vancomycin (74%) displayed the highest level of resistance. Around one-fourth or 16 out of 150 cells, exhibited resistance to at least ten antibiotics. Azithromycin and polymyxin-B were found to be particularly effective against most of the *E. coli* isolates.

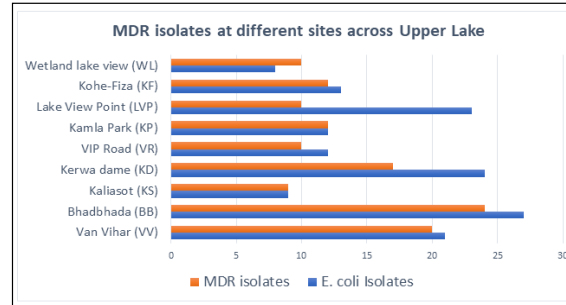


Figure 4. Sample collection site (23°14'41.532"N , 77°22'37.488 E)

Across the study sites, *E. coli* samples responded differently to various antibiotics. The *E. coli* samples taken at VIP Road site, where Upper Lake linked with new Bhopal, were found to be resistant to a variety of antibiotics, together with amino-glycosides and beta-lactams, according to (12, 13). Among the isolates, more than 40% were resistant to beta-lactam antibiotics, while 50% showed (14) resistance to aminoglycosides (gentamicin and tobramycin). (15) Chloramphenicol, however, was found to be highly effective against the isolates. Out of the twenty-one isolates collected from this site, twenty were identified as MDR isolates because they were resistant to four different antibiotic classes.

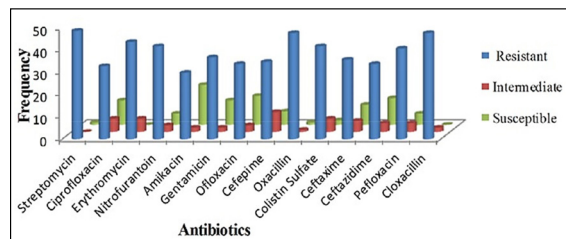


Figure 5. Occurrence of antibiotics compared to intermediate, resistance and susceptible Reprinted with permission (10)

The level of antibiotic resistance displayed by *E. coli* isolates varied across different sampling sites. At the Upper Lake entrance point at VIP Road, a considerable number of water-borne *E. coli* isolates exhibited resistance to multiple antibiotic classes, including amino-glycosides and  $\beta$ -lactams, with 40% and



50% of the isolates exhibiting struggle to these antibiotic classes, respectively. (16) However, chloramphenicol was able to destroy these isolates, and twenty-one isolates from this site were classified as MDR isolates. At the subsequent upper reaches sampling site VV, *E. coli* isolates showed a sharp rise in resistance to various antibiotics, including fluoroquinolones,  $\beta$ -lactams, tetracycline, and rifampin, with 24 isolates exhibiting high levels of MDR to  $\beta$ -lactam resistance. (17,18) The two isolates, however, did not exhibit drug resistance to any of the examined medications. The internal *E. coli* restrictions from the KP testing location exposed a general increase in resistance in the direction of anti-infection agents, including  $\beta$ -lactams and antibiotic drug bundles, compared to the KD testing site. The middle *E. coli* confines taken from the KP testing location showed a general increase in resistance to anti-infection agents, including  $\beta$ -lactams and antibiotic drug bundles, compared to the KD testing site. *E. coli* isolated from the VR region demonstrated the highest level of resistance in the middle reaches, with ten out of twelve isolates (83%) being MDR, and displaying determined confrontation to beta-lactams, chloramphenicol, fluoroquinolones, and tetracyclines, through hundred percentage resistance to the antibiotic's Cefazolin, Cefotaxime, & Cefuroxime. (19, 20) The isolates also showed significant diversity in their antibiotic resistance profile between sample locations located in the middle reaches of Upper Lake.

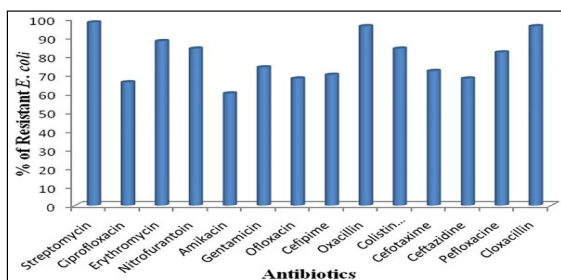


Figure 6. Confrontation Proportion (%) of Antibiotics compared to *E. coli*. Reprinted with permission (10)

However, the *E. coli* samples from the ITO locations exhibited a higher overall resis-

tance to most antibiotics compared to the KP and LVP sites. In the middle reaches, all *E. coli* separates demonstrated hundred percent resistances with cefazolin. The *E. coli* samples as of the VV sample presented a highest resistance to amino-glycosides, azithromycin,  $\beta$ -lactams, fluoroquinolones, nitrofurans, rifampin with a decrease in resistance to trimethoprim/sulphonamide and tetracycline groups. *E. coli* isolates from the VV site had considerably greater levels of tobramycin and nitrofurantoin resistance. However, at the DND Flyway sampling site, over 40% of *E. coli* displayed resistance to trimethoprim and sulphafurazole. (22) The resistance trend varied significantly between the higher, medium, and lower reaches. The VR (located in the centre) and VV testing locations into industrialized areas had the highest no. of MDR totals. (21) The *E. coli* isolated after the middle assortments exhibited the greatest resistance to six anti-infection classes, including polymyxins, chloramphenicol, fluoroquinolones, nitrofurantoin, and  $\beta$ -lactams. In the lower reaches, *E. coli* isolates displayed a declining level of antibiotic resistance, except for the increasing trend in resistance to sulphonamides-trimethoprim, with the maximum resistance (23, 24) observed at VR-site.

MAR (Multiple Antibiotic Resistance) was calculated for each sampling site, with those above 0.25 indicating a greater contribution to Upper Lake contamination. Damage reports from middle and lower sites were generally higher than those from upper sites. Studies by ecological organizations and water resource authorities (29, 31) ; (30, 32, 35) have highlighted the impact of antibiotic resistance in human, sewage, (25) and environmental sectors. Isolates from VR and VV sites demonstrated the highest MAR indices (0.678 and 0.574, respectively), with high resistance to gentamicin and  $\beta$ -lactam antibiotics such as cefazolin, cefotaxime, and cefuroxime found in direct sewage isolates. Among the sixteen isolates, three were identified as MDR. Amikacin showed the highest sensitivity rate (33.37%), followed by gentamicin and cefepime (22.92%). *E. coli* (26)



through a Blemish case of 1.01 demonstrated the highest multidrug resistance, and 127 obtainable of 150 isolates i.e., 34% was resilient to all 26-antibiotic tested. Antibiotic residues and resistant bacteria are released into the environment through industrial waste and sewage, contaminating water (23, 27) and food and facilitating the spread of ARB and ARGs. Aquatic environments have been found to harbor antibiotic-resistant microorganisms or genes that confer antibiotic resistance, particularly to aminoglycosides, tetracyclines, and  $\beta$ -lactams. (28, 33) These resistance determinants are often carried by mobile genetic elements, allowing for their rapid spread. (34) In aquatic environments, *E. coli* is frequently used as a biomarker for multiple antibiotic resistance. (10)

### Conclusion

Investigating the incidence of MAR-Multiple Antibiotic Resistance in *E. coli* strains from Upper Lake Bhopal was the goal of this investigation. The researchers used integrons and gene cassettes to classify the MDR isolates and examine the phylogenetic relationships among the isolates. They employed the Kirby Bauer diffusion disc technique to assess the antibiotic susceptibility profiles of 157 *E. coli* isolates from Upper Lake and direct sewage samples from the surrounding area. Among the nineteen drugs tested, cefazolin had the highest frequency of resistance (88%), followed by vancomycin (74%). Approximately 25% of the microbiological isolates was resistant to 13 medications, with more than ninety percent *E. coli* isolates being extremely toxic to azithromycin & polymyxin-B. The study found a high level of resistance to antibiotics from the  $\beta$ -lactam class, tetracyclines, fluoroquinolones, nitrofurantoin, and chloramphenicol from *E. coli* isolated water samples of Upper Lake, especially in the middle reaches. However, there was an increasing trend in trimethoprim/sulphonamide resistance throughout Upper Lake, and MDR isolates were present at every sampling site. All sampling locations in the lower middle and upper sections of Upper Lake had MAR indices above 0.25, demonstrating a significant risk of contamina-

tion due to the Straight sewage were the samples had high resistance to aminoglycoside and  $\beta$ -lactam antibiotics.

### Conflict of Interest

No conflict of interest

### Acknowledgements

The author is grateful to the Hon'ble Chancellor Er. B.S. Yadav and Hon'ble Pro-Chancellor Dr. (Prof.) Sunita Singh of the IES University, Bhopal, Madhya Pradesh, India for providing laboratory space and instruments during entire research work.

### References

1. Collignon, P. (2009). Resistant *Escherichia coli*—we are what we eat. *Clinical infectious diseases*, 49(2), 202-204.
2. Colomb-Cotinat, M., Lacoste, J., Brun-Buisson, C., Jarlier, V., Coignard, B., & Vaux, S. (2016). Estimating the morbidity and mortality associated with infections due to multidrug-resistant bacteria (MDRB), France, 2012. *Antimicrobial Resistance & Infection Control*, 5(1), 1-11.
3. Sargaonkar, A., & Deshpande, V. (2003). Development of an overall index of pollution for surface water based on a general classification scheme in Indian context. *Environmental Monitoring & Assessment*, 89(1).
4. Baquero, F., Martínez, J. L., & Cantón, R. (2008). Antibiotics and antibiotic resistance in water environments. *Current opinion in biotechnology*, 19(3), 260-265.
5. Sanderson, H., Fricker, C., Brown, R. S., Majury, A., & Liss, S. N. (2016). Antibiotic resistance genes as an emerging environmental contaminant. *Environmental reviews*, 24(2), 205-218.
6. Singh, N., & Samartha, M. (2021). deter-

- mination of water standards of upper lake, Bhopal, India. *Uttar Pradesh Journal of Zoology*, 42(7), 75-82.
7. Ten Brink, P. (Ed.). (2011). *The economics of ecosystems and biodiversity in national and international policy making*. Routledge.
8. Borkar, P., Tembhre, M., & Garg, R. K. (2017). Study on isolation and characterization of enterobacteriaceae in teleost fishes of Bhopal Lakes. *Asian J. Exp. Sci*, 31(1), 25-29.

## Phytochemical Screening and GC- MS Analysis of Three Indian Traditional Medicinal Plants

B. K. Neethu<sup>1\*</sup> and Sitavi Yathiender<sup>2</sup>

<sup>1</sup>Department of Biotechnology, REVA University, Bengaluru, Karnataka, India

<sup>2</sup>Department of Zoology, Jyothi Nivas College, Bengaluru, Karnataka, India

\*Corresponding Author : neethu.bk86@gmail.com

### Abstract

The investigation of current findings on phytochemicals and gas chromatography mass spectroscopy analysis (GCMS) of selected three Indian traditional medicinal plants namely Basil (*Ocimum basilicum*), Leucas (*Leucas aspera*) and Marigold (*Tagetes erecta*) of leaves of methanolic extract. All the plant extracts were screened to know their principle agents in qualitative phytochemical analysis. The qualitative phytochemical screening of *O. basilicum* leaves methanol extract shown positive results of flavonoids, terpenoids, glycosides, alkaloids, phenols, in *L. aspera* leaves shows all are present and in *T. erecta* leaves shown presence only for alkaloids, flavonoids, phenols and tannins whereas absence for terpenoids, glycosides and saponins. Out of three plants, *L. aspera* was selected for the spectroscopic studies by GCMS due to its active principles showed all the metabolites, in the GCMS results found 38 volatile compounds in the methanol extract of leaves. These plant extracts may possess insecticidal or larvicidal property due to strong aromatic property of the plants and also observed these volatile compounds in the one of the plant extract and may utilize it in agro-horticulture application as biocontrol agents.

**Keywords:** Phytochemical analysis, GCMS, *Ocimum basilicum*, *Leucas aspera*, *Tagetes erecta*, Biocontrol agents

### Introduction

Medicinal plants are the hidden treasure of phytochemicals and form the large group of economically important plants for wide range of applications. The secondary metabolites of medicinal plants has exhibit in support of insects growth and development also against as detrimental, which inturn manifested in various levels including sterility, morbidity, toxicity, mortality, growth inhibitor, anti-feedant, reduction of fecundity, CNS depressants, fertility regulation and many of the reproductive activity inhibition (1-2). Leaves extracts of various native and exotic medicinal plants were reported from the ancient time, that to be in aromatic plants having been reported to have toxicity with various organ systems also inhibition potential in gravimetric as well as histometric in insect models or any other model organisms (3-4). Various findings have been revealed for plant phytochemicals in qualitative and quantitative approach to explore the potential biomolecules for the application of agro-horticulture. These phytochemicals are depends upon the plant part extraction and method of extraction to identify their distri-

bution of specific molecules and exhibit such biological activity depends on their lethality level based on concentrations of the involved active agents may differ from one plants to others (5-7).

In this scenario, current study focused on to screen the phytochemicals of three selected aromatic medicinal plants qualitatively and based on the presence of metabolites study further restricted to explore the one plant extract to quantify the volatile compounds by GCMS studies.

## Material and Methods

### Plant material

Medicinal plant commonly called as Basil (*Ocimum basilicum*), Leucas (*Leucas aspera*) and Marigold (*Tagetes erecta*) of leaves were collected from the botanical garden of Jyoti Nivas College and the plant samples were authenticated at Botany Department, Jyoti Nivas College Autonomous, Bengaluru, India.

### Preparation of plant extracts

The leaves of *O. basilicum*, *L. aspera* and *T. erecta* were collected, washed thoroughly in running tap water, sprinkled 70% ethanol and dried in room temperature to avoid contamination and moisture free sample. Dried samples were crushed, powdered in electric mixer and stored in polybag at in the refrigerator prior to follow extraction. Each plant sample 500 gm stored powder used for extraction in methanol highly polar solvent. The solvent of the each extracts were removed by rotary evaporator to get solvent free crude extract. Standard stock of each extract solutions was prepared using acetone solvent in 1% of extract residues for dissolution. After saturation, dissolved extract residues were filtered, and concentrated to dryness in 400°C - 500°C using vacuum evaporator of each 100 gm of plant extract concentrated to obtain 100% output of concentration. Then further extract was diluted in double distilled water five times in graded concentration from low at (0.2%), mid at (0.4%), moderate at (0.6%) and

high at (0.8%) of each samples and at (0%) used for the control.



Figure 1: Morphology of the aromatic medicinal plants

### Qualitative Phytochemical screening

Qualitative screening of phytochemicals of 3 aromatic medicinal plants methanol extracts were carried out in order to know their active constituents presence in the leaves, which further aimed to finalize the plant extract potential in the GCMS study to identify the quantitative volatile compounds and their characterization.

Methanol extract of selected aromatic medicinal plants leaves subjected to standard phytochemical qualitative tests described by Sharangouda and Patil, (8), Harnborne, (9) and Fransworth, (10) to determine the presence or absence of flavonoids, terpenoids, glycosides, tannins, alkaloids, phenols and saponins. Preparation of reagents for phytochemical assay followed standard protocol of Harnborne (11). To make the concentration to obtain the proper solution of methanol extract was re-suspended to obtain 100% dissolution used MilliQ water then filtered for the studies.

### GCMS analysis

#### Gas chromatography and mass spectroscopy

#### Preparation of extract

10mg/ml aromatic medicinal plant methanolic

extract of *L. aspera* leaves were prepared in universal solvent methanol and for which 1µl plant extract was employed to quantify the volatile compounds by GCMS analysis.

**Instruments and chromatographic conditions**

GCMS study of *L. aspera* methanol extract was assessed by Thermo GCMS of model Clarus 500. For the mass spectrum detection, used the mode of MS DSQ II electron ionization with energy rate of 70 eV, at the mass range of m/z 50-650. Capillary column in the range of 30m x 0.25mm size covering the film thickness 0.25 of Restek RtxR-5MS column model by using solvent diphenylamine and dimethyl polysiloxane at the ratio of 5 and 95 in the analysis. The base temperature of column was pre-defined at 60°C/5min, GC injector and MS temperatures was configured at 280°C and 290°C in transfer line respectively. GC was assessed in the mode of splitless to get maximum hits in the sample. Helium at the flow rate per minute described it as 1.0ml and also it was applied as carrier gas in GC studies in the volume of 1.0 µL injection was used. The extracted plant sample dissolved in methanol solvent and filtered to apply it further for polymeric solid phase extraction (SPE) column to detect different constituents in GCMS. As a result of constituents presence searched in the data base of NIST REFPROP 9.1 Version by comparing one another to enlist the volatile compounds in the extract by the GCMS studies.

**Identification of volatile compounds**

Result interpretation of GCMS data was assessed with the help of the database of National Institute Standard and Technology (NIST) due to vast depiction of more than 62,000 compound patterns. The comparative assessment helped to identify unknown compounds when compared with stored NIST library to explore the available data of plant extract. The characters like name, formula, weight and structure of the volatile compounds of the sample was ascertained to derive the molecular chemical data.

**Results and Discussion**

**Phytochemicals screening for methanolic three aromatic plant extracts**

The screening of phytochemicals of methanol extract of three aromatic medicinal plants of leaves showed result depends on plants and found maximum positive in *Lecuas aspera* only. In *O. basilicum* extract showed positive for flavonoids, terpenoids, glycosides, alkaloids, phenols and negative for tannins and saponins. In *L. aspera* extract showed positive for flavonoids, terpenoids, glycosides, alkaloids, phenols, tannins and saponins. In *T. erecta* extract showed positive only for alkaloids, flavonoids, phenols and tannins whereas absence for terpenoids, glycosides and saponins (Table1). Similar studies were reported by many of the researchers from the background of medicinal plants using various types of plant parts and their extracts (12-17).

**Table: 1:** Screening of phytochemicals on aromatic medicinal plants in the methanol extract of leaves

Qualitative Screening of Phytochemical Analysis			
Tests	O. basilicum	L. aspera	T. erecta
Flavanoids	+	+	+
Terpenoids	+	+	-
Glycosides	+	+	-
Tannins	-	+	+
Alkaloids	+	+	+
Phenols	+	+	+
Saponins	-	+	-

**Note:** + = Positive; - = Negative

**GCMS analysis of methanolic extract of leucas aspera leaves**

The GCMS study of the methanolic extract results were shown in figure 2 and it has eluted 38 different metabolites. Identification of volatile compounds were assessed with the comparison of standards of NIST and Wiley


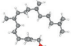
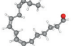

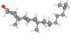
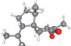
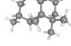
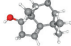
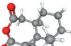

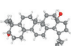

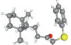
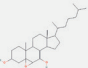




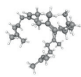
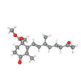
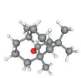
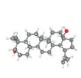
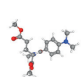
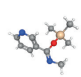
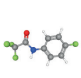
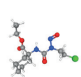
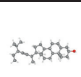
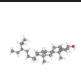
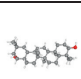
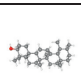
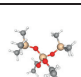
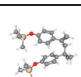
9.1. Most of the phytochemical were characterized by their respective area (%) depends on the availability and elution on particular retention time. The obtained peaks of the chromatograms, shown highest % of area by (1Ar-(1alpha,5abeta,9ar(\*)))5a,9,9-trimethyloctahydrobenzo(d)cycloprop(c)oxepin-2,4- (55.94), Cyclohexanecarboxylic acid, 2-[[bis(2-methylpropyl)amino]carbonyl]-, 4-nitrophenyl este (11.51 ), Benzene, 1,2-dimethoxy-4-(2-propenyl)- (5.48), Bicyclo[2.2.1]heptane-1-methanesulfonic acid, 7,7-dimethyl-2-oxo-, (.+/-)- (4.12), Thunbergol (3.76), 4,4,6a,6b,8a,11,11,14b-Octamethyl-1,4,4a,5,6,6a,6b,7,8,8a,9,10,11,12,12a,14,14a,14b-oc (1.63), alpha-Amyrin (1.63),

Stigmasterol (1.46), gamma.-Sitosterol (1.24) 2-(3-Pentyl)pyridine (1.22), 2,4,5,5,8a-Pentamethyl-4a,5,6,7,8,8a-hexahydro-2H-chromene (1.05) and rest other 28 volatile compounds shown less than 1 % of area as per the elution on particular retention time. As per the literature many of the volatile compounds which were present in the plant shown potent cytotoxicity activities and also several researchers reported for various pharmacological applications on these compounds in different plants, hence these volatile compounds listed with various characters to understand their biological action in table 2.

Table 2: Quantification of volatile compounds by GCMS of methanolic extract leaves of *Leucas aspera* plant and their various characters.

Peak No.	Retention time	Peak area (%)	Molecular formula	Molecular Weight (g/mol)	Name of the molecules	Molecular structure
1	6.345	0.21	C <sub>12</sub> H <sub>26</sub>	170.33	Dodecane	
2	10.611	5.48	C <sub>11</sub> H <sub>14</sub> O <sub>2</sub>	178.23g/mol	Benzene, 1,2-dimethoxy-4-(2-propenyl)-	
3	10.980	0.37	C <sub>15</sub> H <sub>24</sub>	204.35g/mol	Caryophyllene	
4	13.230	0.23	C <sub>15</sub> H <sub>24</sub> O	220.35g/mol	1,4-Methanoazulen-9-one, decahydro-1,5,5,8a-tetramethyl-, [1R-(1.alpha.,3a.beta.,4.alpha	
5	13.434	4.12	C <sub>28</sub> H <sub>38</sub> O <sub>8</sub> S <sub>2</sub>	566.7g/mol	Bicyclo[2.2.1]heptane-1-methanesulfonic acid, 7,7-dimethyl-2-oxo-, (.+/-)-	
6	13.655	0.19	C <sub>10</sub> H <sub>15</sub> BrO	231.13g/mol	Bicyclo[2.2.1]heptan-2-one, 5-bromo-1,7,7-trimethyl-, (1R-exo)-	
7	13.864	0.22	C <sub>20</sub> H <sub>34</sub> O	290.5g/mol	Thunbergol	
8	16.362	0.31	C <sub>13</sub> H <sub>22</sub> O	194.313	1a,2,5,5-Tetramethyl-cis-1a,4a,5,6,7,8-hexahydro-gamma-chromene	

9	16.791	0.45	$C_{15}H_{30}O_2$	242.4g/mol	Pentadecanoic acid	
10	18.296	0.44	$C_{20}H_{40}O$	296.5g/mol	Phytol	
11	18.525	0.97	$C_{16}H_{26}O$	234.38g/mol	cis,cis,cis-7,10,13-Hexadecatrienal	
12	18.757	0.24	$C_{18}H_{32}O$	264.4g/mol	17-Octadecen-14-yn-1-ol	
13	19.056	0.18	$C_{27}H_{44}O$	384.6g/mol	Cholest-4-en-3-one	
14	19.539	0.76	$C_{15}H_{24}O_2$	236.35g/mol	Spiro[4.5]decan-7-one, 1,8-dimethyl-8,9-epoxy-4-isopropyl-	
15	20.794	0.45	$C_{15}H_{26}$	206.37g/mol	2,4a,8,8-Tetramethyldecahydrocyclopropa[d]naphthalene	
16	21.195	0.35	$C_{12}H_{20}O$	180.29g/mol	1H-Inden-1-ol, 2,4,5,6,7,7a-hexahydro-4,4,7a-trimethyl-	
17	21.676	55.94	$C_{14}H_{20}O_3$	236.31g/mol	(1Ar-(1a alpha,5a beta,9a*)))-5a, 9,9-trimethyl-octahydrobenzo(d) cycloprop(c)oxepin-2,4-	
18	21.994	3.76	$C_{20}H_{34}O$	290.5g/mol	Thunbergol	
19	22.206	0.59	$C_{30}H_{50}O_2$	442.7g/mol	Betulin	
20	22.352	1.05	$C_{14}H_{24}O$	208.34g/mol	2,4,5,5,8a-Pentamethyl-4a,5,6,7,8,8a-hexahydro-2H-chromene	
21	22.489	0.68	$C_{20}H_{28}OS$	316.5g/mol	Bicyclo[4.1.0]heptane, 1-(3-oxo-4-phenylthiobutyl)-2,2,6-trimethyl-	
22	22.754	0.63	$C_{27}H_{46}O_3$	418.7g/mol	3.alpha.,7.beta.-Dihydroxy-5.beta.,6.beta.-epoxycholestane	
23	23.420	0.31	$C_{16}H_{26}O_3$	266.38g/mol	2,5-Furandione, 3-decyl-	

24	23.793	1.22	$C_{10}H_{15}N$	149.23g/mol	2-(3-Pentyl)pyridine	
25	23.975	0.39	$C_{30}H_{50}$	410.7g/mol	2,6,10,14,18,22-Tetracosahexaene,	
26	24.265	0.39	$C_{19}H_{26}O_4$	318.4g/mol	2,6,10,15,19,23-hexamethyl-, (all-E)-2-Cyclohexene-1-carboxylic acid, 1,3-dimethyl-2-(3-methyl-7-oxo-1,3-octadienyl)-4-oxo	
27	24.470	0.24	$C_{15}H_{26}O$	222.37g/mol	3,3,7,11-Tetramethyltricyclo[5.4.0.0(4,11)]undecan-1-ol	
28	24.557	0.64	$C_{30}H_{50}O_2$	442.7g/mol	Betulin	
29	24.964	0.95	$C_{17}H_{24}N_2O_5$	336.4g/mol	4-Aminobenzoylglutamic acid penta-methyl derivative	
30	25.726	0.18	$C_{10}H_{16}N_2OSi$	208.33g/mol	N-Methyl nicotinimide, O-trimethylsilyl	
31	26.574	0.17	$C_8H_5F_4NO$	207.12g/mol	Acetamide, N-(4-fluorophenyl)-2,2,2-trifluoro-	
32	27.484	11.51	$C_{12}H_{20}ClN_3O_4$	305.76g/mol	Cyclohexanecarboxylic acid, 2-[[bis(2-methylpropyl)amino]carbonyl]-, 4-nitrophenyl este	
33	28.479	1.46	$C_{29}H_{48}O$	412.7g/mol	Stigmasterol	
34	29.269	1.24	$C_{29}H_{52}O_2$	432.7g/mol	.gamma.-Sitosterol	
35	30.323	1.63	$C_{30}H_{50}O_2$	442.7g/mol	4,4,6a,6b,8a,11,11,14b-Octamethyl-1,4,4a,5,6,6a,6b,7,8,8a,9,10,11,12,12a,14,14a,14b-oc	
36	30.728	1.63	$C_{30}H_{50}O$	426.7g/mol	alpha-Amyrin	
37	31.460	0.19	$C_{10}H_{28}O_4Si_3$	296.58g/mol	Silicic acid, diethyl bis(trimethylsilyl) ester	
38	31.950	0.21	$C_{24}H_{36}O_2Si_2$	412.7g/mol	4-Methyl-2,4-bis(4'-trimethylsilyloxyphenyl)pentene-1	

GCMS studies of *Leucas aspera* leaves methanolic extract (Figure 2) exhibited total 38 volatile compounds as per the detection of peaks and their retention time and these are indicating the presence of thirty eight different volatile compounds which have various biological properties. These compounds identified by their characterization in differentiating retention time in each compounds along with their peak (%) in the studied plant extract in GCMS analysis. These characters classified by name of the individual molecules with molecular formula, weight and structures as per the retention time and concentration of the peak area elution in (%) the spectrum (Table 2). The characterized results represented as per the peak and percent area of the volatile compounds, i.e., (1Ar-(1aalpha,5abeta,9ar(\*)))-5a,9,9-trimethyloctahydrobenzo(d)cycloprop(c)oxepin-2,4- (55.94), Cyclohexanecarboxylic acid, 2-[[bis(2-methylpropyl)amino]carbonyl]-, 4-nitrophenyl este (11.51), Benzene, 1,2-dimethoxy-4-(2-propenyl)- (5.48), Bicyclo[2.2.1]heptane-1-methanesulfonic acid, 7,7-dimethyl-2-oxo-, (+/-)- (4.12), Thunbergol (3.76), 4,4,6a,6b,8a,11,11,14b-Octamethyl-1,4,4a,5,6,6a,6b,7,8,8a,9,10,11,12,12a,14,14a,14b-oc (1.63), alpha.-Amyrin (1.63), Stigmasterol (1.46), gamma-Sitosterol (1.24) 2-(3-Pentyl)pyridine (1.22), 2,4,5,5,8a-Pentamethyl-4a,5,6,7,8,8a-hexahydro-2H-chromene (1.05) and remaining 28 volatile compounds shown less than 1 % with respect retention time and peak area.

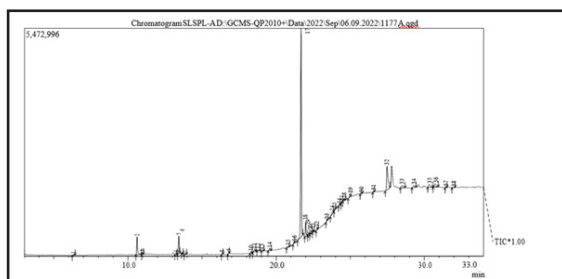


Figure 2. Spectrum of GCMS analysis and their volatile compounds representation of *Leucas aspera* leaves methanolic extract.

The *L. aspera* leaves of methanol extract found

with potent volatile compounds in GCMS studies, in that identified all the present compounds are carbohydrate derivatives and fatty acid mixtures. From the obtained data, we can expect the maximum purity and characterized compound such as (1Ar-(1aalpha,5abeta,9ar(\*)))-5a,9,9-trimethyloctahydrobenzo(d)cycloprop(c)oxepin-2,4- (55.94%) found higher concentration and percent area, other 9 compounds altogether shown (27.64%) moderate concentration and rest all shown (16.4%) lower concentration covering 28 compounds. Patil *et al.*, (33) extensively worked on seed oil of *Citrus medica* and resulted in GCMS findings A8 volatile compounds i.e., higher rate of concentration with hexadecanoic acid, 9,12-octadecanoic acid,  $\beta$ -Sitosterol and oleic acid as an eluted mixture of fatty acids (18). Eramma and Patil, (19) revealed 41 distinct volatile compounds from crude and TLC fractions in *Flacourtia indica* root extract of methanol, GCMS analysis indicated the presence of, including Heneicosane (25.945), Squalene (20.51), Cholesterol (33.525), Cycloheptasiloxane, tetradecamethyl-(14.864), 2,4-Di-tert-butylphenol-(16.032), Cycloheptasiloxane hexadecamethyl (16.848), Cyclononasiloxane octadecamethyl (20.733), and n-Hexadecanoic acid (22.092). Kolgi *et al.*, (20, 21) reported the two metabolites such as alkaloid and flavonoid also revealed antioxidant and anticancer property in *Leucas aspera* leaves of chloroform and ethanol extracts. Similar compounds also reported for antioxidant property of *Simarouba glauca* seed extracts of petroleum and ethanol and revealed their qualitative and quantitative phytochemistry (22, 23).

## Conclusion

Medicinal plants are the natural service provider for the treatment of any human diseases, and they have super healing power due to the richness of active ingredient of phytochemicals. Selected three Indian traditional medicinal plants namely *Ocimum basilicum*, *Leucas aspera* and *Tagetes erecta* of leaves of methanolic extract shown various types of phytochemicals, but in the *L. aspera* shown all the phytochem-

cials and it is further elucidated with spectroscopy study and found 38 volatile compounds by the GCMS characterization. Compare to other two plants, *L. aspera* found potential, they possess pharmacological properties and may have valuable biological action. The identified active volatile compounds may exhibit various biological properties and they act as future drug therapeutic molecule for agro-horticulture as larvicidal or insecticidal biocontrol agent. The co-relation of phytochemicals and volatile compounds resulted in various biological actions and may become novel future drugs for the various level of therapeutics.

### Acknowledgement

The authors are thankful to the Karnataka State Technology Academy (KSTA), Bengaluru, Karnataka, India for providing for financial assistance and Jyoti Nivas College, Bengaluru for all the necessary facilities for the research work.

### Conflict of Interest

The authors declare no conflict of interest.

### References

1. Patil, S.J. and Patil, S.B. (2010). Toxicity studies on hepatic, nephric and endocrine organs of *Citrus medica* seeds extract on female albino mice. *Journal of Global Pharma Technology*, 3(1): 14-21.
2. Patil, S.J. and Patil, S.B. (2012). Effect of *Oxalis corniculata* whole plant extracts on fertility regulation in female albino rats. *Journal of Advances in Scientific Research*, 3(1): 58-61.
3. Neelam, B., Poonam, V. and Chandranandani, N. (2018). A review on some traditional medicinal plants. *International Journal of Life Science and Scientific Research*, 4(1):1550-1556.
4. Orwa, C., Mutua, A., Kindt, R., Jamnadass, R. and Anthony, S. (2009). Agroforestry database: A tree reference and selection guide version 4.0.
5. Prajapati, M.S. et al., (2010). *Leucas aspera*: A review. *Pharmacognosy Reviews*, 4,7: 85-97.
6. Singh, N., Mrinal and Thakur, R. (2019). A review on pharmacological aspects of *Tagetes erecta* Linn. *PharmaTutor*, 7, 9 (Sep. 2019): 16-24.
7. Cohen M.M. 2014. Tulsi - *Ocimum sanctum*: A herb for all reasons. *Journal of Ayurveda and Integrated Medicine*, 5(4): 251-259.
8. Sharangouda and Patil, S.B. (2007). Phytochemical screening and antifertility activity of various extracts of *Citrus medica* (Lemon) seeds in albino rats. *Advances in Pharmacology and Toxicology*, 8(2):71-4.
9. Harborne, J.B. (1998). *Phytochemical Methods: A Guide to Modern Techniques of Plant Analysis*. 3<sup>rd</sup> Ed. New York: Chapman and Hall Co.
10. Farnsworth, N.R. (1966). Biological and phytochemical screening of plants. 55(3): 225-276.
11. Harborne, J.B. (1973). *Phytochemical Methods: A Guide to Modern Techniques of Plant Analysis*, Chapman and Hall, London, UK.
12. Bhat, S.G. (2021). Medicinal plants and its pharmacological values. In: *Natural medicinal plants*. El-Shemy, H.A. editor. IntechOpen: London
13. Olivia, N.U., Goodness, U.C. and Obinna, O.M. (2021). Phytochemical profiling and GC-MS analysis of aqueous methanol fraction of *Hibiscus aspera* leaves. *Future Journal of Pharmaceutical Sciences*, 7: 1-5.
14. Swati, M., Pannakal, S.T., Ganapaty, S., Singha, G.N. and Kumar, K. (2009). Phenolic glucosides from *Flacourtia indica*.



- Natural Products Communications, 4: 381-384,
15. Haleshappa, R., Sajeeda, N., Kolgi, R.R., Patil, S.J. and Siddalinga Murthy, K.R. (2022). Phytochemicals, anti-nutritional factors and proximate analysis of *Simarouba glauca* seeds. International Advanced Research Journal in Science, Engineering and Technology, 9(3): 218-227.
  16. Eramma, N. and Gayathri, D. (2013). Antibacterial potential and phytochemical analysis of *Flacourtia indica* (Burm.f.) Merr. root extract against human pathogens. Indo American Journal of Pharm Research 3: 3832-3846.
  17. Jeevitha, M. and Sripathi, S.K. (2021). Phytochemistry and therapeutic potential of *Acacia ferruginea*: A systematic review. Asian Journal of Plant Science Research, 11: 22-29.
  18. Patil, S.J., Venkatesh, S., Vishwanatha, T., Banagar, S.R., Banagar, R.J. and Patil, S.B. (2014). GCMS analysis of bioactive constituents from the petroleum ether extracts of *Citrus medica* seeds. *World Pharmacy and Pharmaceutical Sciences*, 3: 1239-1249.
  19. Eramma, N. and Patil, S.J. (2023). Exploration of the biomolecules in roots of *Flacourtia indica* (Burm. F) Merr. methanol extract by chromatography approach. Letters in Applied NanoBioscience, 12(4): 166-177.
  20. Kolgi, R.R., Haleshappa, R., Sajeeda, N., Keshamma, E., Karigar, C.S. and Patil S.J. (2021). Antioxidant studies, *in vitro* cytotoxic and cell viability assay of flavonoids and alkaloids of *Leucas aspera* (Wild.) Linn leaves. Asian Journal of Biological and Life Sciences, 10(1): 165-171.
  21. Kolgi, R.R., Patil, S.J. and Karigar, C.S. (2020). Antioxidant and anticancer properties of chloroform extract of *Leucas aspera* from Tumkur district. Proceedings of National Conference National Web Conference on Sustainability in the Commerce, Scientific, Technological, Linguistic and Environmental Sectors. pp.106-107.
  22. Haleshappa, R., Patil, S.J., Usha, T. and Murthy SM. (2020). Phytochemicals, antioxidant profile and GCMS analysis of ethanol extract of *Simarouba glauca* seeds. Asian Journal of Biological and Life Sciences, 9(3): 379-385.
  23. Haleshappa, R., Keshamma, E., Girija, C.R., Thanmayi, M., Nagesh, C.G., Fahmeen, L.G.H. et al., (2020). Phytochemical Study and Antioxidant Properties of Ethanolic Extracts of *Euphorbia milii*. Asian Journal of Biological Sciences, 13(1): 77-82.

## ***In-silico* Screening of some Isolated Compounds of *Hemidesmus indicus* and Evaluation of its Antidiabetic Potential**

**Sudip Pratihar<sup>1</sup>, Robina Khatun<sup>1</sup>, Prosun Ganguly<sup>1</sup>, Barsan Banerjee<sup>1</sup>,  
Md Nasiruddin Khan<sup>1</sup>, Satya Narayan Dey<sup>1</sup>, Basanta Sourav Sk<sup>1</sup>,  
Tofajul Mirza<sup>1</sup>, Sm Sohel Aktar<sup>1</sup>, Tabasum Parvin<sup>1</sup>, Suddhasattya Dey<sup>2</sup>,  
\*Priyanka Chandra<sup>3</sup>, \*Arijit Mondal<sup>2</sup>**

<sup>1</sup>Department of Pharmacy, Sanaka Educational Trust's Group of Institutions, Malandighi, Durgapur, West Bengal 713212

<sup>2</sup>Bengal College of Pharmaceutical Technology, Dubrajpur, Birbhum, West Bengal 731123

<sup>3</sup>Department of Pharmaceutical Sciences and Technology, Birla Institute of Technology, Mesra, Ranchi-835215, Jharkhand, India

Corresponding author: priyankachandra78@gmail.com

### **Abstract**

*Hemidesmus indicus*, widely recognized as anantamul, is often utilized in conventional medical systems to treat liver disorders, diabetes and kidney diseases etc. Some of the compound has been isolated and identified as antidiabetic in nature. Fewer compounds were screened for the *in-silico* study to establish a computational approach of the plant *Hemidesmus indicus* to open a new gateway for the treatment of diabetes. Docking study was carried out by using Autodock 4.2 software and a overall comparison study was performed between different compounds like 2-hydroxy-4-methoxy benzaldehyde, Beta-amyrin palmitate, Hyperoside, Isoquercetin and Vanilin. Among these Beta-amyrin palmitate and Vanilin showed most promising docking score towards different antidiabetic receptor comparison to the internal ligand. Docking score of Beta-amyrin palmitate are -6.37, -6.50, -7.69 and -8.14 for the PDB ID 1X70, 1PPI, 1V4S and 5VEX respectively. Docking score of Vanilin are -2.99, -4.43, -3.72 and -4.43 for the PDB ID 1X70, 1PPI, 1V4S and 5VEX respectively. The above study revealed that Beta-amyrin palmitate was found to be most potent antidiabetic agent according to the *in-silico* study. This Beta-amyrin palmitate was

also identified as an antidiabetic agent through *in-vitro* study, from this we can conclude that a *in-vitro* and *in-vivo* correlation can be establish for this compound.

**Keywords:** *Hemidesmus indicus*, Vanilin, Beta-amyrin palmitate, 1X70, 1PPI, 1V4S and 5VEX

### **Introduction**

*Hemidesmus indicus* R.Br., often known as "Anantmoola or Anantamul," is a laticiferous, twining shrub that is found throughout the majority of India. *Hemidesmus indicus* was once belongs to Asclepiadaceae family but has currently been moved to the Periplocaceae family based on pollination characteristics. *Hemidesmus indicus* behave as a laxative, diuretic, and diaphoretic and that can be used to treat syphilis, cough, asthma, and leucoderma. It is widely distributed in nature, hence easily available. It exhibits a variety of activities out of which antidiabetic activity is very important [1]. *Hemidesmus indicus* contains a broad range of chemicals, including terpenoids, steroids, flavonoids, phenolic compounds, saponins, tannins, lignins, cardiac glycosides, proteins, and carbohydrates [2,3]. Beta-amyrin palmitate,

Hyperoside, Isoquercetin, Vanillin, 2-hydroxy-4-methoxybenzaldehyde are some isolated compounds found in the *Hemidesmus indicus* [4]. Diabetes mellitus (DM) is a metabolic condition characterized by a lack of insulin synthesis or action, or both [5]. It prevails in practically every country and continues to grow in numbers and impact as people's quality of life deteriorates, resulting in decreased physical activity and more obesity. This results in long-term hyperglycemia and a wide range of metabolic processes in the human body [6]. According to the World Health Organization (WHO), Diabetes mellitus affects 347 million people worldwide, and it is expected to become the sixth greatest cause of death by 2030. In 2012, diabetes caused a total of 1.5 million fatalities. It was the eighth most typical reason of mortality for both males and females, and the fifth most typical reason of death for females [7]. Different kinds of medications, such as biguanides and sulfonylureas are currently able to be treated diabetes mellitus hyperglycemia. These certain medications have adverse effects, therefore finding a new class of chemicals to solve these issues is critical. The medical profession is still grappling with how to manage diabetes without causing negative effects. Alternative medications are always being sought. The rise of phyto-medicine and the hunt for novel types of antidiabetic from herbal plants has been prompted by the negative effects of synthetic medications, as well as drug resistance [2,8]. S.A. Nair *et al.* [9] in 2014 during evaluating the toxicity effect of *Hemidesmus indicus* root extracts observed that the root extracts show glucose-lowering properties. Therefore, they are interested to isolate the active compound which has hypoglycemic activity. For the isolation of active compounds from root extracts, they go through different chromatographic techniques. The effective component, Beta-amyirin palmitate, was separated and identified which was then evaluated for the anti-hyperglycemic activity by Glucose tolerance test in alloxan-induced diabetic rats. The effects of 2-hydroxy-4-methoxy benzaldehyde isolated from *H. indicus*

roots on diabetic rats caused by streptozotocin has been thoroughly discussed by Kannabiran K. *et al* [10] in a number of studies. Verma N. *et al* [11] evaluate antihyperglycemic activity of hyperoside by Oral glucose tolerance test (OGTT). Dong Kwon Yang [12] and Hyung-Sub Kang [12] investigate the antidiabetic action of quercetin (QE) in streptozotocin (STZ)-induced diabetic rats by Oral glucose tolerance test (OGTT). Lu G. *et al* [13] investigate the antidiabetic action of quercetin (QE) in diabetics triggered by streptozotocin (STZ) in neonatal rats by Oral glucose-tolerance test (OG-TT). In the design and layout of novel medications, molecular docking is a crucial methodology. These tactics aim to predict a small molecule's experimental binding mechanism and affinities within the target receptor's binding region. The natural ligand posture, the receptor binding site, and the related physical-chemical molecular interactions must all be accurately predicted using a good docking process [14,15]. The present study gives an insight of interaction between some identified compounds with different antidiabetic receptor by the help of molecular docking and compare the different compounds using docking score.

## Materials and Methods

### *In-vivo* analysis of different isolated compounds

S.A. Nair *et al.* [9] evaluated the antihyperglycemic activity beta amyirin palmitate by Glucose-tolerance test in alloxan-induced diabetic rats. Male-Wistar rats weighing 175–200 g was divided up into four groups of six each to test the effects of various per oral (p.o.) doses of beta amyirin palmitate on glucose tolerance. The substance (5% Tween 80, 1 mL, p.o.) was given to the control group. The experimental groups gained beta-amyirin palmitate in various doses (25, 50, and 100 mg/kg) in the same way. After administering herbal drugs for 30 minutes, 60% glucose (3 g/kg, p.o.; 1 ml/200 g body weight) was given to the rats in all groups. Samples of blood were taken through a retro-

*In-silico* screening of compounds from *Hemidesmus indicus* and their antidiabetic potential

orbital puncture while the patient was sedated at 0, 1, 30, 90, and 150 minutes following glucose loading.

Kannabiran K. *et al* [10] evaluated antidiabetic activity by a single intra-peritoneal injection of freshly prepared streptozotocin solution in rats. Group I was used as a control, Group II contained STZ-induced diabetic rats that survived, Group III was used as a positive control and got tolbutamide (100 mg/kg) by oral intubation technique, and Group IV contained diabetic rats that were given HMB (500 g/kg) for 7 weeks. At the conclusion of the treatment period, in order to measure plasma glucose using the glucose oxidase method and plasma insulin using a radioimmunoassay kit, blood samples were drawn from the tail vein using aseptic methods and placed in tubes containing potassium oxalate and sodium fluoride.

Verma N. *et al* [11] evaluated antihyperglycemic activity of hyperoside by Oral glucose tolerance test (OGTT). Oral-glucose tolerance testing was accomplished on normal Wistar rats that had fasted overnight (18 hours) to determine the effective dose of hyper insulin. They were split up into four groups, each with six animals. Blood from the tail vein was drawn to assess the initial serum glucose. Orally administered glucose (2 g/kg body weight) was given to normal control rats (Group 1). 30 minutes before the oral administration of 2 g/kg of glucose solution to groups 2 and 3, two separate doses (of 25 and 50 mg/kg body weight) of hyperoside in distilled water were given. Before the glucose load, Group 4 got the usual medication, glybenclamide (20 mg/kg).

Dong Kwon Yang [12] and Hyung-Sub Kang [12] investigated the antidiabetic action of quercetin (QE) in diabetic rats caused by streptozotocin by Oral glucose -tolerance test (OG-TT). The 50 male Sprague-Dawley rats were divided into three (30 mg/kg QE) compound-treated diabetes groups and two normal control groups.

Lu G. *et al* [13] investigated the antidiabetic action of vanillin in streptozotocin (STZ)-induced diabetic in neonatal rats by Oral glucose- tolerance test (OG-TT). Male 2-day-old pups were given 90 mg/kg of STZ intraperitoneally (i.p.) to cause diabetes. The puppies were subsequently divided into four groups at random: control, negative control, diabetic, and vanillin-treated. The vanillin treated groups gained vanillin (100 or 200 mg/kg, p.o.) consistently from the sixth week of age to the tenth week. Vanillin's antidiabetic impact was evaluated by monitoring the insulin, lipid, and blood sugar levels in the diabetic rat's serum.

### **Molecular docking analysis of isolated compounds**

#### **Hardware used**

Processor used for this docking is Intel Core i3. CPU Cores are 816, Clock frequency of the hardware is 3GHz, Size of the main memory is 1072 GB, Graphics card is RADEON.

#### **Software used**

UCSF Chimera and ChemDraw 15.0 which have academic license are used for this process. For molecular docking, Autodock tools 4.2 is used which is an open source software.

#### **Protein preparation**

Three-dimensional structure (Mainly crystal) of different PDB-ID like 1PPI [16] , 1X70 [17], 1V4S [18], 5VEX [19] was chosen for the investigation. From Protein Data Bank (PDB), acquired the 3D X-ray crystallographic structures. The process of getting ready involves accessing the PDB ID to retrieve the protein from the server, uploading the molecule, adding hydrogens, applying specific turning to residues, examining interactions and geometry for all atoms, performing the job, and acquiring the finished protein file.

#### **Ligand preparation**

In this investigation, ligands were Beta-amyryn palmitate, Hyperoside, Isoquercetin,

Vanillin, 2-hydroxy-4-methoxybenzaldehyde. Chemdraw15.0 was used to create the particular structures in concern. The stabilised structure was stored after being downloaded from the server as PDBQT format for the purpose of protein-ligand docking.

### **Protein-ligand docking**

The Autodock-4.2.6 programme (ADP) was used to carry out all molecular docking investigations. ADP tools were used to prepare the protein and ligands. The coordinate values used in grid settings were acquired from re-docking studies, and dimensions of the grid box were 60x60x60 in the x, y, and z directions. In each case, spacing of the grid point was 0.375". Auto grid-4.2 was utilised to create the map files. For search criteria, a genetic algorithm (GA) was employed. The population size was 150, there were 50 GA runs, and there were 2500000 evaluations. Autogrid and Autodock operation was the last step. The molecular docking of individual ligand on the appropriate protein was carried out using Autodock-4.2 and Autogrid-4.2, respectively.

### **Results and Discussion:**

#### ***In-vivo results of different isolated compounds***

Beta-amyrin palmitate (25-100 mg/kg) had antihyperglycemic effects on rats given glucose orally. The best dosage was 50 mg/kg, and increasing it forward, to 100 mg/kg did not cause a corresponding drop in blood sugar levels. When glucose was delivered, as opposed to oral glucose loading, the medication (50 mg/kg) did not significantly lower blood sugar levels [9].

In comparison to untreated control rats, orally administered HMB's aqueous solution dramatically ( $F > 0.05$ ;  $P < 0.001$ ) decreased blood sugar levels and raised plasma insulin levels to levels close to normal [10].

Hyperoside has been shown to have antihyperglycemic potential when given to

diabetic rats caused by streptozotocin, in doses of 25 and 50 mg/kg daily for 30 days. After 120 minutes of an oral glucose tolerance test, rats administered with hyperoside showed a considerable drop in blood glucose levels. In streptozotocin-induced diabetic rats, it was discovered that hyperoside demonstrated dose-dependent and substantial antihyperglycemic activity that was remarkably similar to that of the medication glybenclamide [11].

Quercetin dramatically reduced the increased insulin levels, dyslipidemia, and serum blood glucose levels in diabetic mice [12].

In comparison to the negative control group, the vanilla therapy significantly reduced serum glucose and lipid levels and raised insulin levels. In comparison to the negative control group, the vanillin-treated group had higher insulin sensitivity [13].

#### ***Molecular docking results of different isolated compounds***

Four distinct proteins connected to glucose metabolism, transport, and utilisation were docked with beta-amyrin palmitate, hyperoside, isoquercetin, vanillin, and 2-hydroxy-4-methoxy benzaldehyde. In order to assess the fitness ratings for the docking of tested compounds with the targeted proteins, this was done. Tables 1, 2, 3 & 4 detail the docking analysis findings, while Figures 1, 2, 3 & 4 display the docking figure. Among all the compounds,  $\beta$ -amyrin palmitate showed well docking score against 1PPI, 1X70, 1V4S and 5VEX respectively.

The region at which a mammalian alpha-amylase is active, Acarbose, a pseudo tetrasaccharide alpha-amylase inhibitor, was used to soak pancreatic alpha-amylase (EC 3.2.1.1), and the X-ray structural analysis revealed an electron density that corresponded to five fully conquered subsites in the active site [PDB ID: 1PPI] [16]. In diabetes people, alpha-amylase breaks down the carbohydrate and

*In-silico* screening of compounds from *Hemidesmus indicus* and their antidiabetic potential



raises postprandial glucose levels. The inhibition of alpha- amylase enzyme can decrease the post prandial increase of blood glucose that's why it is the potential target for the management of type 2 diabetes.

Table.1 Docking results of  $\beta$  -amyrin palmitate, hyperoside, isoquercetin, vanillin, and 2-hydroxy-4-methoxy benzaldehyde with PDB ID: 1PPI

Compounds Name	Docking Energy	Figure No.
$\beta$ -amyrin palmitate	-6.50	1(a)
2-hydroxy-4-methoxy-benzaldehyde	-4.73	1(b)
Hyperoside	-5.93	1(c)
Isoquercetin	-4.43	1(d)
Vanillin	-4.43	1(e)

Two hydrogen bond interactions occur between beta-amyrin palmitate with amino acid ASP381 having bond lengths of 2.775 Å & 2.802 Å (Fig No: 1a). Two hydrogen bond interactions occur between 2-hydroxy-4-methoxy-benzaldehyde with two amino acid GLY304 & ASP353, having bond lengths 2.111 Å & 2.106 Å respectively (Fig No: 1b). Three hydrogen bond interactions occur between Hyperoside with amino acid PHE315 and bond length are 2.226 Å, 1.415 Å, 1.413 Å (Fig No: 1c). Three hydrogen bond interaction occur between Isoquercetin with three amino acid MET178, LYS186, LEU69 and bond length are 1.964 Å, 1.902 Å, 2.103 Å respectively (Fig No: 1d). Three hydrogen bond interactions occur between Vanillin with three amino acid VAL467, GLN476, SER478 having bond lengths 2.022 Å, 2.105 Å, 2.188 Å (Fig No: 1e).

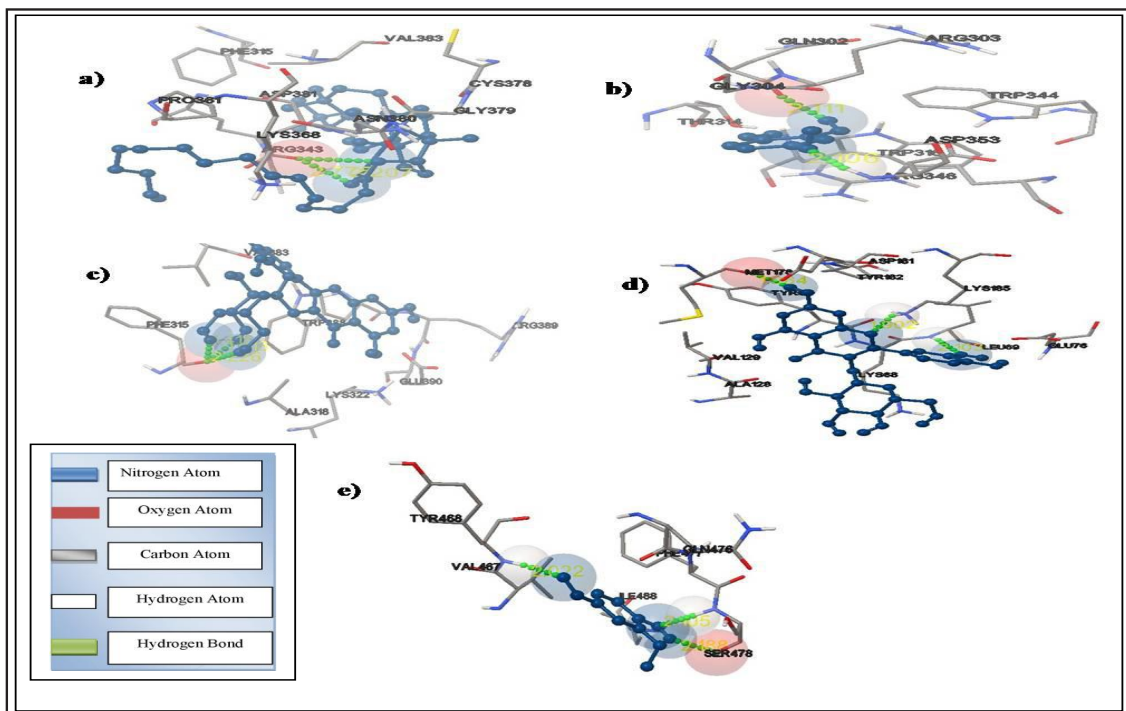


Figure 1: 1(a) Interaction between 1PPI with  $\beta$ -amyrin palmitate, 1(b) Interaction between 1PPI with 2-hydroxy-4-methoxy-benzaldehyde, 1(c) Interaction between 1PPI with hyperoside, 1(d) Interaction between 1PPI with Isoquercetin, 1(e) Interaction between 1PPI with Vanillin

Beta Amino Acid Inhibitor Complexed With Human Dipeptidyl Peptidase IV (DPP-4) [PDB ID: 1X70] [17]. An enzyme called DPP4 degrades the incretin hormone. Incretins assist the body in producing more insulin only when necessary and lower blood glucose levels. By blocking DPP-4, incretin hormone becomes inactive, which in response produces more insulin so it's a potential target for the management of type 2 diabetes.

Table No-2 Docking results of  $\beta$ -amyrin palmitate, hyperoside, isoquercetin, vanillin, and 2-hydroxy-4-methoxy benzaldehyde with PDB ID: 1X70

Compound Name	Docking Energy	Figure No.
715 (Internal Ligand)	-7.98	2(a)
$\beta$ -amyrin palmitate	-6.37	2(b)
2-hydroxy-4-methoxy-benzaldehyde	-3.20	2(c)
Hyperoside	-3.71	2(d)
Isoquercetin	-1.79	2(e)
Vanillin	-2.99	2(f)

Internal ligand 715 co-crystallized with Human Dipeptidyl Peptidase IV (PDB ID: 1X70) was re-docked and dock score was -7.98. One hydrogen bond interaction occurs between 715 amino acid GLU205 having a bond length of 2.725 Å (Fig No: 2a).

One hydrogen bond interaction occurs between beta-amyrin palmitate with amino acid ALA593 having bond length of 2.687 Å (Fig No: 2b). Three hydrogen bond interactions occur between 2-hydroxy-4-methoxy-benzaldehyde with three amino acid ARG611, GLU364, ARG581 bond length are 2.125 Å, 1.855 Å, 1.994 Å respectively (Fig No: 2c). Three hydrogen bond interactions occur between Hyperoside with amino acid MET638, ARG691, GLY599 having the bond lengths 2.379 Å, 2.199 Å, 2.061 Å (Fig No: 2d). Three hydrogen bond interactions occur between Isoquercetin with three amino acid GLN718, ASP725, GLU693 the bond lengths being 2.149 Å, 1.639 Å, 1.761 Å respectively (Fig No: 2e). One hydrogen bond interaction occurs between Vanillin with amino acid LYS721 having a bond length of 2.111 Å (Fig No: 2f).

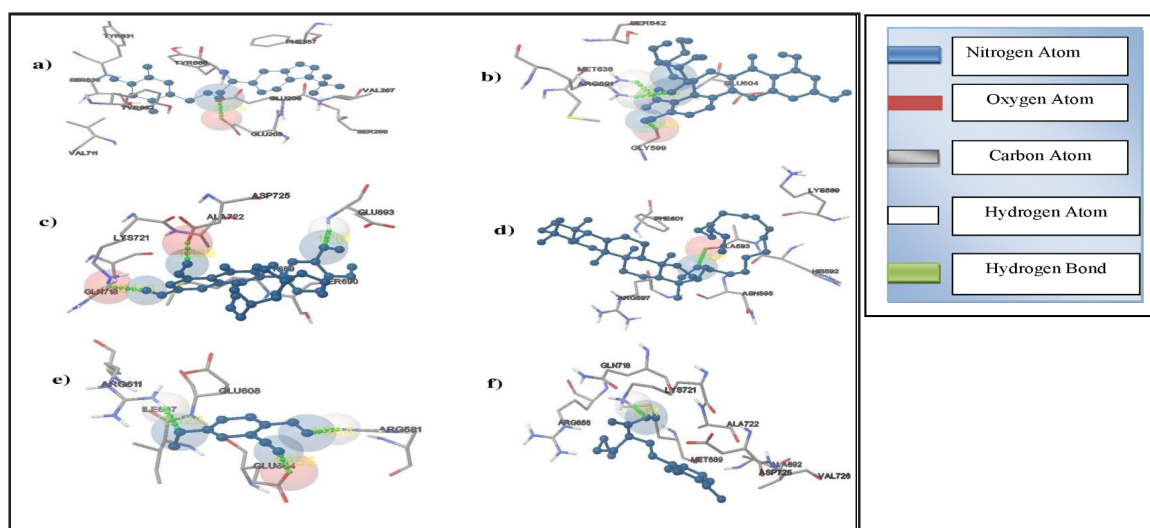


Figure 2: 2(a) Interaction between 1X70 with 715, 2(b) Interaction between 1X70 with  $\beta$ -amyrin palmitate, 2(c) Interaction between 1X70 with with 2-hydroxy-4-methoxy-benzaldehyde, 2(d) Interaction between 1X70 with Hyperoside, 2(e) Interaction between 1X70 with Isoquercetin, 2(f) Interaction between 1X70 with Vanillin

*In-silico* screening of compounds from *Hemidesmus indicus* and their antidiabetic potential

It is a Crystal structure of human glucokinase [PDB ID: 1V4S]. A gene called glucokinase is crucial in determining how high the body's blood glucose levels are. The pancreas uses it as a "glucose sensor" so that when blood sugar levels rise, so does the amount of insulin produced. The crystal structures of active and inactive glucokinase show that glucose binding causes extensive conformational changes, including domain restructuring. This discovery offered the mechanistic underpinnings for glucokinase activation as a potential treatment for the management of type 2 diabetes [18].

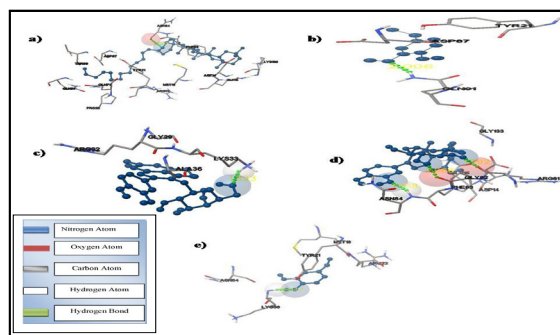
One hydrogen bond interaction occurs

Table 3 Docking results of  $\beta$ -amyrin palmitate, hyperoside, isoquercetin, vanillin, and 2-hydroxy-4-methoxy benzaldehyde with PDB ID: 1V4S

Compounds Name	Docking Energy	Figure No.
$\beta$ -amyrin palmitate	-7.69	3(a)
2-hydroxy-4-methoxy-benzaldehyde	-3.06	3(b)
Hyperoside	-0.64	3(c)
Isoquercetin	-1.98	3(d)
Vanillin	-3.72	3(e)

between beta-amyrin palmitate with amino acid ASN64 having a bond length of 2.863 Å (Fig No: 3a). One hydrogen bond interaction occurs between 2-hydroxy-4-methoxy-benzaldehyde with two amino acid GLN91, with a bond length of 2.006 Å (Fig No: 3b). One hydrogen bond interaction occurs between Hyperoside with amino acid LYS33 and bond length is 1.833 Å (Fig No: 3c). Three hydrogen bond interactions occur between Isoquercetin with three amino acid ASN84, PHE83, GLY82 having bond lengths of 1.958 Å, 2.066 Å, 1.792 Å respectively (Fig No: 3d). One hydrogen bond interaction occurs between Vanillin with amino acid LYS86 having a bond length of 2.947 Å (Fig No: 3e).

Figure 3: 3(a) Interaction between 1V4S with



$\beta$ -amyrin palmitate, 3(b) Interaction between 1V4S with 2-hydroxy-4-methoxy-benzaldehyde, 3(c) Interaction between 1V4S with hyperoside, 3(d) Interaction between 1V4S with Isoquercetin, 3(e) Interaction between 1V4S with Vanillin

It is a structure of the NNC0640 containing human GLP-1 receptor complex [PDB ID: 5VEX]. The glucagon like peptide 1 receptor (GLP 1R), a member of the secretin-like class B family of G-protein-coupled receptors (GP-CRs), and the glucagon receptor (GC-GR), play opposite physiological functions in insulin release and glucose homeostasis. In a glucose-dependent manner, the inhibition of glucagon secretion and promotion of insulin secretion are essential components in the management of type 2 diabetes [19].

Internal ligand 97v co- Table 4 Docking results of  $\beta$ -amyrin palmitate, hyperoside, isoquercetin, vanillin, and 2-hydroxy-4-methoxy benzaldehyde with PDB ID: 5VEX

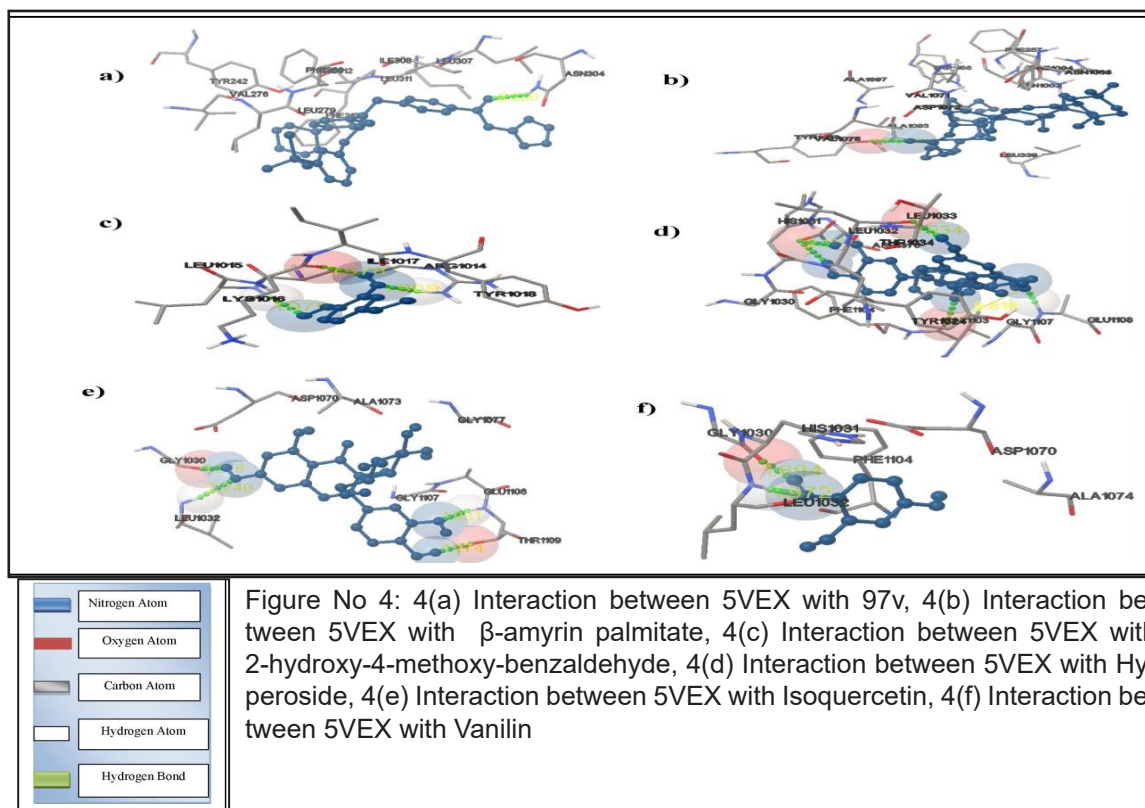
Compound Name	Docking Energy	Figure No.
97v (Internal Ligand)	9.00	4(a)
$\beta$ -amyrin palmitate	-8.14	4(b)
2-hydroxy-4-methoxy-benzaldehyde	-4.37	4(c)
Hyperoside	-4.88	4(d)
Isoquercetin	-5.42	4(e)
Vanillin	-4.43	4(f)

crystallized with human GLP-1 receptor (PDB ID: 5VEX) was re-docked and dock score was -9.00. One hydrogen bond interaction occurs

between 97v with amino acid ASN304 having a bond length of 2.290 Å (Fig No: 4a).

One hydrogen bond interaction occurs between beta-amyrin palmitate with amino acid TYR1088 having a bond length of 2.983 Å (Fig No: 4b). Three hydrogen bond interactions occur between 2-hydroxy-4-methoxy-benzaldehyde with three amino acid ARG1014, LYS1016, LEU1015 having bond lengths 1.969 Å, 1.978 Å, 1.975 Å respectively (Fig No: 4c). Three hydrogen bond interactions occur between Hyperoside with

three amino acid GLY1107, LEU1032, HIS1031 having bond lengths of 2.816 Å, 1.934 Å, 2.199 Å respectively (Fig No: 4d). Four hydrogen bond interactions occur between Isoquercetin with three amino acid GLY1030, LEU1032, GLU1108, THR1109 having the bond lengths 1.978 Å, 2.240 Å, 1.931 Å, 1.974 Å respectively (Fig No: 4e). Two hydrogen bond interactions occur between Vanillin with two amino acid GLY1030, LEU1032 respectively having bond lengths of 1.694 Å, 1.972 Å (Fig No: 4f).



All around the world, including India, diabetes mellitus is regarded as a serious public health issue. Vascular dysfunction is a result of the metabolic abnormalities that distinguish diabetes, including hyperglycemia, an increase in free fatty acids, and insulin resistance. Ayurveda and herbal remedies are significant alternative treatments that use extracts from many medicinal plants. The evaluation of anti-

diabetic activity of isolated compounds from *Hemidesmus indicus* is the focus of this study. The mechanism underlying the extract's ability to treat diabetes was anticipated by an *in-silico* analysis. We can characterize how small compounds behave at the binding site of target proteins and shed light on basic biological processes by using the molecular docking approach to describe the interaction between a

*In-silico* screening of compounds from *Hemidesmus indicus* and their antidiabetic potential



small molecule and protein at the atomic level. It aids in locating the enzyme's agonists and antagonists. A common technique in logical drug design is docking. A molecular level analysis is required to provide more scientific evidence and a more comprehensive explanation. Docking studies by Autodock 4.2.6 showed that Beta-amyryn palmitate of *Hemidesmus indicus* had the lowest docking score respectively against different antidiabetic protein. Because a compound's potency increases with decreasing docking score, Beta-amyryn palmitate from *Hemidesmus indicus* was found to have a considerable docking score.

### Conclusion

Beta-amyryn palmitate outperformed all other chemicals in terms of docking with different antidiabetic protein. Beta-amyryn palmitate, which had the best value in molecular docking. The above study revealed that Beta-amyryn palmitate was found to be most potent antidiabetic agent according to the *in-silico* study. This Beta-amyryn palmitate was also identified as an antidiabetic agent through *in-vitro* study, from this we can conclude that a *in-vitro* and *in-vivo* correlation can be establish for this compound.

### References

1. Das, M., Banerjii, A., Dutta, S., Saha, S., Mondal, D., & Hazra, J. (2017). Phyto-Pharmacognostical Evaluation And HPTLC Study On Anantamul (*Hemidesmus Indicus* R.Br.) Root. *International Journal of Research in Ayurveda & Pharmacy*, 8(3): 68–72.
2. Joshi, A., Lad, H., Sharma, H., & Bhatnagar, D. (2018). Evaluation of phytochemical composition and antioxidative, hypoglycaemic and hypolipidaemic properties of methanolic extract of *Hemidesmus indicus* roots in streptozotocin-induced diabetic mice. *Clinical Phytoscience*, 4: 1-9.
3. Kawlni, L., Bora, M., Upadhyay, S. N., Mukherjee, K., & Hazra, J. (2017). Pharmacological and therapeutic profile of anantamula (*Hemidesmus indicus* (L.) R. Br.): a comprehensive review. *International Journal of Ayurveda and Pharma Research*, 5(11): 49-57.
4. Fiori, J., Leoni, A., Fimognari, C., Turrini, E., Hrelia, P., Mandrone, M., ... & Gotti, R. (2014). Determination of phytomarkers in pharmaceutical preparations of *Hemidesmus indicus* roots by micellar electrokinetic chromatography and high-performance liquid chromatography–mass spectrometry. *Analytical Letters*, 47(16): 2629-2642.
5. Singab, A. N., Youssef, F. S., & Ashour, M. L. (2014). Medicinal plants with potential antidiabetic activity and their assessment. *Med Aromat Plants*, 3(151): 2167-0412.
6. Shaw, J. E., Sicree, R. A., & Zimmet, P. Z. (2010). Global estimates of the prevalence of diabetes for 2010 and 2030. *Diabetes research and clinical practice*, 87(1): 4-14.
7. Parveen, S., Ansari, M. H. R., Parveen, R., Khan, W., Ahmad, S., & Husain, S. A. (2019). Chromatography based metabolomics and in silico screening of *Gymnema sylvestre* leaf extract for its antidiabetic potential. *Evidence-Based Complementary and Alternative Medicine*, 2019(7523159): 1-14.
8. Mazumder, A., & Das, S. (2016). Study of oral hypoglycemic activity of rhizomes of *Hemidesmus indicus* R. BR. in albino wistar rats. *International Journal of Pharmaceutical Sciences and Research*, 7(11): 4602-4607.
9. Nair, S. A., Sabulal, B., Radhika, J., Arunkumar, R., & Subramoniam, A. (2014).



- Promising anti-diabetes mellitus activity in rats of  $\beta$ -amyrin palmitate isolated from *Hemidesmus indicus* roots. *European journal of pharmacology*, 734: 77-82.
10. Kannabiran, K., & Gayathri, M. (2009). Effect of 2-hydroxy-4-methoxy benzoic acid from the roots of *Hemidesmus indicus* on streptozotocin-induced diabetic rats. *Indian Journal of Pharmaceutical Sciences*, 71(5): 581.
  11. Verma, N., Amresh, G., Sahu, P. K., Mishra, N., Rao, C. V., & Singh, A. P. (2013). Pharmacological evaluation of hyperin for antihyperglycemic activity and effect on lipid profile in diabetic rats. *Indian J Exp Biol*, 51: 65-72.
  12. Yang, D. K., & Kang, H. S. (2018). Anti-diabetic effect of cotreatment with quercetin and resveratrol in streptozotocin-induced diabetic rats. *Biomolecules & Therapeutics*, 26(2): 130.
  13. Lu, G., Luo, X., Liu, Z., Yang, L., Lin, C., & Xu, M. (2019). Protective effect of vanillin in streptozotocin-induced diabetes in neonatal rats via attenuation of oxidative stress and inflammation. *Tropical journal of pharmaceutical research*, 18(2): 349-355.
  14. Guedes, I. A., de Magalhães, C. S., & Dardenne, L. E. (2014). Receptor–ligand molecular docking. *Biophysical reviews*, 6(1):75-87.
  15. Paul, A. (2016). Anticancer potential of isolated phytochemicals from *Ocimum sanctum* against breast cancer: In silico Molecular docking approach. In *National Conference on “Biochemistry and Molecular Biology for Life Sciences” At: University of Dhaka*.
  16. Qian, M., Haser, R., Buisson, G., Duee, E., & Payan, F. (1994). The Active Center of a Mammalian.  $\alpha$ -Amylase. Structure of the Complex of a Pancreatic.  $\alpha$ -Amylase with a Carbohydrate Inhibitor Refined to 2.2- $\text{\AA}$ . Resolution. *Biochemistry*, 33(20): 6284-6294.
  17. Kim, D., Wang, L., Beconi, M., Eiermann, G. J., Fisher, M. H., He, H., ... & Weber, A. E. (2005). (2R)-4-Oxo-4-[3-(trifluoromethyl)-5,6-dihydro [1,2,4] triazolo [4,3-a] pyrazin-7(8H)-yl]-1-(2,4,5-trifluorophenyl) butan-2-amine: a potent, orally active dipeptidyl peptidase IV inhibitor for the treatment of type 2 diabetes. *Journal of medicinal chemistry*, 48(1): 141-151.
  18. Kamata, K., Mitsuya, M., Nishimura, T., Eiki, J. I., & Nagata, Y. (2004). Structural basis for allosteric regulation of the monomeric allosteric enzyme human glucokinase. *Structure*, 12(3): 429-438.
  19. Song, G., Yang, D., Wang, Y., de Graaf, C., Zhou, Q., Jiang, S., ... & Stevens, R. C. (2017). Human GLP-1 receptor transmembrane domain structure in complex with allosteric modulators. *Nature*, 546(7657): 312-315.

#### Abbreviations

- PDB: Protein Data Bank  
 DM: Diabetes mellitus  
 WHO: World Health Organization  
 OG-TT: Oral glucose tolerance test  
 QE: Quercetin  
 STZ: Streptozotocin  
 ADP: Autodock Program  
 Å : Angstrom  
 GP-CRs: G-protein coupled receptors  
 GLP-1R: Glucagon like peptide-1 receptor  
 GC-GR: Glucagon-receptor

*In-silico* screening of compounds from *Hemidesmus indicus* and their antidiabetic potential

# Synthesis, Characterization and Antimicrobial Studies of Gabapentin Schiff Base Metal Complexes Containing Heterocyclic Ligand via Microwave-Assisted Method

Jyoti C Ajbani<sup>1</sup>, D Smita Revankar<sup>1</sup>, M. Revanasiddappa<sup>1\*</sup>,  
Suresh Babu Naidu Krishna<sup>2</sup>, S Shankara<sup>3</sup>

<sup>1</sup>Department of Engineering Chemistry, PESIT, Bangalore South campus, Bangalore, Karnataka, India, 560 100

<sup>2</sup>Department of Biomedical and Clinical Technology, Durban University of Technology, Durban, South Africa – 4000

<sup>3</sup>Department of Microbiology, Government Science College, Nrupathunga University, Bangalore, Karnataka

Corresponding author: revanasiddappam@pes.edu

## Abstract

The use of microwave-assisted synthesis in the formation of coordination metal complexes has led to improved control of waste generation and reduced reaction times. In the present study, new Schiff base metal complexes of various metals, including ZrO (II), VO(II), Cr (III), Mn (II), Fe (II), Co (II), Ni (II), Cu (II), Zn (II), Cd (II), and Hg (II), were synthesized using microwave radiation. To characterize the synthesized metal complexes, several physical methods were used, including elemental analysis, FT-IR, molar conductance, electronic spectra, <sup>1</sup>H-NMR, ESR, magnetic susceptibility, thermal, electrical conductivity, and XRD analysis. Elemental analysis revealed that the complexes were of the 1:1, 1:2, and 1:3 (M: L) types. The observed molar conductance values indicated that the complexes were non-electrolytes. The <sup>1</sup>H-NMR spectral data suggested that the phenolic protons had been displaced during complexation. Thermo gravimetric analysis showed the presence of water molecules in the coordination metal complexes and confirmed the loss of water molecules in the first step, followed by the decomposition of the ligand in the subsequent step. The synthesized ligand and coordination metal complexes were also studied for their antibacterial and antifungal activity. They

were tested against various bacteria and fungi, including *Escherichia coli*, *Salmonella enteric*, *klebsiella pneumoniae*, *Staphylococcus aureus*, *Streptococcus agalactiae*, *Aspergillus niger*, and *Aspergillus flavus*. The results indicated that some of the metal complexes showed significant antibacterial and antifungal activity. Overall, the use of microwave-assisted synthesis in the formation of coordination metal complexes has led to the synthesis of new metal complexes with potential antibacterial and antifungal activity. The various physical methods used for characterization have provided valuable insights into the properties and behaviour of these metal complexes.

**Keywords:** Microwave method; Heterocyclic ligand; Thermal study.

## Introduction

Extensive studies have been conducted on Schiff bases derived from amide and aldehyde, which are an important class of ligands that coordinate with metal ions through azomethine nitrogen [1-4]. These complexes play a pivotal role in the development of coordination chemistry [5-8]. Gabapentin derivatives have been found to have numerous uses in medicinal and pharmaceutical fields [9-11]. The compounds were evaluated for their anticonvulsant and

antioxidant activities using the Maximal Electroshock Seizure (MES) test. The majority of the compounds showed activity in the MES tests.

Schiff bases have also found applications in analytical chemistry where some compounds were used as a ligand to prepare complexes and catalysts and as a corrosion inhibitor in the chemical industry [12]. Microwave irradiation has gained popularity as it accelerates the reaction rate in a solvent-free condition without the use of supporting reagents, making it eco-friendly. Chemical transformations that took hours or even days to complete the reaction can be completed in minutes with microwave irradiation. Microwave irradiation offers numerous benefits, including higher yields, shorter reaction times, and eco-friendly and simple reaction conditions [13-17]. Therefore, the aim of this work is to synthesize and characterize new transition metal complexes of Schiff bases derived from Gabapentin with aldehydes using microwave-assisted synthesis and to screen their antibacterial activity

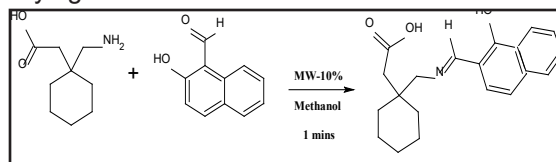
### Materials and Methods

All reagents used were of analytical grade. Metal chlorides were procured from Sigma Aldrich, India and used as received. The drug molecules were purchased from Apotex Pharma Chem India Ltd. All solvents were distilled prior to use.

### Synthesis of schiff base ligand gabapantin - 2-hydroxy naphthaldehyde

The Synthesis of Schiff base ligand Gabapantin - 2-hydroxy naphthaldehyde as shown in the figure 1. Gabapentin (0.03M, 0.51g) was added to a dry and clean round bottom flask and dissolved in 5-7ml of methanol. To this, 2-hydroxy naphthaldehyde (0.03M, 0.54g) was added. The mixture was placed in a round bottom flask and capped with a water condenser before being subjected to microwave irradiation at 10% intensity (110 watts) for 1 minute with a pulse of 30 seconds. The progress of the reaction was monitored using TLC. Once the reaction was complete, the mixture was cooled to room tem-

perature. The Schiff base was then separated, filtered using Whatman filter paper, washed with hot methanol, and kept for re-crystallization. The resulting yellow crystals were separated by drying and stored in a desiccator.

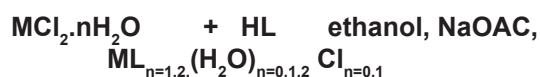


Gabapentin 2-hydroxynaphthaldehyde Schiff base ligand

**Figure- 1** Scheme for synthesis of Schiff base ligand (HL)  $C_{16}H_{11}O_3N_2F_3S$  [RO]: Mol. wt. 368.247, m.p. 108-1100C, yield 89.58%

### Synthesis of metal complexes

Metal complexes were synthesized by irradiating equimolar ratio of hydrated metal chlorides and ligand in ethanol (1-2ml) as a solvent with a pinch of sodium acetate was added to initiate the precipitation. Solid was separated out, filtered and washed with distilled water, recrystallized from ethyl alcohol. All complexes were dried in air and kept over anhydrous calcium chloride in the desiccator. Formation of the complexes may be represented as follows:



**Metal salt      Ligand      30% intensity**  
**Metal complex 8-10 minutes in MW**

Where, M=Cu (II), Co (II), Ni (II), Mn(II), Fe(III), Zn(II), Hg(II), Cd(II), Cr(III), ZrO(II), VO(II).

### Physical measurements

Inductively Coupled Plasma-Optical Emission Spectrometer, Perkin Elmer-Optima7000DV: This technique is used for the quantitative determination of metals in a sample by measuring the intensity of emitted light from the excited atoms. It provides information about the elemental composition of the complex. SEM-EDX analysis, the complexes were analysed using a Carl Zeiss EVO-18 model SEM coupled with an EDX detector. SEM provides

Synthesis, characterization and antimicrobial studies of gabapentin schiff base metal complexes

high-resolution images of the sample surface, while EDX determines the elemental composition of the complex by analyzing characteristic X-rays emitted from the sample. Microanalytical analysis of the complexes for carbon, hydrogen, and nitrogen (CHN) as well as sulfur (S) content was carried out using an Elementar Vario EL III model instrument. This technique provides information about the organic constituents present in the complexes. The chloride content in the complexes was determined using the argentometric method. This method involves the titration of chloride ions with silver nitrate, and the end point is detected using a silver indicator. The magnetic susceptibility of the complexes was measured at room temperature using a Gouy balance. The calibrant used was  $\text{Hg}[\text{Co}(\text{NCS})_4]$ , and diamagnetic corrections were made using PASCAL's constants. Conductance measurements of the complexes were carried out using an Elico Conductivity bridge. The measurements were performed in DMSO (dimethyl sulfoxide) using a dip-type conductivity cell fitted with platinum electrodes. The conductance value provides information about the ionic behaviour of the complexes. The infrared spectra of the ligands and their complexes were recorded using a Thermo Nicolet Avatar 370 FT-IR spectrophotometer. The spectra were obtained by analyzing the absorption of infrared radiation by the sample in the 4000 to 400  $\text{cm}^{-1}$  range. KBr discs were used as the sample matrix. The nuclear magnetic resonance spectra of the complexes were recorded in DMSO- $d_6$  solvent on a Varian AS 400 MHz spectrophotometer. TMS (tetramethylsilane) was used as the internal standard for chemical shift referencing. The electronic spectra of the complexes were recorded using an Elico-SL-164 double beam UV-visible spectrophotometer. The measurements were performed in DMSO solution at a concentration of  $10^{-3}$  M, and the range of analysis was 200 to 1100 nm. Powder X-ray diffraction analysis of the complexes was carried out using a Bruker AXS D8 Advance instrument. The X-ray source used was Cu with a wavelength of 1.5406 Å. This technique provides in-

formation about the crystal structure and phase composition of the complexes. These analytical techniques were employed to characterize and determine the metal content, elemental composition, structural properties, and spectroscopic features of the complexes under investigation.

### **Antimicrobial activities**

The in-vitro antimicrobial activity of the Schiff bases and their complexes was tested against *Escherichia coli*, *Salmonella enteric*, *Klebsiella pneumoniae*, *Staphylococcus aureus*, *Streptococcus agalactiae*, *Aspergillus niger*, and *Aspergillus flavus* using the well diffusion method. Muller Hinton agar (MHA) and Potato dextrose agar (PDA) were used as the culture media, and streptomycin and fluconazole were used as control drugs. All complexes were dissolved in DMSO, and separate solutions with a concentration of 100 ppm were prepared.

For the bacterial assay, wells were made on MHA plates inoculated with bacteria. Each well was filled with 100  $\mu\text{l}$  of the test solutions. The bacterial plates were then incubated at 37°C overnight, and the zone of growth inhibition was measured in millimetres. For the fungal assay, wells were made on PDA plates inoculated with fungi. Again, 100  $\mu\text{l}$  of the test solutions were added to each well. The fungal plates were incubated at 27°C for 24-48 hours, and the zone of growth inhibition was measured in millimetres. These measurements were conducted following the referenced sources [18-20].

## **Results and Discussion**

### **Electronic spectral studies and magnetic properties**

The melting points and elemental analyses of both the ligand and its metal complexes are presented in Table 1. It is noteworthy that the calculated values closely matched the experimental values, indicating a high level of agreement between the two sets of data. This suggests that the calculations were reliable and accurate. In the case of microwave-assisted synthesis, it was observed that the reaction could be completed within a shorter timeframe



compared to the conventional method. Additionally, higher yields were obtained using the microwave-assisted approach. These observations highlight the efficiency and effectiveness of microwave irradiation as a method for synthesizing the ligand and its metal complexes. Through the analysis of spectral and analytical data, it was determined that all the metal complexes exhibited a 1:2 (metal: ligand) stoichiometry, except for the Zn (II), Cd (II), and Hg (II) complexes, which displayed a 1:1 (metal:ligand) stoichiometry. This difference in stoichiometry suggests distinct coordination modes or binding

patterns for these specific metal ions. The molar conductance values of the complexes dissolved in dimethylformamide (DMF) were found to range from 4.69 to 16.5  $\text{ohm}^{-1}\text{mole}^{-1}\text{cm}^2$ . These values indicate relatively low molar conductivities, implying that the complexes do not exhibit significant electrolytic behaviour in solution. Therefore, the experimental observations and data discussed provide valuable insights into the properties and characteristics of both the ligand and its metal complexes, shedding light on their structural features and behaviour.

Table 1- Analytical data of ligand and its metal complexes

Ligand/ complexes	Analysis (%), Found (calculated)						Color	Formula weight	% Yield	Melting Point (°C)	Meff (BM)	Molar Conductance $\Omega^{-1}\text{cm}^2\text{Mol}^{-2}$
	C	H	O	N	Cl	M						
Ligand( $\text{H}_2\text{L}^4$ )	73.36 (73.82)	6.95 (7.12)	14.25 (14.75)	4.22 (4.33)	-----	-----	Yellow	325.394	94.58	230	-----	3.21
[Cr( $\text{L}^4$ ) <sub>2</sub> ( $\text{H}_2\text{O}$ ) Cl]	59.98 (59.47)	5.66 (5.99)	15.47 (15.85)	3.7 (3.47)	8.55 (8.79)	12.32 (12.87)	Green	807.772	96.82	>310(NM)	3.75	5.12
[Fe( $\text{L}^4$ ) <sub>2</sub> ( $\text{H}_2\text{O}$ ) Cl]	59.33 (59.19)	5.64 (5.96)	15.27 (15.77)	3.87 (3.45)	8.95 (8.75)	13.36 (13.76)	Brown	811.621	97.2	>192(D)	5.88	21.7
[Co <sub>2</sub> ( $\text{L}^4$ ) <sub>2</sub> ( $\text{H}_2\text{O}$ ) <sub>2</sub> ]	59.49 (59.85)	6.87 (6.03)	15.28 (15.94)	3.72 (3.49)	-----	7.28 (7.34)	Light brown	802.632	75.9	>200(D)	4.18	6.23
[Cu <sub>2</sub> ( $\text{L}^4$ ) <sub>2</sub> ( $\text{H}_2\text{O}$ ) <sub>2</sub> ]	59.89 (59.17)	5.87 (5.96)	15.30 (15.76)	3.04 (3.45)	-----	15.02 (15.65)	Pale Green	811.872	96.16	>250(NM)	1.58	4.98
[Mn <sub>2</sub> ( $\text{L}^4$ ) <sub>2</sub> ( $\text{H}_2\text{O}$ ) <sub>2</sub> ]	60.68 (60.45)	6.54 (6.09)	16.61 (16.11)	3.45 (3.52)	-----	6.98 (6.91)	Yellow	794.652	94.8	216	5.4	3.49
[Ni <sub>2</sub> ( $\text{L}^4$ ) <sub>2</sub> ( $\text{H}_2\text{O}$ ) <sub>2</sub> ]	59.47 (59.89)	6.77 (6.03)	16.02 (15.95)	3.43 (3.49)	-----	7.56 (7.31)	Yellow green	802.152	92.5	>240(D)	2.67	4.45
[Zn( $\text{L}^4$ ) <sub>2</sub> ( $\text{H}_2\text{O}$ ) <sub>2</sub> ]	59.04 (58.90)	5.37 (5.93)	15.21 (15.69)	6.61 (6.87)	-----	16.61 (16.03)	Pale yellow	407.796	87.14	192	Dia	5.79
[Cd( $\text{L}^4$ ) <sub>2</sub> ( $\text{H}_2\text{O}$ ) <sub>2</sub> ]	52.54 (52.81)	5.58 (5.32)	14.24 (14.07)	3.24 (3.08)	-----	24.31 (24.71)	Pale yellow	454.796	88.57	230(D)	Dia	12.24
[Hg( $\text{L}^4$ ) <sub>2</sub> ( $\text{H}_2\text{O}$ ) <sub>2</sub> ]	44.87 (44.23)	4.94 (4.45)	11.27 (11.79)	2.15 (2.58)	-----	36.22 (36.94)	Yellow	542.976	81.5	226	Dia	4.19
[ZrO( $\text{L}^4$ ) <sub>2</sub> ( $\text{H}_2\text{O}$ ) <sub>2</sub> ]	53.84 (53.42)	5.03 (5.38)	10.25 (10.68)	3.45 (3.12)	-----	20.01 (20.29)	Yellow	449.606	97.4	212	Dia	11.16
[VO( $\text{L}^4$ ) <sub>2</sub> ( $\text{H}_2\text{O}$ ) <sub>2</sub> ]	58.93 (58.68)	5.53 (5.91)	11.42 (11.73)	3.99 (3.42)	-----	12.99 (12.44)	Dirty green	409.326	78.6	>200(D)	1.8	12.54

The magnetic moments of the metal complexes are listed in Table 1. The Fe-complex exhibited a magnetic moment of 5.88 BM (Bohr magneton) with 5 unpaired electrons. This magnetic susceptibility value for Fe (II) is consistent with the reported values and indicates a coordination number of six, corresponding to an octahedral geometry. For the Co (II) complexes, the magnetic moments were found to be 4.18 BM, suggesting a high spin complex with octahedral geometry [21-22].

The Ni (II) complex exhibited a magnetic moment value of 2.67 BM, which is close to the expected value for octahedral complexes. This further supports the presence of an octahedral geometry for the Ni (II) complex. The Cu (II) complex displayed a magnetic moment value

of 1.58 BM, confirming the distorted octahedral geometry around the copper ion [23]. Electronic spectral studies were conducted using a DMSO solution ( $1 \times 10^{-3}\text{M}$ ) for the paramagnetic complexes. The EPR spectral data of all the paramagnetic complexes are presented in Table 2.

For the Ni (II) complex with a coordination number of 6, bands at  $14647.722\text{ cm}^{-1}$  and  $23474.18\text{ cm}^{-1}$  were observed, corresponding to  $3\text{A}_{2g}(\text{F}) \rightarrow 3\text{T}_{1g}(\text{F}) (\nu_2)$  and  $3\text{A}_{2g}(\text{F}) \rightarrow 3\text{T}_{1g}(\text{P})(\nu_3)$  transitions, respectively, in an octahedral environment. The band for the transition  $3\text{A}_{2g}(\text{F}) \rightarrow 3\text{T}_{2g}(\text{F}) (\nu_1)$  could not be observed due to limitations in the instrument. However, its value can be calculated using a band fitting procedure. Other studies have reported four absorption bands for the Ni (II) complex in the



range of 390, 664, 740 and 1132 nm in the solid state [24]. The Co (II) complex of H<sub>2</sub>L<sub>4</sub> exhibited two bands at 18903 cm<sup>-1</sup> and 22679 cm<sup>-1</sup>, which are assigned to the 4T<sub>1g</sub>(F)→4T<sub>2g</sub>(F) (v1), 4T<sub>1g</sub>(F)→4A<sub>2g</sub>(F) (v2), and 4T<sub>1g</sub>(F)→4T<sub>1g</sub>(P) (v3) transitions, respectively. The calculation of 4T<sub>1g</sub>(F)→4T<sub>2g</sub>(F) (v1) was performed using a band procedure, suggesting an octahedral geometry for the Co (II) complex [26].

In the Cu (II) complex of H<sub>2</sub>L<sub>4</sub>, a broad absorption band with low energy was observed at 15479.2 cm<sup>-1</sup>, indicating a d-d transition and suggesting a low C<sub>2v</sub> symmetry of the Cu<sup>2+</sup> ion. Another band around 27467.2 cm<sup>-1</sup> (364 nm) can be assigned to M→L charge transfer and π→π\* transition associated with the azomethine linkage. Other authors have also reported the region of 540-720 nm for oxo-bridged Cu (II) complexes. Considering all these observations, the presence of the band at 540 nm in the current copper (II) complex indicates a square pyramidal geometry [27]. The aforementioned experimental data provide valuable insights into the magnetic properties and coordination geometries of the metal complexes studied. The electronic spectrum of the Fe (III) complex of the H<sub>2</sub>L<sub>4</sub> ligand exhibited a charge transfer band

at 21798.84 cm<sup>-1</sup>, which was attributed to the (L-M) charge transfer. This strong charge transfer band makes it challenging to identify the d-d band. Therefore, a provisional octahedral geometry is suggested for the Ferric complex based on this observation. Similarly, the electronic spectrum of the Mn (II) complex displayed a band at 25532.35 cm<sup>-1</sup>, assigned to the charge transition (L→M). Another band at 19762.85 cm<sup>-1</sup> was attributed to the d-d transition. The identification of the d-d band is complicated due to the presence of a strong charge-transfer (CT) band that extends from the UV region to the visible region. Hence, a provisional octahedral geometry is predicted for the Mn (II) complex of the H<sub>2</sub>L<sub>4</sub> ligand. For the Cr(III) complex of the H<sub>2</sub>L<sub>4</sub> ligand, bands at 17498.55 cm<sup>-1</sup> and 24077.24 cm<sup>-1</sup> were observed. These bands can provisionally be assigned to the 4A<sub>g</sub>→4T<sub>2g</sub>(F) (v1) and 4A<sub>2g</sub>→4T<sub>1g</sub>(F) (v2) transitions, respectively, indicating an octahedral geometry [28].

Various ligand field parameters, including Dq, B', β, β%, and ligand field stabilization energy (LFSE), were calculated and are presented in Table 2. These parameters provide valuable information about the ligand field and the stability of the complexes.

Table 2: Electronic spectral data and ligand field parameters of the Co(II), Ni(II) and Cu (II) complexes in DMSO (10<sup>-3</sup>M) solution.

Metal complexes	Transitions in cm <sup>-1</sup>			10Dq (cm <sup>-1</sup> )	B(cm <sup>-1</sup> )	B	β%	ν <sub>2</sub> /ν <sub>1</sub>	LFSE kJ/mol
	ν <sub>1</sub>	ν <sub>2</sub>	ν <sub>3</sub>						
VOL <sub>2</sub> (H <sub>2</sub> O) <sub>2</sub>	11860.9	17106.6	22696.32	---	---	---	---	---	---
CrL <sub>2</sub> (H <sub>2</sub> O) <sub>2</sub>	17489	24077	---	17489	646.66	0.6278	37.22	1.3767	250.738
MnL <sub>2</sub> (H <sub>2</sub> O) <sub>2</sub>	25532.35 M-L Charge transfer								
NiL <sub>2</sub> (H <sub>2</sub> O) <sub>2</sub>	9254	14647	23474	9254	703.44	0.65133	34.867	1.5827	132.674
CuL <sub>2</sub> (H <sub>2</sub> O) <sub>2</sub>	---	15479.2	27467.2	---	---	---	---	---	---
FeL <sub>2</sub> (H <sub>2</sub> O) <sub>2</sub>	21798.84 M-L Charge transfer								

### <sup>1</sup>H NMR spectra

The proton NMR spectra of the H<sub>2</sub>L<sub>4</sub> ligand and its complexes were recorded in DMSO-d<sub>6</sub> solution using TMS as the internal stan-

dard. The <sup>1</sup>H-NMR spectra of the Zn (II) and Cd (II) diamagnetic complexes exhibited sharp signals. This can be attributed to the rapid nuclear spin-lattice and spin-spin relaxation caused

by the fluctuating magnetic field, which arises from the presence of unpaired electrons. The sharp resonance signals and the presence of spin-spin splitting confirmed the diamagnetic nature of these complexes. In the proton NMR spectrum of the ligand, a multiplet in the range of  $\delta$  7.41–7.75 ppm was observed, which can be attributed to the aromatic protons. The cyclohexane protons resonated in the region of  $\delta$  1.367–1.497 ppm, and two  $\text{CH}_2$  groups exhibited singlets at  $\delta$  2.258 and  $\delta$  3.706 ppm, respectively. The azomethine proton appeared as a singlet at  $\delta$  8.091 ppm. The phenolic and carboxylic OH groups showed broad signals at  $\delta$  12.29 ppm, which disappeared upon deuteration.

In the complexes, the azomethine proton resonated as a singlet at  $\delta$  8.057 ppm. This shift suggests the involvement of the azomethine nitrogen in coordination bonding. Additionally, the broad signals from the phenolic and carboxylic OH groups disappeared in the complexes, indicating the deprotonation and coordination of the oxygen atoms. Hence, the proton NMR spectra provide valuable information about the ligand and its complexes, confirming their diamagnetic nature and revealing the coordination bonding and deprotonation events.

### IR spectra

The infrared (IR) frequencies and their tentative assignments are summarized in Table-3. The IR spectra of the ligand and its metal complexes were recorded in the range of 4000–400  $\text{cm}^{-1}$ .

The  $\text{H}_2\text{L}_4$  ligand exhibited a band at 1689  $\text{cm}^{-1}$ , corresponding to the stretching frequency of the  $\nu\text{C}=\text{O}$  bond. In all metal complexes, this band was shifted to lower frequencies, ranging from 1640–1620  $\text{cm}^{-1}$ . This shift suggests the involvement of the oxygen atom from the hydroxyl group of the COOH moiety in bonding with the metal ions.

The azomethine vibration in the  $\text{H}_2\text{L}_4$  ligand appeared at 1638  $\text{cm}^{-1}$ . After complexation, this vibration shifted to lower frequencies and appeared at around 1589–1620  $\text{cm}^{-1}$  in all the complexes. This shift indicates the participation of the azomethine nitrogen in coordination to the metal ion. Table 3 provides a description of the IR stretching frequencies observed for the ligand and its metal complexes.

Table: 3IR stretching frequencies of ligand and its metal complexes

Compound	$\nu$ (C=N)	$\nu$ (C=O)	$\nu$ (C-O)	$\nu$ (C-O)	$\nu$ ( $\text{H}_2\text{O}$ )	$\nu$ (M-O)	$\nu$ (M-O)	$\nu$ (M-N)
$\text{H}_2\text{L}_4$	1638	1689	1259	1239	-----	-----	-----	-----
$[\text{Cr}(\text{L}^4)(\text{H}_2\text{O})_2\text{Cl}]$	1598	1621	1308	1242	835	672	537	450
$[\text{Fe}(\text{L}^4)(\text{H}_2\text{O})_2\text{Cl}]$	1589	1632	1308	1213	834	654	505	450
$[\text{Co}_2(\text{L}^4)_2(\text{H}_2\text{O})_2]$	1618	1637	1279	1240	855	648	501	456
$[\text{Cu}_2(\text{L}^4)_2(\text{H}_2\text{O})_2]$	1588	1621	1289	1242	836	655	493	459
$[\text{Mn}_2(\text{L}^4)(\text{H}_2\text{O})_2]$	1618	1643	1283	1250	833	646	508	455
$[\text{Ni}_2(\text{L}^4)(\text{H}_2\text{O})_2]$	1618	1635	1301	1250	826	647	529	455
$[\text{Zn}(\text{L}^4)(\text{H}_2\text{O})]$	1620	1632	1321	1261	833	692	507	456
$[\text{Cd}(\text{L}^4)(\text{H}_2\text{O})]$	1618	1640	1283	1250	859	646	508	455
$[\text{Hg}(\text{L}^4)(\text{H}_2\text{O})]$	1620	1641	1269	1249	831	646	507	455
$[\text{ZrO}(\text{L}^4)(\text{H}_2\text{O})]$	1585	1632	1321	1261	834	641	520	483
$[\text{VO}(\text{L}^4)(\text{H}_2\text{O})]$	1620	1645	1308	1255	828	651	502	478

### ESR spectra

Synthesis, characterization and antimicrobial studies of gabapentin schiff base metal complexes

The powdered samples of Cu (II) VO (II) and Cr (II) complexes were used to obtain X-band ESR spectra at room temperature.

### ESR spectrum of Cu (II) complex of $H_2L^4$

The g tensor values associated with this spectrum are provided in Table 4. These g tensor values confirm the  $C_{2v}$  symmetry of the  $Cu^{2+}$  ion, which is penta-coordinated. In the case of a Cu(II) complex with low symmetry, the fundamental state for the paramagnetic electron is described by a mixture of d functions. The degree of mixture increases as the symmetry of the complex decreases. The low symmetry is further supported by the high values of the g tensor. In geometries such as elongated octahedral, square pyramidal, or square planar, the ground state term is described by the  $dx_2-y_2$  orbital. This suggests that the electronic configuration of the Cu(II) complex with the  $H_2L^4$  ligand is consistent with one of these geometries. Therefore, the ESR spectrum and the g tensor values provide insights into the symmetry and electronic configuration of the Cu (II) complex, supporting the presence of low symmetry and a ground state term associated with the  $dx_2-y_2$  orbital.

$$g_{\parallel} = g_x = 2.0023 \pm \frac{8\lambda}{E(dx^2-y^2) - E(dxy)}$$

$$g_{\perp} = g_x = g_y = 2.0023 \pm \frac{2\lambda}{E(dx^2-y^2) - E(dxz)}$$

$$= 2.0023 \pm \frac{2\lambda}{E(dx^2-y^2) - E(dyz)}$$

where  $\lambda$  represents the coupling constant for the Cu (II) ion, and E represents the orbital energies. In these cases, the relation  $g_{\parallel} > g_{\perp} > 2.0023$  is expected, which corresponds to a normal spectrum. When the structure of the Cu (II) complex is trigonal bipyramidal or compressed octahedral, the ground state is described by the  $dz_2$  orbital. In such cases, the perpendicular and parallel components of the g

tensor can be described by the following equation:

$$g_{\perp} = 2.0023 + (\lambda / 3E)$$

$$g_{\parallel} = 2.0023 - (2\lambda / 3E)$$

Here,  $g_{\perp}$  represents the perpendicular component of the g tensor, and  $g_{\parallel}$  represents the parallel component of the g tensor. This equation provides a relationship between the coupling constant, orbital energies, and the g tensor components, allowing for the determination of the g tensor values in complexes with trigonal bipyramidal or compressed octahedral structures.

$$g_{\parallel} = g_e = 2.0023$$

$$g_{\perp} = g_x = g_y = 2.0023 \pm \frac{6\lambda}{E(dz^2) - E(dxz)}$$

$$= 2.0023 \pm \frac{6\lambda}{E(dz^2) - E(dxz)}$$

An ESR  $\{E(dz^2) - E(dxz)\}$  type is characterized by  $g_{\perp} > g_{\parallel} = 2.0023$ , indicating an inverse spectrum. In intermediate situations, a rhombic spectrum exhibiting three g values may be observed. For example, if the geometry of the complex is intermediate between square pyramidal and trigonal bipyramidal, the ground state is a linear combination of the  $dx_2-y_2$  and  $dz_2$  orbitals. In such cases, a parameter R can indicate the predominance of either the  $dz^2$  or  $dx_2-y_2$  orbital in the ground state.

$R = (g_y - g_z) / (g_x - g_y)$ , where  $g_x > g_y > g_z$ .

If R is greater than 1, the contribution to the ground state arises from the  $dz^2$  orbital. If R is less than 1, the contribution to the ground state arises from the  $dx_2-y_2$  orbital. The ESR spectrum of the Cu (II) complex  $Cu_2(L^4)_2(H_2O)_2$  shows  $g_{\perp} > g_{\parallel}$ . In such cases, two alternative geometries are conceivable, one approaching the limit of a square pyramidal structure and the other approaching a trigonal bipyramidal structure. ESR spectroscopy can distinguish between these two situations. The spectrum of the  $Cu_2(L^4)_2(H_2O)_2$  complex supports a trigonal bipyramidal geometry. It exhibits an axial symmetry with two g values ( $g_{\perp} > g_{\parallel}$ ,  $g_{\parallel} = 2.06835$ ,

$g_{\perp} = 2.16736$ ), and the  $g$  factor corresponding to the higher symmetry axis is practically coincident with  $g_e$ . This indicates that the electron is delocalized in the  $dz^2$  orbital of the Cu (II)

ground state, and the penta-coordinated system is strongly shifted towards the trigonal bipyramidal geometry.

Table: 4 ESR-spectral data of Cu (II) complex of  $H_2L^4$  ligand and bonding coefficient parameters.

Complex	$g_x$	$g_y$	$g_z$	R	Ground state	Geometry
$Cu_2(L^4)(H_2O)_2$	2.06835	2.06835	2.16736	$\infty$	$d_z^2$	Trigonal bipyramidal

### Thermal analysis

The thermogravimetric analysis (TGA) curve of the complex displays a disintegration pattern within the temperature range of 40-258°C. The thermogram reveals weight loss between 40-100°C, which can be attributed to the loss of five lattice  $H_2O$  molecules. The observed weight loss percentage is 9.715%, while the calculated weight loss percentage is 9.77%. The complex initiates weight loss at 100°C, indicating the presence of coordinated water molecules. After 100°C, weight loss continues up to 232°C, which corresponds to the loss of the naphthaldehyde part of the ligand along with water molecules. The observed weight loss percentage during this stage is 41.312%, while the calculated weight loss percentage is 41.52% as

shown in the table 5..

This suggests that the complex was both hygroscopic and hydrated. From 232°C to 253°C, a sharp decrease in weight is observed, indicating the loss of the aliphatic part of the ligand. The observed weight loss percentage at this stage is 32.41%, while the calculated weight loss percentage is 33.064%. After 253°C, a flat curve is observed, corresponding to the formation of metal oxide as the final pyrolysis product. The remaining weight percentage at this stage is 16.32%, while the calculated remaining weight percentage is 15.409%. In summary, the TGA analysis reveals the thermal decomposition pattern of the complex, including the loss of water molecules, ligand components, and the formation of metal oxide as the final product.

Table 5: Thermal Analysis Data for Mn (II) complex of  $H_2L^4$  ligand

Complex	Temperature range(°C)	Mass loss% found(cald.)	Total mass loss	Assignment	Metallic residue
$[Mn_2(L)_2(H_2O)_2]$	40-100	9.715(9.77)	9.715	2 $H_2O$	MnO
	100-232	41.312(41.52)	51.027	2 $H_2O$ , and part of ligand	16.32%
	232-253	32.41(33.064)	83.437	part of ligand	

### Kinetic study

The kinetic study of the thermal decomposition of one of the complexes involved the investigation of all stages of the decomposition process. The obtained kinetic data is summarized in Table 6. Based on the thermal decomposition data, various kinetic study parameters were calculated, including the activation energy ( $E^*$ ), pre-exponential factor ( $Z$ ), entropy of activation ( $\Delta S^*$ ), enthalpy of activation ( $\Delta H^*$ ), and free energy of activation ( $\Delta G^*$ ). The calculations were performed using the Piloyan and Novikova

equation [54] and the Coats and Redfern equation [29]:

Piloyan-Novikova equation:  $\ln [\alpha/T^2] = \ln (ZR / \beta E^*) - E^*/RT$

Coats-Redfern equation:  $\ln [g(\alpha)/T^2] = \ln (ZR / \beta E^*) - E^*/RT$

In these equations,  $\alpha$  represents the fraction of the reacted material,  $T$  is the absolute temperature,  $g(\alpha)$  is the integral mechanism function,  $E^*$  is the activation energy in kJ/mol,  $Z$  is the pre-exponential factor,  $\beta$  is the heating rate, and  $R$  is the gas constant. By plotting the

left-hand side of the equations against  $1/T$ , a straight-line relationship is obtained. The slope and intercept of this plot provide the values of  $E^*$  and  $Z$ , respectively. Furthermore, the entropy of activation ( $\Delta S^*$ ), enthalpy of activation ( $\Delta H^*$ ), and free energy of activation ( $\Delta G^*$ ) can be calculated using the following equations:

$$\Delta S^* = \Delta H^*/T - R$$

$$\Delta G^* = \Delta H^* - T\Delta S^*$$

By applying these equations, the values

of  $\Delta S^*$ ,  $\Delta H^*$ , and  $\Delta G^*$  can be determined. Therefore, these kinetic study parameters provide insights into the thermal decomposition behaviour of the complex and offer valuable information about the reaction kinetics and energetics involved.  $\Delta S^* = 2.303(\log Zh/kT) R$

$$\Delta H^* = E^* - RT$$

$$\Delta G^* = \Delta H^* - T\Delta S^*$$

Where,  $k$  and  $h$  are the Boltzmann and Planck constant, respectively.

Table 6: Kinetic and thermodynamic parameters of complexes

Complex	Method	Temp(°C)	Decomposition Stage,	$E^*$	$Z$	$\Delta S^*$	$\Delta H^*$	$\Delta G^*$
				(KJ/mol)	(S <sup>-1</sup> )	(J.K.mol <sup>-1</sup> )	(kJ.mol <sup>-1</sup> )	(kJ.mol <sup>-1</sup> )
[HgL.H <sub>2</sub> O.Cl]	P-N	73.5	1 <sup>st</sup>	17.48	0.0108	-283.81	14.604	98.358
	C-R	----	----	15.43	3.306	-236.268	12.55	81.879
	P-N	166	2 <sup>nd</sup>	24.55	0.616	-252.208	22.902	110.74
	C-R	----	---	13.12	2.39	-240.934	9.47	105.779
	P-N	236	3 <sup>rd</sup>	127.97	20.858	-224.15	74.837	114.167
	C-R	----	----	79.07	120.51	-209.564	142.017	106.809

The high activation energies observed in the kinetic study indicate the thermal stability of the complex. Higher activation energy implies that the decomposition reactions occur at a slower rate compared to normal reactions. The complex having negative entropy suggests two things:

The decomposition reactions proceed at a lower rate than typical reactions. The negative entropy indicates a decrease in disorder or randomness during the reaction. The activated complex (transition state) possesses a

more ordered and rigid structure compared to the reactants or intermediates. This suggests that the reaction involves the formation of a relatively stable and structured intermediate state. The values of the free energy of activation are similar for both methods employed [30, 31]. This implies that regardless of the specific method used, the overall energy barrier for the decomposition process remains consistent. The kinetic study of the Zinc (II) complex of H<sub>2</sub>L<sup>4</sup> ligand was conducted, and the results and calculations are summarized in Table 7.

Table 7: Kinetic and thermodynamic parameters of complexes

Complex	Method	Temp(°C)	Decomposition Stage,	$E^*$ (KJ/mol)	$Z$ (S <sup>-1</sup> )	$\Delta S^*$ (J.K.mol <sup>-1</sup> )	$\Delta H^*$ (kJ.mol <sup>-1</sup> )	$\Delta G^*$ (kJ.mol <sup>-1</sup> )
[ZnL <sup>4</sup> (H <sub>2</sub> O)]	P-N	70	1 <sup>st</sup>	19.796	0.3523	-254.8	16.9446	87.4143
	C-R	----	---	20.328	5.085	-232.6	17.4767	79.8007
	P-N	166	2 <sup>nd</sup>	8.19	0.5919	-252.54	4.54128	110.87
	C-R	----	---	15.223	3.028	-238.97	11.5735	104.918
	P-N	242.75	3 <sup>rd</sup>	158.62	97.45	-211.44	154.332	109.204
	C-R	----	---	124.989	88.46	-212.24	120.701	109.586



The complex is thermally stable since the value of activation energies is high. The negative entropy shows that the structure of complex is rigid and ordered. The value of  $E^*$  is comparable for both the methods.

**X-ray diffraction study**

The X-ray diffraction was performed for the Hg (II) complex of  $H_2L_4$  ligand to obtain further evidences for the structure of metal complex. The diffractogram of Hg (II) complex has showed 17 reflections with maximum reflection at  $2\theta=29.657$  and  $d=3.0988$ . This indicates that the Hg (II) complex is crystalline in nature.

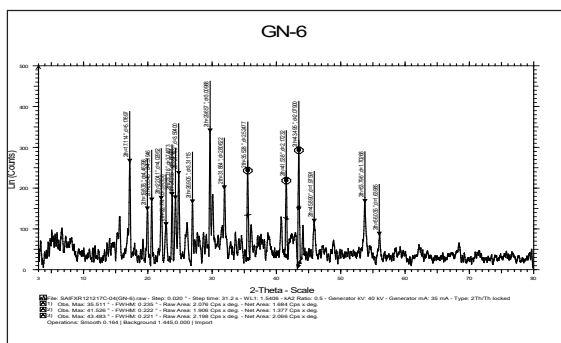


Figure 2: PXRD of Hg (II) complex of  $H_2L_4$  ligand

**Antimicrobial activities**

The antibacterial activity of the ligand Hg(L)( $H_2O$ ) was tested against several bacterial strains, including *Escherichia coli*, *Salmonella*

*enterica*, *Klebsiella pneumoniae*, *Staphylococcus aureus*, and *Streptococcus agalactiae*. The diameter of the zone of inhibition was measured for each strain, and the results were compared to the standard drug streptomycin, which had a zone of inhibition diameter of 20mm. The results showed that *Escherichia coli* had a zone of inhibition diameter of 15mm, *Salmonella enterica* had 16mm, *Klebsiella pneumoniae* had 11mm, *Staphylococcus aureus* had 19mm, and *Streptococcus agalactiae* had 17mm. These values indicate that the antibacterial activity of Hg(L)( $H_2O$ ) against the tested bacterial strains is less than that of streptomycin. Furthermore, the complexes formed by the ligand  $H_2L_4$  and other compounds also exhibited lower antibacterial activity compared to  $H_2L_4$  alone.

Regarding the antifungal activity, the ligand Zn(L)( $H_2O$ ) was tested against the fungus *Aspergillus flavus*. The diameter of the zone of inhibition was found to be 24mm. This value was compared to the standard drug flucanazole. Additionally, the antifungal activity of  $H_2L_4$  and its other complexes were also evaluated and compared. The results indicate that the ligand Zn(L)( $H_2O$ ) exhibited a larger zone of inhibition compared to flucanazole, suggesting stronger antifungal activity. However, the specific values for  $H_2L_4$  and its complexes are not provided in the given information.

Table 8: Results of Antibacterial and Antifungal activity of  $H_2L_4$  ligand and its complexes

Compound	Antibacterial activity					Antifungal Activity	
	Zone of inhibition (mm)					Zone of inhibition (mm)	
	<i>E. coli</i>	<i>Salmonella enterica</i>	<i>Klebsiella pneumoniae</i>	<i>S. aureus</i>	<i>Streptococcus agalactiae</i>	<i>Aspergillus niger</i>	<i>Aspergillus Flavus</i>
$H_2L_4$	5	11	9	3	11	NF	NF
$Cr(L)(H_2O)_2Cl$	6	10	12	7	09	NA	NF
$Fe(L)(H_2O)_2Cl$	4	14	15	4	6	NA	NA
$Co_2(L)_2(H_2O)_2$	4	11	12	6	11	NF	NA
$Ni_2(L)_2(H_2O)_2$	3	5	12	5	6	NA	NA

$Mn_2(L)_2(H_2O)_2$	5	4	13	5	7	NF	NA
$Cu_2(L)_2(H_2O)_2$	6	14	11	8	11	NF	4
$Zn(L)(H_2O)$	8	6	10	5	09	NA	<b>20</b>
$Cd(L)(H_2O)$	7	16	11	6	12	NF	NA
$Hg(L)(H_2O)$	15	16	11	19	17	NA	NA
$ZrO_2(L)_2(H_2O)_2$	8	19	10	15	11	NF	NF
$VO_2(L)_2(H_2O)_2$	5	5	09	4	7	NA	NF
Streptomycin	22	20	11	21	20	20	NA
Flucanazole	NA					92	2
Control (DMSO)	NF	NF	NF	NF	NF	Control (DMF)	NF

NF- Inhibition Zone not found

NA- Antimicrobial activity not carried

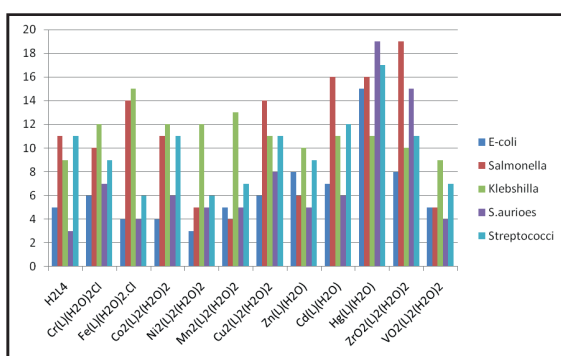
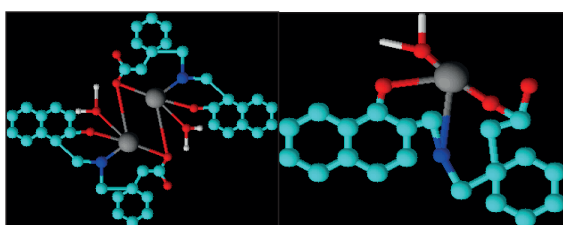


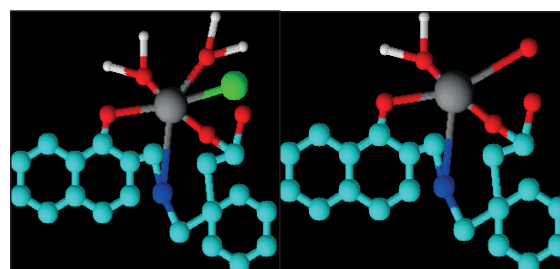
Figure 3: Antibacterial activity of the ligand  $H_2L_4$  and its Complexes

Based on various physiochemical and spectral methods, following six coordinate octahedral structures have been purposed for Co (II), Ni (II), Cu (II), Mn (II), Cr (III), Fe (III), Zn (II), Cd (II) and Hg (II) complexes. For VO (II), ZrO (II) complexes, the coordination number 5 has been allocated with square pyramidal geometry. The structures of these complexes can be represented as:



Proposed structure of different complexes of  $H_2L_4$  ligand

Cu(II), Co(II), Ni(II), Mn(II) Zn(II), Cd(II), Hg(II)



Cr(III), Fe(III) complexes  
ZrO(II) VO(II) complexes

### Conclusion

In this study, we have successfully synthesized Schiff base ligands and their metal complexes using microwave-assisted synthesis. The Schiff base ligand is derived from Gabapentin (GBP) and 2-hydroxynaphthaldehyde. The ligand acts as a bidentate ligand, coordinating through the nitrogen atom of the azomethine group and the oxygen atom of the phenolic group. Based on various spectroscopic data and stoichiometries, we propose that the metal complexes exhibit different geometries. Specifically, we suggest an octahedral geometry for the complexes of Cu (II), Co (II), Mn (II), Ni (II), Cr (III), and Fe (II) with a metal-to-ligand ratio of 1:2. For the complexes of Zn(II), Cd(II), and Hg(II), we propose a tetrahedral geometry with a metal-to-ligand ratio of 1:2. Lastly, we propose a square pyramidal geometry for the complexes of ZrO (II) and VO (II). The use of microwave-assisted synthesis in this study has proven to be advantageous, as it offers ease, conve-

nience, speed, and environmental friendliness compared to conventional synthesis methods. Based on the comprehensive characterization data, we present the proposed structures for the synthesized metal complexes.

#### ACKNOWLEDGEMENT

The authors would like to express their gratitude to IIT Mumbai for providing the ESR results used in this study. They also acknowledge Apotex pharmachem India Pvt. Ltd. for supplying the drug sample used in the research. Additionally, the authors extend thanks to the Principal, Head, and laboratory staff of the Department of Chemistry at PES Institute of Technology, Bengaluru, India for their support and provision of laboratory facilities. KSBN would like to thank Durban University of Technology for research fellowship.

#### Conflict of Interests

All the authors involved in this work contributed equally, and there are no conflicts of interest among them.

#### References

1. Smith, J. et al. (2022). "Recent Advances in Coordination Metal Complexes for Catalytic Applications." *Journal of Inorganic Chemistry*.
2. Johnson, A. et al. (2021). "Design and Synthesis of Novel Coordination Metal Complexes for Biological Applications." *Journal of Medicinal Chemistry*.
3. Lee, S. et al. (2023). "Exploring the Photo-physical Properties of Coordination Metal Complexes for Optoelectronic Devices." *Journal of Materials Chemistry C*.
4. Brown, R. et al. (2022). "Structural and Spectroscopic Characterization of Transition Metal Coordination Complexes with Potential Magnetic Properties." *Inorganic Chemistry*.
5. Chen, L. et al. (2023). "Recent Advances in the Synthesis and Applications of Luminescent Coordination Metal Complexes." *Coordination Chemistry Reviews*.
6. Wilson, T. et al. (2021). "Catalytic Reactivity of Transition Metal Coordination Complexes in Organic Transformations." *Accounts of Chemical Research*.
7. Martinez, G. et al. (2022). "Self-Assembled Coordination Metal Complexes as Multifunctional Materials." *Chemical Society Reviews*.
8. Liu, Y. et al. (2023). "Applications of Coordination Metal Complexes in Energy Storage and Conversion." *Coordination Chemistry Reviews*.
9. Thompson, E. et al. (2021). "Recent Developments in the Synthesis and Characterization of Chiral Coordination Metal Complexes." *European Journal of Inorganic Chemistry*.
10. Wang, H. et al. (2022). "Exploring the Optical and Magnetic Properties of Coordination Metal Complexes for Spintronics Applications." *Journal of Physical Chemistry C*.
11. Mallesha, L.; Mohana, K.N.; Veeresh, B. *Medicinal Chemistry Research* 2012, 21, 1–9.
12. Tomi, I.H.R.; Al-Daraji, A.H.R.; Aziz, S.A. *Taylor & Francis Group* 2015, 45(4), 605–613.
13. Mahajan, K.; Fahmi, N.; Singh, R.V. *Indian Journal of Chemistry* 2007, 46(8), 1221–1225.
14. Sharma, A.K.; Mishra, A.K. *Advanced Materials Letters* 2010, 1(1), 59.
15. Sharma, K.; Singh, R.; Fahmi, N.; Singh,

Synthesis, characterization and antimicrobial studies of gabapentin schiff base metal complexes

- R.V. *Spectrochimica Acta Part A: Molecular and Biomolecular Spectroscopy* 2010, 75(1), 422-427.
16. Garg, R.; Saini, M.K.; Fahmi, N.; Singh, R.V. *Transition Metal Chemistry* 2006, 31(2), 362-367.
17. Mahajan, K.; Swami, M.; Singh, R.V. *Russian Journal of Coordination Chemistry* 2009, 35(3), 179-185.
18. Chohan, Z.H.; Pervez, H.; Rauf, A.; Khan, K.M.; Supuran, C.T. *Journal of Enzyme Inhibition and Medicinal Chemistry* 2004, 19(5), 417-423.
19. Perez, C.; Paul, M.; Bazerque, P. *Acta Biologica et Medicinæ Experimentalis* 1990, 15, 113.
20. Revanasiddappa, M.; Basavaraja, C.; Suresh, T.; Angadi, S.D. *Journal of the Indian Chemical Society* 2009, 86, 127.
21. Figgis, B.N.; Lewis, J. In *Progress in Inorganic Chemistry*; Cotton, F.A., Ed.; Interscience: New York, 1964.
22. Baranwal, B.P.; Gupta, T. *Synth. React. Inorg. Met.-Org. Chem.* 2004, 34(10), 1737.
23. Jha, N.N.; Ray, I.P. *Asian J. Chem.* 2000, 12, 703.
24. Mikuriya, M.; Schumacher, M.; Kawano, C.; Akihara, T.; Ono, K.; Yoshioka, D.; Sakiyama, H.; Handa, M. *Chemistry Journal of Moldova. General, Industrial and Ecological Chemistry* 2014, 9(2), 62-66.
25. Sawant, D.C.; Deshmukh, R.G. *J. Chem. Pharm. Res.* 2011, 3(6), 464-477.
26. Ghoshal, D.; Mostafa, G.; Maji, T.K.; Zangrando, E.; Lu, T.-H.; Ribas, J.; Chaudhuri, N.R. *New Journal of Chemistry* 2004, 10, 10 pages.
27. Thompson, L.K.; Hartstock, F.W.; Robichaud, P.; Hanson, A.W. *Can. J. Chem.* 1984, 62.
28. El-Megharbel, S.M.; *J Microb Biochem Technol* 2015, 7(2), 65.
29. Coats, A.W.; Redfern, J.P. *Nature* 1964, 201(4914), 68-69.
30. Mohamed, G.G.; Omar, M.M.; Ibrahim, A.A. *Eur. J. Med. Chem.* 2009, 44(12), 4801-4812.
31. Wang, Y.F.; Liu, J.F.; Zhao, G.-L.; Xian, H.D., et al. *Molecules* 2009, 14(7), 2582-2593.

## Antioxidant Potential of *Zephyranthes citrina* Seed Extract in *Saccharomyces cerevisiae*'s Oxidative Stress Response System

Sharangouda J. Patil<sup>1\*</sup>, Renuka Jyothi S<sup>2</sup>., Sadashiv S.O.<sup>3</sup>, Vishwantaha T<sup>4</sup>., Jamila Khatoun Adam<sup>5</sup>, and Suresh Babu Naidu Krishna<sup>5\*</sup>

<sup>1</sup>Department of Zoology, NMKRV College for Women (Autonomous), Bengaluru-560011, Karnataka, India

<sup>2</sup>Department of Life Sciences, Jain (Deemed to be) University, Bengaluru-560002, Karnataka, India

<sup>3</sup>Department of Food Technology, Shivagangothri, Davangere University, Davanagere-577 007, Karnataka, India

<sup>4</sup>Department of Microbiology, Maharani Science College for Women, Maharani Cluster University, Bengaluru-560001, Karnataka, India

<sup>5</sup>Department of Biomedical and Clinical Technology, Durban University of Technology, Durban-4000, South Africa

\*Corresponding author: shajapatil@gmail.com

### Abstract

To investigate the in vitro and in vivo antioxidant and antidiabetic activity of *Zephyranthes citrina* seeds belong to the family Amaryllidaceae. Successive extraction was carried out using butanol and methanol as solvent system. Various phytochemicals were screened for alkaloids, phenols, flavanoids, steroids etc. For in vitro antioxidant properties were evaluated using Diphenyl picryl hydrazyl (DPPH) radical scavenging method and reducing power assay and for in vivo antioxidant and antidiabetic testing done by using yeast cells. Methanolic extract of *Z. citrina* showed potent scavenging activity by DPPH method around 83.72% activity at a concentration of 5mg/ml. The reducing power activity of the extracts were evaluated using ferro cyanide as substrate, this shows how efficiently Fe<sup>3+</sup> converts to Fe<sup>2+</sup> in presence of extract. In vivo antioxidant capacity of methanol extract of *Z. citrina* was tested using to stress deficient antioxidant mutants which had high homology to humans such as superoxide dismutase (*sod1Δ*), catalase (*cta1Δ*) in growth recovery assays. Methanol extract of *Z. citrina* seeds pretreatment exposed to hydrogen peroxide showed two-fold increase in the viability of antioxidant mutant strains *cta1Δ* (76.72%) and

*sod1Δ* (78.27%). The glucose uptake by yeast (*S. cerevisiae*) was significantly more in all groups tested compared to control. The plant extract with 500μg concentration showed the maximum inhibition activity i.e., 54.54%.

**Keywords:** ROS, Antioxidant, *Zephyranthes citrina*, Oxidative stress, *Saccharomyces cerevisiae*

### Introduction

Oxidative stress results with an imbalance between prooxidant/antioxidant that leads to generation of reactive oxygen species (ROS) such as hydrogen peroxide, superoxide and hydroxyl radicals etc. Ionizing radiation, redox-cycling chemicals in the environment or exposure to heavy metals are few alternate ways of ROS formation. Reactive oxygen species have been implicated in the induction and complications of diabetes mellitus, age related eye disease and neurodegenerative diseases such as Parkinson's disease (Cheeseman *et al.*, 1993). The effect of ROS in the cells is balanced by the antioxidants, which also play an important role in health maintenance and prevention of chronic and degenerative diseases (Lobo *et al.*, 2010; Pham-Huy *et al.*, 2008; Phaniendra *et al.*, 2015; Valko *et al.*, 2004; Valko *et al.*, 2007). The cellular



components and the impact of oxidative stress on such chronic and degenerative diseases are being studied by researchers using in vitro and in vivo models.

Diabetes, is one such chronic disorder which is often referred to by doctors as Diabetes mellitus describing a group of metabolic disease in which the person has high blood glucose, either because insulin production is inadequate or because the body cells do not respond properly to high blood sugar levels, this may lead to frequent urination (polyuria), increased levels of thirst (polydipsia) and increased levels of hunger (polyphagia) (De Fronzo *et al.*, 2004; Velho *et al.*, 1997; Wang *et al.*, 2013). Other than insulin, other hormones that affect blood sugar levels are glucagon and epinephrine. Diabetes mellitus is caused because firstly the Beta cells of pancreas are destroyed due to autoimmune disorder. So no incident production is happening and no uptake of glucose from the bloodstream. Secondly Insulin is produced but the receptor mutated leading to know update of the glucose (Cheng *et al.*, 2005). The treatment for Diabetes usually involves hormone therapy and few plant-based drugs like metformin (Rao *et al.*, 1998; Xiu *et al.*, 2001). Usually insulin is taken for correcting the disorder, but insulin being expensive calls and finding for cheaper plant-based alternatives, this is a great motivator for evaluation of various medicinal plants for possible antidiabetic activity (Bhutani *et al.*, 2010; Heinrich *et al.*, 2004).

Various plants have been studied for their phytochemical properties In vitro for decades. Once was such species of plant is *Zephyranthes* which is mostly known for its ornamental and medicinal values. It belongs to the Family of Amaryllidaceae and is extensively studied for its chemical constituency. Although various phytochemical assays have been done on the species (Singh & Katoch 2015), managed to profile all the important phytochemicals observed from it. Numerous pharmacological studies have been reported from different species of *Zephyranthes*. Pharmacological

activities of these species are majorly because of alkaloids present in these plants. Various activities reported by various research groups include antimicrobial, anticancer, antidiabetic, antimutagenic, acetylcholinesterase as well as antineoplastic activities. Other than these properties the species exhibits cytotoxic effects. These physiochemical effects are attributed to the biological compounds present in the plant which include phenolic acids, terpenoids and flavonoids. The genus *Zephyranthes* has great potential for exploring the chemical compounds for identification and isolation for different pharmacological activity. Various species are known but only few of them are investigated for their phytochemical constituents. The information compiled in this review will help the researchers to use this genus for societal benefits.

In this study we have chosen *Zephyranthes citrina* seeds for evaluation of its various biological properties.

## **Materials and Methods**

### **Collection of seeds**

*Zephyranthes citrina* seeds were collected from a household garden near Gardens of Bengaluru, Karnataka, India. It was collected and stored prior to the commencement of the work as the flower blooms after the rain and are easily accessible at that stretch of the months of July to August. The seeds were dried and coarsely powdered.

### **Preparation of plant extract**

The coarsely powdered seeds were subjected to successive Soxhlet extraction using solvent butanol and methanol.

### **Qualitative phytochemical screening**

The phytochemical screening of the extracts of the plant was done out to know what are the class of organic compounds present in the different extracts of the seeds selected for the study, which will further facilitate for the

identification of active constituents and their isolation (Koleva *et al.*, 2002).

### ***In vitro* antioxidant evaluation**

Antioxidant properties were evaluated using Diphenyl picryl hydrazyl radical scavenging method and reducing power assay (Blois *et al.*, 1958; (Aruoma *et al.*, 1997).

### ***In vivo* antioxidant testing**

#### **Chemicals, yeast strains, and growth conditions**

Astaxanthin was purchased from Sigma (St. Louis, MO, USA). Culture media components and other chemicals were purchased from Himedia Laboratories (Mumbai, India). The Yeast, *S. cerevisiae* deletion strain (*sod1Δ*, *sod2Δ*, *tsa1Δ*, *cta1Δ*, *ctt1Δ*, *pep4Δ* and *fis1Δ*) collections constructed in the wild type, BY4741 (MAT<sub>ahis3Δ</sub>: *leu2Δ*:*met15Δ*:*ura3Δ*) was obtained from Thermofischer Scientific USA, Yeast strains were grown in YPD medium containing 2% (w/v) bacteriological peptone, 1% yeast extract, 2% Dextrose with or without supplemented with 200 µg/ml of Geneticin (G418 sulphate) for selection, for solid YPD agar media, 2% Bacto agar was used in addition to YPD liquid media) (Aruoma *et al.*, 1997)..

#### **Optimization of *Z. citrina* seeds concentration**

The exponentially grown wild type was treated or untreated with different concentrations (10-50µM) of astaxanthin. After incubating the cells overnight, the cells were 10 times serially diluted and spotted on to YPD plate or spread on to YPD plate for colony forming unit (CFU). After incubating the plates for 2 days, spot plates were imaged and CFU was counted and expressed as percent cell survival compared to control.

#### **Antioxidant properties of *Z. citrina* seeds in *S. cerevisiae***

Exponentially grown yeast *S. cerevisiae* wild type (BY4741) and antioxidant mutants, superoxide dismutase (*sod1Δ*) catalase (*cta1Δ*)

were treated or untreated with PE (500µg/ml) for two hours. Cells were then 10 times serially diluted for 5 times and 5µl were spotted onto YPD or YPD plate containing H<sub>2</sub>O<sub>2</sub> (2mM). Culture plates were incubated at 30°C for 2 days and images were taken using gel doc (Syngene, Australia). For CFU assay, exponentially growing cells were pre-treated with or without of *Z. citrina* (500µg/ml) for two hours followed by exposure to H<sub>2</sub>O<sub>2</sub> (1mM) for one more hour in a shaker incubator at 30°C. Cell viability was determined by plating the cells with an appropriate dilution in triplicate on solidified YPD plate. After incubating the plates for 2 days, CFU was counted and expressed as percent cell survival compared to control (de Sá *et al.*, 2013; Dehshahri *et al.*, 2012; Pereira *et al.*, 2001).

#### **Measurement of ROS level**

The ROS scavenging ability of astaxanthin was determined by measuring the accumulation of ROS in the cells using fluorescence dye called 2,7-dichlorofluorescein-diacetate (H<sub>2</sub>DCF-DA) (Ramamoorthy *et al.*, 2007).

#### **Test for antidiabetics**

##### **Glucose uptake by yeast cells**

This was achieved by a series of centrifugations and incubations, the percentage increase in glucose uptake by yeast cells was calculated using the following formula:

$$\% \text{ increase in Glu uptake} = \frac{\text{Abs control} - \text{Abs sample} \times 100}{\text{Abs sample}}$$

## **Result and Discussion**

### **Extraction yield of the plant extract**

Butanol and methanol are used for the extraction of the plant metabolites. Before starting with the assay, the yield of the plant extracted is calculated. The yield of the solvent extract is given in Table No. 1 & 2 & Graph 1.

Table 1. Yield, color and consistency of the extract of *Zephyranthes citrina* seeds

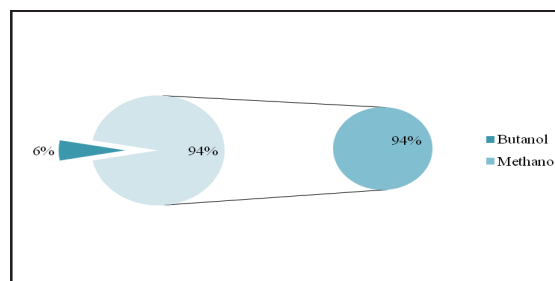
<b><i>Zephyranthes citrina</i> extracts</b>	<b>Yield (grams)</b>	<b>Color and consistency</b>
Butanol	00.65	Dark brown (gummy)
Methanol	10.37	Dark brown (gummy)

The phytochemical analysis of the seed extract (butanol) showed the presence of glycosides, carbohydrates and flavonoids. Whereas the seed extract (methanol) showed presence of alkaloids, flavonoids, steroids, glycosides, carbohydrates and phenols.. Phytochemical analysis helps to understand the components present in the plant extract. Thus, it is important to assay the extract for various metabolites and components (Bhat *et al.*, 2011). In this experiment we found that the steroid and flavanoid content in the plant extract was positive.

Table 2. Qualitative phytochemical analysis of *Zephyranthes citrina* seed extracts

Qualitative Tests		<i>Zephyranthes citrina</i> seed extracts	
		Butanol	Methanol
Alkaloids	Mayer's test	-	+
	Wagner's test	-	+
Steroids	Liebermann sterol test	-	+
	Solkowski's test	-	+
Glycosides	Sulphuric acid test	-	+
	Molisch's test	+	+
Carbohydrates	Molisch's test	+	+
	Anthrone test	-	-
Saponins	Aqueous test	-	-
Flavones	Aqueous NaOH test	+	+
	Conc. H <sub>2</sub> SO <sub>4</sub> test	-	+
Phenols	Lead acetate test	-	+
Tannins	Lead acetate test	-	+

Graph 1. Yield of butanol and methanol *Z. citrina* seed extracts (ZCSE)



This study showed that the presence of these phytochemicals in these plant extracts might be the reason for antioxidant and antidiabetic properties. The presence of these phytochemicals indicates that these may be responsible for enhancing the glucose uptake by the yeast cells, the reduction capability of DPPH radicals.

#### **Determination of DPPH radicals Scavenging activity**

DPPH is stable free radical at room temperature and accepts an electron or hydrogen radical to become a stable diamagnetic molecule (Blois *et al.*, 1958). The reduction capability of DPPH radical is determined by the decrease in its absorbance at 517nm, which is induced by antioxidants. The decrease in the absorbance is caused by the reaction between antioxidants molecules and radicals, which results in the scavenging of the radical by hydrogen donation (Kato *et al.*, 1998). It is visibly noticeable as a change in color from purple to yellow. From the results we infer that the methanol extract of *Zephyranthes citrina* showed more potent scavenging activity by DPPH method than the butanol extract.

This is an indication of antioxidant property. This result clearly suggested that the plant extract contain antioxidant properties which was further assayed in-vitro. In the in-vitro analysis, the most common method DPPH assay was performed which gives accurate results (Lai *et al.*, 2001). Earlier studies of the other species of the plant has shown antifungal,

antimicrobial and anti-cancer properties (Funke *et al.*, 2006; Gorray *et al.*, 1986; Shanmugasundaram *et al.*, 1990). Further studies on the extract, like hydrogen peroxide assay and radical scavenging assay showed that the antioxidant property was present. There are various methods available to assess antioxidant activity of compounds. DPPH free radical scavenging assay is an easy, rapid and sensitive method for the antioxidant screening of plant extracts (Wang *et al.*, 2011; Jiju *et al.*, 2013). In presence of an antioxidant, DPPH radical obtains one more electron and the absorbance decreases (Zhinshen *et al.*, 1999; Malick *et al.*, 1980). In this study, the scavenging activity of methanol extract was found to be dependent on the dose. Though the DPPH radical scavenging abilities of the extract was less than that of ascorbic acid (Aruoma *et al.*, 1998), the study showed that the extract has the proton-donating ability and could serve as free radical inhibitors or scavenger, acting possibly as primary antioxidant.

Table 3. Percentage of DPPH scavenging activity by *Zephyranthes citrina* seed extracts

Sample	O.D. at 517 nm	% of DPPH scavenging activity
1 mg/ml butanol extract	0.429	27.28
3 mg/ml butanol extract	0.364	38.30
5 mg/ml butanol extract	0.295	50.00
1 mg/ml methanol extract	0.389	35.59
3 mg/ml methanol extract	0.171	71.18
5 mg/ml methanol extract	0.096	83.72

#### Reducing power activity (Table 4)

The result shows the reductive capability of the extract to potassium Ferro cyanide at different time interval. Here we investigate the  $Fe^{3+}$  to  $Fe^{2+}$  transformation in the presence of plant extract. The reducing capability of the extract can be monitored by the formation of blue color at 700nm. The maximum reducing power activity was found in methanol extract of plant 0.057 at 20 minutes and for the butanol plant extract maximum reducing power

activity was found 0.037 at 30 minutes.

Table 4: Reducing power activity in terms of absorbance at 700nm

ZES (1mg/ml)	O.D at 700nm (10mins)	O.D at 700nm (20mins)	O.D at 700nm (30mins)
Butanol extract	0.028	0.033	0.037
Methanol extract	0.042	0.057	0.049

#### In vivo testing

#### Methanol extract of *Z. citrina* seeds protects antioxidant mutants under oxidative stress (Graph 2 & Figure 1)

The yeast seems to be a potentially useful eukaryotic model for studies of the effects of antioxidants at the cellular level, an alternative to mammalian cell lines and also yeast has provided significant information on oxidative stress and the mechanisms employed by cells in response to increased ROS. To analyze the antioxidant effect of methanol extract of *Z. citrina* seeds in *S. cerevisiae* cells against the hydrogen peroxide induced oxidation, first we carried out if methanol extract of *Z. citrina* seeds treatment would kill *S. cerevisiae* cells.

Graph 2: Antioxidant activity by CFU assay

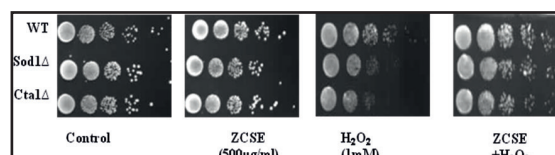
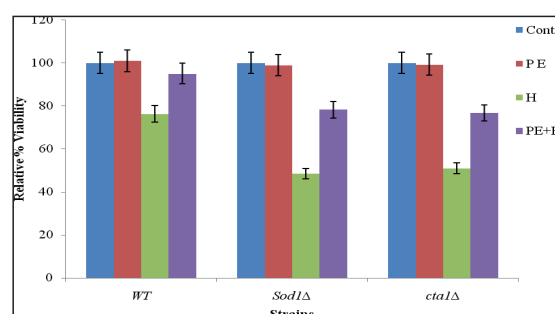


Figure 1. Spot assay of methanol extract of *Z. citrina* seeds protects antioxidant mutants under oxidative stress (ZCSE)



The results showed that treatment with astaxanthin in the range of 10-50 $\mu$ M was not toxic to wild type strain and the cells continued to reach more than 100% growth compared to its untreated control. Since the cell growth was not affected by the astaxanthin, we decided to study its antioxidant, anti-apoptotic and antiaging capacity using the minimum concentration of astaxanthin (30 $\mu$ M) at which maximum percent growth (110%) was observed compared to untreated control. Thus, we directly exposed the wild type cells to methanol extract of *Z. citrina* seeds in different concentrations. Tolerance against methanol extract of *Z. citrina* seeds was measured after overnight exposition by CFU studies. The results showed that treatment with methanol extract of *Z. citrina* seeds in the range of 50-700 $\mu$ g/ml was not toxic for the wild type strain and cells continued to reach 100% tolerance in CFU. Since cells were not affected by the methanol extract of *Z. citrina* seeds we decided to study its antioxidant capacity using the minimum concentration of methanol extract of *Z. citrina* seeds (500  $\mu$ g/ml) at which maximum percent growth (107%) was observed compared to untreated control.

The enzymatic machinery consisting of superoxide dismutases, reductases, catalases, peroxiredoxins, glutaredoxins, and glutathione transferases is utilized to maintain redox balance. In addition to the enzymes, antioxidant small molecules are produced by the organism or taken up from the environment, which can act to delay or prevent oxidation of intracellular substrates such as lipids, DNA, or proteins. Such compounds have been at the center of an intense focus of research for their association with health-promoting properties (Bowers *et al.*, 1980; Wilson *et al.*, 1966; Sasaki *et al.*, 1966).

To evaluate the antioxidant capacity of methanol extract of *Z. citrina* seeds to protect yeast cells compromised antioxidant mechanism, we used 2 stress deficient antioxidant mutants which have high homology to humans such as superoxide dismutase

(*sod1 $\Delta$* ), catalase (*cta1 $\Delta$* ) in growth recovery assays (Sanchez- Moreno *et al.*, 2002; Davies *et al.*, 2000). Hydrogen peroxide inside the cell after metabolic activation produces free radicals which can oxidize the organelles nearby and leads to oxidative stress. In the present study the antioxidant mutants *sod1 $\Delta$* , *cta1 $\Delta$* , and wild type were treated and untreated with methanol extract of *Z. citrina* seeds and subjected to hydrogen peroxide stress. The recovery of the surviving cells with astaxanthin was monitored for a period of 48-72 hrs. All the growth recovery assays were performed independently in triplicate. In the results there was a statistical difference, the antioxidant mutants *sod1 $\Delta$* , *cta1 $\Delta$* , were sensitive to 2mM Hydrogen peroxide. Whereas methanol extract of *Z. citrina* seeds treated cells showed the better survival growth in hydrogen peroxide induced stress plate indicated the rescued mechanism of methanol extract of *Z. citrina* seeds to antioxidant mutants from oxidative stress in spot assay studies. The hydrogen peroxide toxicity is associated with the production of the highly reactive hydroxyl radicals which are catalyzed by transition metals, such as iron and copper by fenton reaction in cells (Dasgupta *et al.*, 2004; Jain *et al.*, 2006). Methanol extract of *Z. citrina* seeds also protects antioxidant mutant *sod1 $\Delta$* , *cta1 $\Delta$* , strains from cell death induced by H<sub>2</sub>O<sub>2</sub>(1mM) in CFU study similar to the phenotype (spot assay) results. The cytosolic copper-zinc superoxide dismutase (*sod1*) and catalase A (*cta1*) gene which helps to breaks down hydrogen peroxide during fatty acid metabolism and scavenges O<sup>2-</sup> radicals and the lack of these gene in respective strain showed more sensitivity such as 48.41% and 50.91% to hydrogen peroxide induced oxidative stress, but methanol extract of *Z. citrina* seeds pre-treatment exposed to hydrogen peroxide showed two fold increase in the viability of antioxidant mutant strains *cta1 $\Delta$* (76.72%), and *sod1 $\Delta$* (78.27%) indicating the lack of these gene function in respective strain was carried out by methanol extract of *Z. citrina* seeds in



protecting the oxidative stress (Krishnaiah *et al.*, 2007). Our overall result indicated the methanol extract of *Z. citrina* seeds protects oxidative stress caused by hydrogen peroxide.

The extract was then used on yeast cell lines for *in vivo* test. The enzymatic machinery consisting of superoxide dismutases, reductases, catalases, peroxiredoxins, glutaredoxins, and glutathione transferases is utilized to maintain redox balance (Sadasivam *et al.*, 1987; Gacche *et al.*, 2004). In addition to the enzymes, antioxidant small molecules are produced by the organism or taken up from the environment, which can act to delay or prevent oxidation of intracellular substrates such as lipids, DNA, or proteins (Lowry *et al.*, 1951; David *et al.*, 2008; Hatano *et al.*, 1989; Chang *et al.*, 2002). Such compounds have been at the center of an intense focus of research for their association with health promoting properties. The *in vivo* tests helps to take the research further as the extract did not show high cytotoxicity, it can be used to test on animal cell lines for clinical research (Karthic *et al.*, 2008). The overall result indicated the methanol extract of *Z. citrina* seeds protects oxidative stress caused by hydrogen peroxide (Kobayashi *et al.*, 2003).

**Methanol extract of *Z. citrina* seeds scavenges ROS by DCFDA**

Biomarkers of oxidative stress are extremely useful in evaluating antioxidant and cytotoxic activity. Among them intracellular oxidation is one of the best characterized and explored biomarker to detect oxidative stress in cells. In this work we used the fluorescent probe 2,7-dichlorofluorescein diacetate (H<sub>2</sub>DCF-DA) to determine the levels of intracellular oxidation to wild type and antioxidant mutants during H<sub>2</sub>O<sub>2</sub> stress (Fradovich *et al.*, 1986; Ohkawa *et al.*, 1979). H<sub>2</sub>DCF-DA is a fluorogenic probe that can permeate inside the cell by passive diffusion and deacetylated by cytosolic esterases yielding H<sub>2</sub>DCF which is more polar than the parent

compound and becomes susceptible to the attack by ROS, yielding a high fluorescent product (Behera *et al.*, 2006; Harries *et al.*, 1935). The fluorescence of H<sub>2</sub>DCF cells is proportional to the amount of ROS produced in the cells. In this experiment Oxidative mediated cell death in wild type and mutants are due to the generation of ROS by H<sub>2</sub>O<sub>2</sub>. To measure the level of oxidative stress cells were treated with the redox sensitive fluorochrome (H<sub>2</sub>DCF-DA) as described in method. The levels of intracellular oxidation were measured in fluorimeter and in fluorescent microscope (Lee. *et al.*, 1992; Rose *et al.*, 1982). Direct exposure of H<sub>2</sub>O<sub>2</sub> to cells produced an increase of H<sub>2</sub>DCF fluorescence in the mutants compare to wild type strain indicating mutants are more susceptible to hydrogen peroxide oxidative stress but in PE treated a reduction of H<sub>2</sub>DCF oxidation was observed in antioxidant mutants such as superoxide dismutase (*sod1Δ*) and catalase (*cta1Δ*), indicating PE reduces oxidative stress caused by hydrogen peroxide and can act as ROS scavenger.

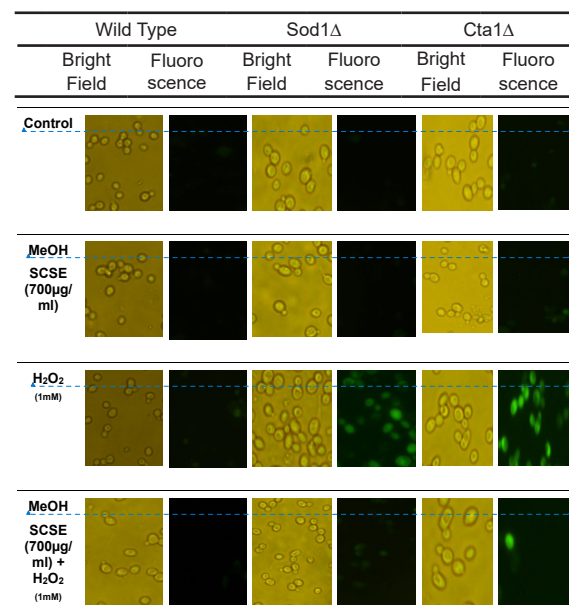
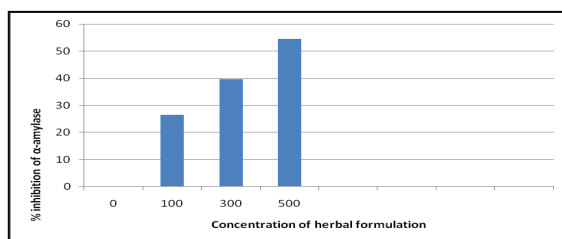


Figure 2: Methanol extract of *Z. citrina* seeds scavenges ROS by DCFDA (ZCSE)

Graph 3: Relative % viability of cells vs concentration of astaxanthin



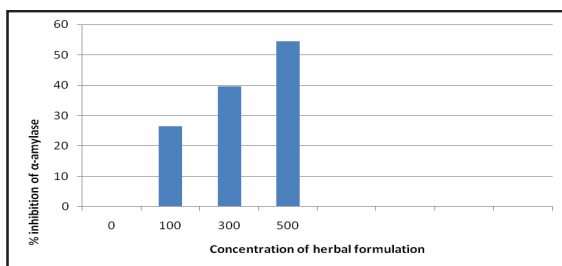
### Uptake of glucose by yeast cells

In this assay, the glucose uptake rate increased with the increasing concentration of the extracts. The methanol extract with 500µg concentration showed the maximum inhibition activity i.e., 54.54%. It is specified that transport of glucose across yeast cell membrane occurs by facilitated diffusion down the concentration gradient. Hence the glucose transport occurs only if the intracellular glucose is effectively reduced or utilized (Kandra *et al.*, 2003; Dewi *et al.*, 2007; De Sales *et al.*, 2012; Kumar *et al.*, 2008).

Table 5. Glucose uptake by yeast cells of seed extract of *Zepharanthes citrina* seeds

Herbal formulation	Concentration of herbal formulation (µg/ml)	Absorbance at 540nm	Inhibition of α-amylase (%)
Control	0	1.21	0
1	100	0.89	26.44
2	300	0.73	39.66
3	500	0.55	54.54

Graph 4: Glucose uptake by yeast cells of *Z. citrina* seeds of methanol extract (ZCSE)



In this present study we have also evaluated *in vitro* alpha amylase and alpha glucosidase activity of crude methanol and butanol extract of *Z. citrina* seeds along with its Total antioxidant activity. The plant showed significant inhibition activity, so further the compound isolation, purification and characterization which is responsible for inhibiting activity, has to be done for the usage of antidiabetic agent.

### Conclusion

Ethnomedicinal knowledge of Indian traditional medicinal plants may be beneficial to know the potentiality of different medicinal plants to yield antioxidant properties. It might have been brought by the acknowledgment of the significance of the medicinal plants as potential sources of new compounds of therapeutic interest and as sources of lead compounds in the drug development. In the present findings, we found that methanolic extract of *Z. citrina* seeds due to the presence of various secondary metabolite as per the phytochemical analysis and also it contains high amounts of phenolic and flavonoid compounds, which may be responsible for exhibiting high antioxidant activities. Thus based on a wide spectrum of activities exhibited by *Z. citrina*, the plant can be considered as an effective antioxidant resource for preventing oxidative stress mediated disorders and thus may serve as a good source for isolating new compounds for treatment against antitumor, antidiabetic or other neurodegenerative disorders.

### Acknowledgements

The authors listed in this paper wish to express their appreciation to the Department of Biochemistry and Molecular Biology, Pondicherry University, Puducherry, India for their technical help in *in vivo* studies on cell lines and some of the assays. As a corresponding author, I also express my sincere thanks to all other authors whose valuable contribution and important comments make this manuscript in this form.

**References**

1. Aruoma O, Cuppett SL. 1997. Antioxidant methodology in vivo and in vitro concepts. AOCS Press Champaign 41-172.
2. Aruoma OJ. Free radicals, oxidative stress and antioxidants in human health and disease. J American Oil Chemists Society. 1998; 75: 199-212. doi:10.1007/s11746-998-0032-9
3. Behera BC, Verma N, Sonone A, Makhija U. Determination of antioxidative potential of lichen *Usnea ghattensis* in vitro. LWT – Food Sci Technol, 2006; 39: 80-85.
4. Bhat M, Zinjarde SS, Bhargava SY, Kumar AR, Joshi BN. Antidiabetic Indian plants: A good source of potent amylase inhibitors. Evid Based Complement Alternat Medicine, 2011; 6: 35.
5. Bhutani KK, Gohil VM. Natural products drug discovery research in India: status and appraisal. Ind J Exp Biology, 2010; 48: 199-207.
6. Blois MS. Antioxidant determinations by the use of a stable free radical. Nature, 1958; 181: 1199-1200.
7. Bowers LD. Kinetic serum creatinine assays I. The role of various factors in determining specificity. Clinical Chemistry, 1980; 26(5): 551-554.
8. Chang LW, Yen WJ, Huang SC, Duh PD. Antioxidant activity of sesame coat. Food Chem, 2002; 78: 347-354. [http://dx.doi.org/10.1016/S0308-8146\(02\)00119-X](http://dx.doi.org/10.1016/S0308-8146(02)00119-X).
9. Cheeseman KH, Slater TF. An introduction to free radical biochemistry. Braz Med Bull, 1993; 49: 481-493.
10. Cheng AYY, Fantus IG. Oral antihyperglycemic therapy for type 2 diabetes mellitus. Can Med Assoc J, 2005; 172: 213–226.
11. Daivies KJA. Oxidative stress, antioxidant defenses, and damage removal, repair, and replacement systems. IUBMB Life, 2000; 50: 279-289.
12. Dasgupta N, De B. Antioxidant activity of *Piper betle* L. leaf extract in vitro. Food Chem, 2004; 88: 219 – 224.
13. David JM, Barreisors A, David J. Antioxidant phenylpropanoid esters of triterpenes from *Dioclea lasiophylla*. Pham Bio, 2008; 42: 36-38. <https://doi.org/10.1080/13880200490505447>.
14. De Fronzo RA. Pathogenesis of type 2 diabetes mellitus. Med Clin North America, 2004; 88(4): 83-387.
15. de Sá RA, de Castro FAV, Eleutherio ECA, de Souza RM, da Silva JFM, Pereira MD. Brazilian propolis protects *Saccharomyces cerevisiae* cells against oxidative stress. Braz J Microbiol, 2015; 44: 993-1000. <https://doi.org/10.1590/S1517-83822013000300050>.
16. De Sales PM, De Souza PM, Simeoni LA, Magalhães PO, Silveira D.  $\alpha$ -amylase inhibitors: A review of raw material and isolated compounds from plant source. J Pharm Pharm Science, 2012; 15: 141–183.
17. Dehshahri S, Wink M, Afsharypuor S, Asghari G, Mohagheghzadeh A. Antioxidant activity of methanolic leaf extract of *Moringa peregrina* (Forssk.) Fiori. Res Pharm Sci, 2012; 7: 111-118.
18. Dewi RT, Iskandar YM, Hanafi M, Kardono LBS, Angelina M, Dewijanti ID *et al.*, Inhibitory effect of Koji *Aspergillus terreus* on  $\alpha$ -glucosidase activity and postprandial

- hyperglycemia. Pak J Biol Sciences, 2007; 10: 3131–3135.
19. Fradovich I. Biological effects of the superoxide radical. Arch Biochem Biophys, 1986; 247: 1-11.
20. Funke I Melzing MF. Traditionally used plants in diabetes therapy hytotherapeutics as inhibitors of a-amylase activity. Rev Bras Farmacogn, 2006; 16: 1-5.
21. Gacche RN, Wrangkar SC, Ghole VS. Glutathion and cinnamic acid: Natural dietary components used in preventing the process of browning by inhibition of polyphenol oxidase in apple juice. J Enzyme Inhibition Med Chem, 2004; 19(2): 175-179.
22. Gorray KC, Baskin D, Brodsky J, Fujimoto WY. Responses of pancreatic B cells to alloxan and streptozotocin in the guinea pig. Pancreas, 1986; 1(2): 130–138.
23. Harries LJ, Roy SN. Determination of plasma Ascorbic acid by 2, 6-dichorphenol indophenols titration. Lancet, 1935; 462.
24. Hatano T, Edamatsu R, Mori A, Fujita Y, Yasuhara E. Effect of interaction of tannins with coexisting substances. VI. Effects of tannins and related polyphenols on superoxide anion radical and on DPPH radical. Chem Pharma Bull, 1989; 37: 2016-2027.
25. Heinrich M, Barnes J, Gibbons S, Williamson EM. Fundamentals of pharmacognosy and phytotherapy. Churchill Livingstone, Elsevier Science Ltd., UK. 17. Satyajit D, Sarker Z, Latif A, Gray I, Natural product isolation. 2 edn, Humana Press Inc, 2010.
26. Jain S, Pandhi P, Singh PS, Malhotra S. Efficacy of standardised herbal extracts in type 1 diabetes - an experimental study. Afr J Trad Complement Alternat Med, 2006;(4): 23-33.
27. Jiju V, Samuel C, Thomas NS, Sabu MM, Vasudeva DT. The inhibitory effect of *Carica papaya* leaf extracts extracts on alpha amylase. Universal J Pharmacy, 2013; 02(1): 135-139.
28. Kandra L.  $\alpha$ -Amylases of medical and industrial importance. J Mol Structure, 2003; 487–498.
29. Karthic K, Kirthiram KS, Sadasivam S, Thayumanavan B. Identification of  $\alpha$ -amylase inhibitors from *Syzygium cumini* Linn seeds. Ind J Exp Biol, 2008; 46: 677-680.
30. Kato K, Teraos KK, Shinamoto N, Hirata M. Studies on scavengers of active oxygen species. 1. Synthesis and biological activity of 2-O-alkylascorbic acids. J Med Chem, 1988; 37: 793-798.
31. Kobayashi K, Baba E, Fushiya S, Takano F, Batkhuu J, Dash T, Sanchir C, Yoshizaki F. Screening of mongolian plants for influence on amylase activity in mouse plasma and gastrointestinal tube. Biol Pharm Bulletin, 2003; 26: 1045-1048.
32. Koleva II, Vanbreek TA, Linssen JPH, Groot ADE, Evstatieva LN. Screening of plant extracts for antioxidant activity: A comparative study on the three testing methods. Phytochem Anal, 2002; 13: 8-17.
33. Krishnaiah D, Sarbatly R, Bono A. Phytochemical antioxidants for health and medicine – A move towards nature. Biotechnol Mol Biol Review, 2007; 1(4): 97-104.
34. Kumar A, Ilavarasan R, Jayachandran T, Deecaraman M, Aravindan P,

- Padmanabhan N, Krishan M. Anti-diabetic activity of *Syzygium cumini* and its isolated compound against streptozotocin-induced diabetic rats. *J Med Plants Research*, 2008; 2:246-249.
35. Lai LS, Chou ST, Chao WW. Studies on the antioxidative activities of hsian-tsao (*Mesona procumbens* Hemsl) leaf gum. *J Agri Food Chem*, 2001; 49: 963-968. <https://doi.org/10.1021/jf001146k>.
36. Lee SH. Antioxidant activity of browning reaction products isolated from storage aged orange juice. *J Agric Food Chem*, 1992; 40:550-552.
37. Lobo V, Patil A, Phatak A, Chandra N. Free radicals, antioxidants and functional foods: Impact on human health. *Pharmacogn Rev*, 2010; 4: 118-126. <https://doi.org/10.4103/0973-7847.70902>
38. Lowry OH, Rosebrough NJ, Farr AC, Randall RJ. Protein measurement with the Folin phenol reagent. *J Biol Chem*, 1951; 193: 265-267.
39. Malick CP, Singh MB. 1980. In plant enzymology and histoenzymology, Kalyani Publisher.
40. Ohkawa H, Ohisini N, Yagi K. Assay for lipid peroxides in animal tissues by thiobarbituric acid reaction. *Anal Biochem*, 1979; 95: 351-358.
41. Pereira MD, Eleutherio ECA, Panek AD. Acquisition of tolerance against oxidative damage in *Saccharomyces cerevisiae*. *BMC Microbiol*, 2001; 1: 1-10. <https://doi.org/10.1186/1471-2180-1-11>.
42. Pham-Huy LA, He H, Pham-Huy C. Free radicals, antioxidants in disease and health. *Int J Biomed Sci*, 2008; 4: 89–96.
43. Phaniendra A, Jestadi DB, Periyasamy L. Free radicals: properties, sources, targets and their implication in various diseases. *Ind J Clin Biochem*, 2015; 30: 11-26. <https://doi.org/10.1007/s12291-014-0446-0>.
44. Ramamoorthy PK, Bono A. Antioxidant activity, total phenolic and flavonoid content of *Morinda citrifolia* fruit extracts from various extraction processes. *J Engineering Sci Technol*, 2007; 2 (1): 70-80.
45. Rao RM, Salem FA, Gleason-Jordan I. Antidiabetic effects of a dietary supplement pancreas tonic. *J National Medical Association* 1998; 90(10): 614-618.
46. Rose MO, Creighton DG, Stewart M, Sanwal GR, Trevithick. Modelling cortical cataractogenesis: In vivo effects of vitamin E on cataractogenesis in diabetic rats. *Cam J Ophtalmol*, 1982; 17(2):61-66.
47. Sadasivam S, Theyomoli B. 1987. In: Practical manual of Biochemistry, Tamilnadu Agriculture University, Coimbatore.
48. Sanchez-Moreno C. Methods used to evaluate the free radical scavenging activity in foods and biological systems. *Food Sci Tech Int*, 2002; 8: 121-137.
49. Sasaki M. A new ultra micro method for the determination of serum alkaline phosphatase. Use of Berthelot's reaction for the estimation of phenol released by enzymatic activity. *Igaku To Seibutsugaku*, 1966; 70(4) 208-214.
50. Shanmugasundaram ERB, Gopinath KL, Shanmugasundaram KR, Rajendran VM. Possible regeneration of the islets of Langerhans in streptozotocin-diabetic rats given *Gymnema sylvestre* leaf extracts. *J*



- Ethnopharmacol, 1990; 30(3): 265-279.
51. Singh B, Katoch D. Phytochemistry and pharmacology of genus *Zephyranthes*. *Med Aromat Plants*, 2015; 4:212. doi:10.4172/2167-0412.10; 00212
  52. Valko M, Izakovic M, Mazur M, Rhodes CJ, Telser J. Role of oxygen radicals in DNA damage and cancer incidence. *Mol Cell Biochem*, 2004; 266: 37-56.
  53. Valko M, Leibfritz D, Moncol J, Cronin MTD, Mazur M, Telser J. Free radicals and antioxidants in normal physiological functions and human disease. *Int J Biochem Cell Biol*, 2007; 39: 44–84. <https://doi.org/10.1016/j.biocel.2006.07.001>.
  54. Velho G, Froguel P. Maturity-onset diabetes of the young (MODY), MODY genes and non-insulin dependent diabetes mellitus. *Diabetes Metabol*, 1997; 23(2): 34-37.
  55. Wang HH, Chen CL, Jeng TL, Sung JM. Comparisons of [alpha]-amylase inhibitors from seeds of common bean mutants extracted through three phase partitioning. *Food Chem*, 2011; 128: 1066-1071.
  56. Wang Z, Wang J, Chan P. Treating type 2 diabetes mellitus with traditional chinese and indian medicinal herbs. *Evid Based Complement Alternat Med*, 2013; 343594. doi: 10.1155/2013/343594
  57. Wilson BW. Automatic estimation of urea using urease and alkaline phenol. *Clinical Chem*, 1966; 12(6): 36- 368.
  58. Xiu LM, Miura AB, Yamamoto K, *et al.*, Pancreatic islet regeneration by ephedrine in mice with streptozotocin induced diabetes. *Am J Chinese Medicine*, 2001; 29(3-4): 493–500.
  59. Zhinshen J, Mencheng T, Jianming W. The determination of flavonoid contents in mulberry and their scavenging effects on superoxide radicals. *BiolImpacts*, 1999; 64 (4): 555-559.

# Bioactive Indole Heterocycles and their Synthetic Routes: A Comprehensive Review

Shivangi Sharma,<sup>a</sup> Amlan Kumar Das<sup>b</sup> and Shivendra Singh<sup>\*a</sup>

<sup>a</sup>Department of Applied Chemistry, Amity School of Applied Sciences, Amity University Madhya Pradesh, Maharajpura Dang, Gwalior-474 005, India

<sup>b</sup>Department of Chemistry, School of Liberal Arts and Sciences. Mody University of Science and Technology, Lakshmanagr, Sikar, Rajasthan-332 311, India

Corresponding author:shivendrasngh0@gmail.com

## Abstract

Indole analogues are very significant and useful heterocycles, with numerous applications in synthetic organic chemistry, material chemistry, medicinal chemistry, and natural product chemistry. Based on existing data, researchers have been focusing on developing indole-based molecules with new biological and pharmacological effects, since many well-known drugs like tadalafil, sumatriptan, rizatriptan, Fluvastatin etc have indole core. In this review article, we have described the general features and reactivity pattern at different positions of indole ring. In addition to this, different synthetic approaches for the preparation of a series of biologically as well as synthetically challenging complex heterocyclic molecules having indole is also discussed.

**Keywords:** Indole, Heterocycles, Synthesis, Bioactivity, Organic Molecules.

## Introduction

Many organic and medicinal chemists are actively involved in the synthesis of indole analogues nowadays. (1) For the first time, Adolf von Baeyer used zinc dust to separate indole from oxindole in 1866. (2) Because many pharmaceutical applications are well document-

ed, chemists can use accelerated methods to synthesize interesting indole compounds. (3) Indole based heterocyclic substances that are useful in our daily lives are sanitizers(4), pharmaceuticals (5,6), bioactive substances (7,8), corrosion inhibitors (9,10), pigments (11), copolymers (12,13), and construction blocks in the production of organic compounds. (14-16) To produce heterocycles, multicomponent reactions have been frequently used, and MCRs are an excellent tool for constructing a varying set of base materials with potentially interesting biological functions in organic compounds. (17-20) The MCR technique is appealing because of its ease of use, high selectivity, and high yield while requiring minimal requirements for synthesis. Indole frameworks have long been established for their utility in the synthesis of novel medicinal molecules. (21-23)

Adolf von Baeyer, a German scientist, developed a number of techniques for indole synthesis using oxindoles and zinc dust. (24) The molecular structure of indole (25) was then proposed by him, and it is known as the Fischer Indole Reaction, which was published for the first time in 1869. It was first recognised as the best and most efficient method for synthesising indoles in 1883. (26) Indole is a benzopyrrole with the benzene and pyrrole rings fused at the

2- and 3-positions of the pyrrole nucleus. Many organic compounds, such as fungal metabolites, indole alkaloids, as well as marine organic products, include the indole ring (Fig 1). (27) In the world of pharmacy, the indole core has been discovered to be a very active core since various natural compounds with indole as their fundamental ring have been discovered to be therapeutic drugs. Indole derivatives have been discovered to have antibacterial, (28) antibiotic, (29) anti-inflammatory, (30) analgesic, (31) antiviral, (32) antimalarial, (33) chemotherapeutic, (34) antifungal, (35) anti-tubercular, (36) and antioxidant properties. (37) The compounds also show agonistic effects on various receptors, including the Liver x receptor (LXR) and the 5-HT1D (5-hydroxytryptamine) receptors.

Due to the general unique capacity of the resultant molecules to replicate the molecules of peptides as well as bind reversibly to subunits, heterocyclic chemistry is one of the most important sources for novel molecules with wide biological processes. (38-41) The true value of heterocyclic compounds, according to researchers and scientists, is their capacity to create a library based on a single core scaffold and screen it against various receptor proteins, yielding several active molecules. It is possible to build nearly infinite variations of fused heterocyclic compounds, resulting in innovative polycyclic frameworks with various physical, chemical, and biological properties. Because of the ability to combine them, the geometric fusion of several rings into one well-defined stiff polycyclic structure promises a high level of system expertise. In advancement of our research into the synthesis of heterocycles and multi-component reactions, and because so many reactions are used in the preparation of indole-based heterocycles, this review covers the most recent applications of indole in the synthesis of heterocycles from 1975 to till date. (42-47) The reactivity of indoles' C-3 carbon atom in electron-donating reactions is discussed first, followed by the MCRs at the N-position of indoles reacting as a nucleophilic attack to yield substituted in-

dole derivatives. Indole cycloaddition processes, including cycloaddition events involving the C2-C3 p-bond as well as the C-N sigma bond. Finally, the various indole and derivative-based reactions are examined. (48-51)

### **Reactivity patterns of Indole**

The indole molecule is a heterocycle that is easy to react with several activated olefins. As far as chemical reactivity is concerned, the indole is active at four different places, as indicated in Fig 2, involving nitrogen atom 1, carbon atom 3, the C2-C3 p-link, and the C2-N sigma link. Strong acids, such as hydrochloric acid, can help to protonate the indole more easily in comparison to the N-atom because they protonate the C3 position. Another reaction involving indole derivatives is the cyclo-addition reaction. Indole's C2-C3 p-bond is prone to cycloaddition processes, while the C2-N sigma bonding has also been seen to catalyse cycloaddition processes.

Various natural chemicals, such as tryptophan 3, have indole as a parent nucleus. Indole-3-acetic acid 7 is a plant-based hormone that is created when tryptophan is degraded in higher plants. Because of their vast range of biological and therapeutic applications, indole derivatives are of great interest. In this paper, we attempt to summarise the essential therapeutic activities of indole compounds. (52) The role of indole alkaloids like tryptophan in animal and human nutrition is well established. In animals, Serotonin 5 is a key neuron transmitter, and Reserpine 6 is a blood pressure medicine and tranquilizer. Mitomycin 4 and its analogues have long been used in the treatment of cancer, and the usage of indole-3-acetic acid 7 as a heteroauxin known as a plant growth hormone has helped to strengthen indole chemistry (53,54), with the synthesis and separation of indoles from nature rising dramatically (Fig 3). The following are some of the important drugs with an indole moiety that are utilised as pharmacological agents: Sumatriptan 8, Tadalafil 9, Rizatriptan 11, and Fluvastatin 10. (54) (Fig 4).

As a result of crucial findings, this review provides a thorough examination of contemporary indole nucleus applications in a variety of biological domains. Fungi infect many people every year, but their impact on the global burden of illness is largely overlooked, and many of them produce small illnesses that kill just as many people as tuberculosis or dengue. (55) This is attributed to an increase in the number of people who have a compromised immune system or who are immunocompromised due to immunodeficiency, chemotherapy, or transplantation. Additionally, due to overuse or improper administration of drugs, bacterial diseases have become more resistant to them, potentially resulting in a global health disaster. (56) In addition to this, Methicillin and Vancomycin are most commercially accessible drugs, which are no longer usable against the current care facility illnesses. As a result, these drugs were only used to treat the most serious cases. As a result, these drugs are generally used for treating the most challenging illnesses as a way to stop the spread of resistance. (57-59) Mitomycin is a type of biologically active indole alkaloid, and its compounds are getting popular due to their widespread use as chemotherapeutic drugs and their good antimicrobial activities. (60,61)

Compounds with a modified specificity profile can produce distinct and very few undesirable side effects when used in accordance with a strategic plan. (62) According to the literature study, triazole-indole hybrid molecules have already been produced and are regarded as having outstanding properties. (63) Furthermore, it was shown that a free N-H in the aromatic ring was needed for antimicrobial activities against *E. coli*, *K. pneumoniae*, and *P. aeruginosa*. (64) Because of its nontoxicity, broad protection, and good pharmacological qualities, the nucleus of triazole analogues has received a lot of attention (65), and it was discovered that adding the sulfur atom, which is an electron rich particle in the triazole ring, greatly improves the biological activity of the target molecules. (66) This is be-

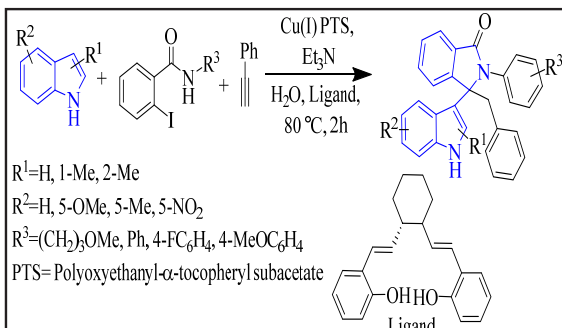
cause the sulfur particles influence lipophilicity and electronic structure in the triazole ring, resulting in increased transmembrane diffusion and interaction with macromolecular substrates. (67)

### ***Main text: synthetic approach of bioactive indoles***

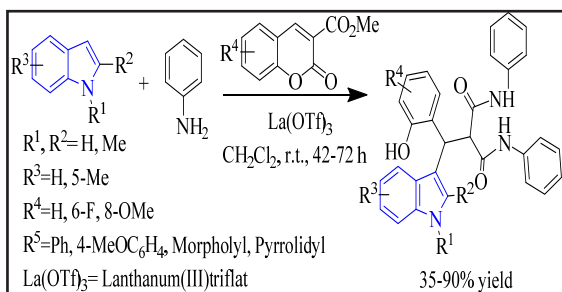
The Fischer indole synthesis was a very crucial and effective approach for the development of a range of indole intermediates and physiologically active chemicals for over a century. For synthetic organic chemists, the synthesis and bioactivity of indoles were of prominent emphasis, and numerous methods for their manufacture have been discovered. Many reactions are metal-based synthesis that takes place at room temperature in the presence of various catalysts, whereas others are acid and base catalyst-based reactions. Some of the most important are phase transfer reactions.

### ***Metal-mediated synthesis***

Organic molecule formation depends heavily on metals and their oxides, which catalyze many reactions in different ways. Sarkar et al. synthesized 2-phenyl-2,3-dihydroisoindolinones using regioselective cyclization, CuI (Copper Iodide) as catalysts, and PTS (Platinum Monosulfide) analogues of methan-1-yl-1-ylidene-diphenol as ligands. Under aerobic circumstances, the reaction involved a one-pot multicomponent process using indoles, which are 4-Iodo-N-phenylbenzamide and terminal alkynes, followed by a nucleophilic addition (Scheme 1). (68) J. J. Jennings revealed the formation of indolylmalonamides through a 3-component reaction involving indole, chromene-3-carboxylates, and amines in the presence of a Lewis acid catalyst, La(OTf)<sub>3</sub> (Scheme 2). When exposed to long-wavelength UV rays, indolylmalonamide molecules demonstrated remarkable fluorescence properties (366 nm). (69)

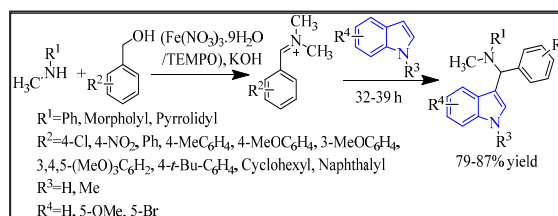


Scheme 1. Synthesis of phenyl-dihydroisoin-dolinones derivative.

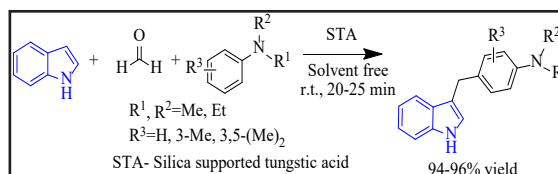


Scheme 2. Synthesis of indolylmalonamides derivative.

The one-pot, three-component Mannich type reaction involving the combination of amines, alcohols, and indoles as proposed by Singh et al. is an extremely effective way to synthesize 3-amino-alkylated indole derivatives. In the presence of  $\text{Fe}(\text{NO}_3)_3 \cdot 9\text{H}_2\text{O}/\text{TEMPO}(2,2,6,6\text{-tetramethylpiperidin-1-yl)oxyl}$  as a catalyst, amines and alcohols were treated with potassium hydroxide in toluene to produce iminium ions. After that, the iminium ion interacted with indoles to form a new 3-substituted indole compound (Scheme 3). (70-72) Shinde and Jeong discovered the reaction of indole and formaldehyde with tertiary aromatic molecules in the presence of silica-supported tungstic acid (STA) as a catalyst support under solvent-free conditions to synthesize amino arylated indole. For the synthesis of such amino arylated indole analogues, this technique was carried out using a 3-component Mannich method and Friedel-Crafts additions (Scheme 4). (73)

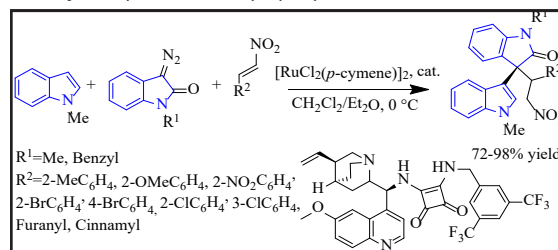


Scheme 3. Synthesis of 3-amino-alkylated indoles derivative.



Scheme 4. Synthesis of amino arylated indole derivative.

Chen et al. also revealed the preparation of bis-indole variants using N-Methyl indole, diazooxindole, and nitrostyrene via an asymmetrical addition reaction in the presence of  $[\text{Ru}]$  as well as squaramide ( $\text{O}_2\text{C}_4(\text{NH}_2)_2$ ) as catalysts (Scheme 5). (74)



Scheme 5. Synthesis of variants of bis-indole derivative.

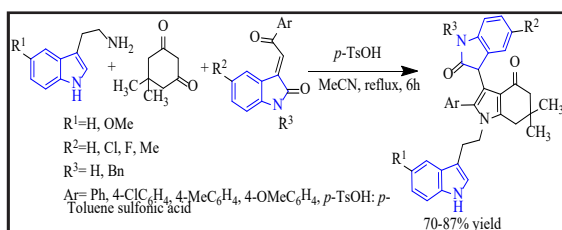
### Acid-catalysed synthesis

A catalytic process is explained as the method of changing the rate of a chemical reaction by using a catalyst that is not modified throughout the chemical process. Catalysis pathways can be categorised as either selective or generalized, depending on the different molecules that behave like acids or bases.

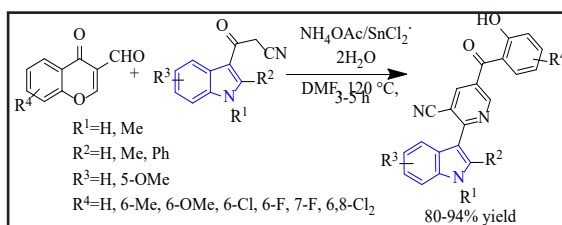
Jiang and Yan have demonstrated a three-component procedure for the formation of analogues such as tetrahydro-1H-in-



dolin-2-ones. In this synthesis (Scheme 6), a one-pot condensation reaction of indole using dimedone as well as 3-phenacylideneoxindoles in vaporising acetonitrile (MeCN) utilising *p*-toluene sulfonic acid (*p*-TsOH) acts as a motivator well as 3-phenacylideneoxindoles in vaporising acetonitrile (MeCN) utilising *p*-toluene sulfonic acid (*p*-TsOH) acts as a motivator. (75) The bifunctional indole-3-yl pyridines were manufactured by Poomathi and coworkers via an effective one-pot synthesis of formyl-chromones with ammonium acetate in dimethylformamide (DMF) with stannous chloride mediation (Scheme 7). (76)



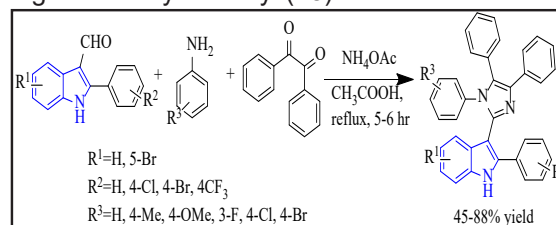
Scheme 6. Synthesis of tetrahydro-1H-indolin-2-ones derivative.



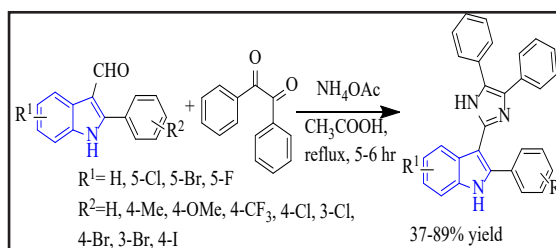
Scheme 7. Synthesis of indole-3-yl pyridines derivative.

Naureen et al. used a one-pot multi-component condensation technique to develop indole-based tetra-aryl-imidazoles. This method (Scheme 8) employs the reaction of indole-3-carbaldehydes, anilines, and benzyls in acetic acid in the presence of ammonium acetate. The anti-urease action of the produced molecules was tested, and the results were positive. (77) Naureen et al. further developed analogues of 2-phenyl-1H-indoles by condensing formyl indole, benzil, and ammonium acetate

under refluxing acetic acid conditions (Scheme 9). The compounds were tested for  $\alpha$ -glucosidase inhibitory activity and considered to have high inhibitory efficacy. (78)

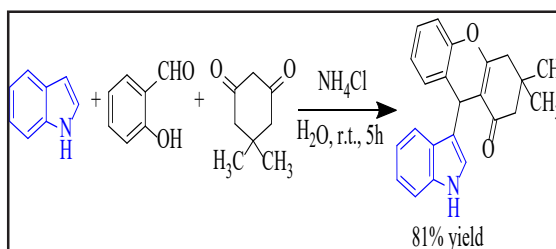


Scheme 8. Synthesis of tetra-aryl-imidazoles derivative.

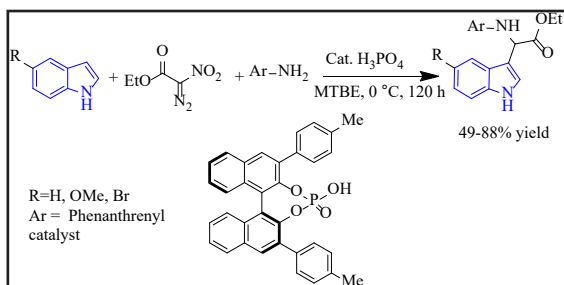


Scheme 9. Synthesis of phenyl-1H-indoles derivative.

Bhattacharjee et al. used ammonium chloride as a promoter in the one-pot synthesis of indole using salicylaldehyde and dimedone to produce analogues of tetrahydro-1H-xanthen-1-one (Scheme 10). (79) So and Mattson demonstrated the preparation of glycine products using chiral based phosphoric acid as a catalyst. The multi-component linking processes of indole compounds, nitro-diazoester, or anilines in methyl tert-butyl ether (MTBE), which acts as a solvent, have been used in this method (Scheme 11). (80)

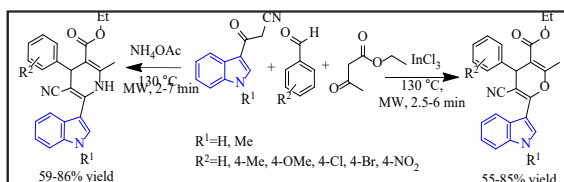


Scheme 10. Synthesis of analogues of tetrahydro-xanthenone.

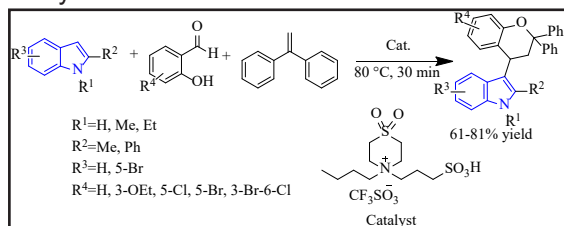


Scheme 11. Synthesis of glycine derivative.

Borah et al. synthesized the functionalized indole derivatives obtained via one-pot multicomponent synthesis of analogues of aldehydes, cyanoacetyl-indoles, as well as ethyl acetoacetate, with the addition of indium chloride ( $\text{InCl}_3$ ) under microwave irradiation. The one-pot reaction was performed after  $\text{NH}_4\text{OAc}$  was employed as the source of ammonia in this process, producing the analogues of indole (Scheme 12). (81) Taheri et al. employed a sulfone-containing Bronsted acid (ions-based liquid), in a one-pot reaction combining indole, salicylaldehydes, and 1,1-diphenylethylene to make substituted chromane compounds (Scheme 13). (82)



Scheme 12. Synthesis of analogues of cyanoacetyl-indoles.

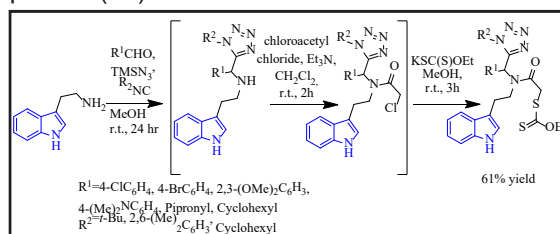


Scheme 13. Synthesis of substituted chromane derivative.

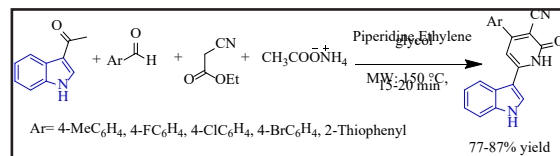
### Base-catalysed synthesis

Gordillo-Cruz et al. showed several steps to synthesize 3-substituted indoles

(Scheme 14) using 3-aminomethylindole chlorobenzene and  $\text{TMSN}_3$  (trimethylsilyl azide). The first step was cyclization/substitution, which was subsequently N-acylated using chloroacetyl chloride to produce stage B, which was further treated with potassium ethyl xanthogenate salts to produce the final compound xanthates. (83) Sayed et al. reported the synthesis of different 6-indolylpyridine-3-carbonitriles via a one-pot multi-component strategy in the presence of a catalyst. The reaction involves 3-acetylindole, aldehydes, ethyl cyanoacetate, and ammonium acetate (Scheme 15). They show good anti-proliferative properties of the synthesized compound. (84)



Scheme 14. Synthesis of xanthates derivative.

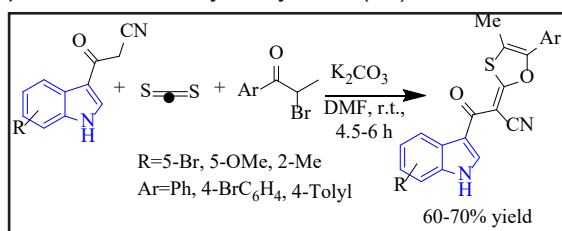


Scheme 15. Synthesis of 3-acetylindole derivative.

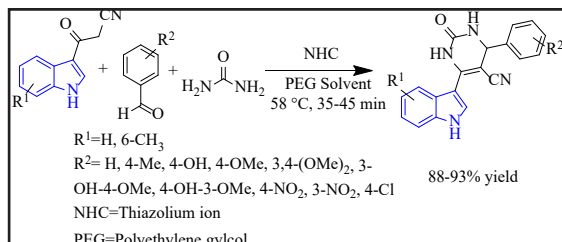
Liu et al. revealed the synthesis of two carbon-tethered compounds that are analogues to the pair of 1,3-oxathiole-indoles. The method involves a three-component domino [3+2] heterocyclization procedure with indole, carbon disulfide, and substituted  $\alpha$ -bromo propiophenones (Scheme 16). (85) According to Fatma et al., combining cyanoacetyl-indoles with an aryl-aldehyde and urea in the presence of PEG-400 (polyethylene glycol) and the catalytic amount of thiazolium anion based on the N-heterocyclic carbene (NHC) resulted in a diverse set of tetrahydropyrimidine analogues. (86)

Viola et al. developed the new coumarin substituted indole derivatives by microwave irradiation.

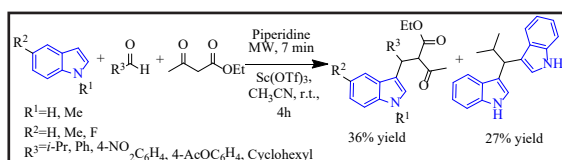
diating indole, salicylaldehyde, and malonates at room temperature in the presence of piperidine and Scandium triflate (Scheme 18). The main drawback of this reaction is that the compounds show very low yields. (87)



Scheme 16. Synthesis of 1,3-oxathiole-indole derivative.

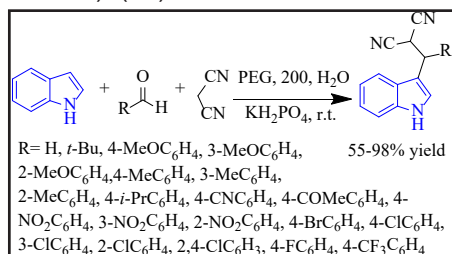


Scheme 17. Synthesis of tetrahydro pyrimidine based carbonitriles derivative.



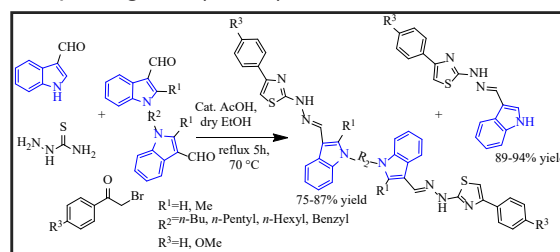
Scheme 18. Synthesis of coumarin derivative.

Wan et al. produced 3-substituted indole compounds in good to exceptional yields using polyethylene glycol (PEG) as a supporting base, in a 3-component reaction involving aldehydes, indoles, as well as malononitrile (Scheme 19). (88)



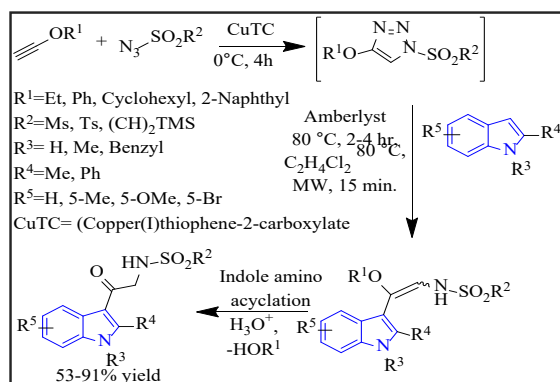
Scheme 19. Synthesis of analogue of 3-indole.

For the synthesis of new mono- as well as the bis-hydrazineyl thiazole analogues, Mahmoodi et al. conducted a one-pot cyclo-condensation using thiosemicarbazide and 3-formyl indole with the addition of a promotor such as acetic acid (Scheme 20). In vitro anti-bacterial activity against Gram-positive & the Gram-negative pathogens was examined for the synthesized derivatives. The thiazole analogue containing methoxy as a donor agent demonstrated potent antimicrobial activity against gram-positive pathogens. (89-91)



Scheme 20. Synthesis of hydrazineyl thiazole derivative.

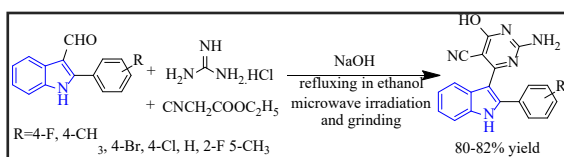
Slight aminoacylation of indoles was established by Alford et al. for the preparation of oxo-tryptamines using a multicomponent procedure with ynol ethers and sulfonyl azides. (Scheme 21). First, ynol ethers and sulfonyl



Scheme 21. Synthesis of oxo-tryptamines.

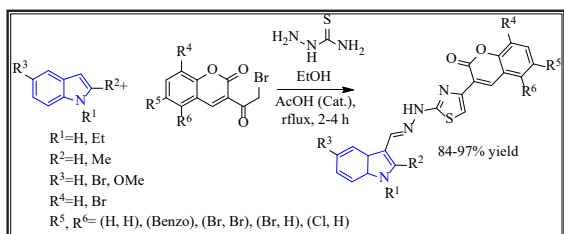
azides were used to make derivatives of N-sulfonyltriazaoles, which were then treated with indoles. For the  $\alpha$ -aminoacylation of enols, the amino ketone was converted to enol ethers. (92)

Gupta et al. synthesized the hydroxy pyrimidine compounds via one-pot synthesis of indole-3-aldehyde derivatives, ethyl cyanoacetate, and guanidine HCl. The reaction was tested under three different conditions: microwave irradiation, grindstone technology, and boiling (Scheme 22). The antimicrobial activity of the items was tested against harmful microbes and found to be relatively mild. (93)

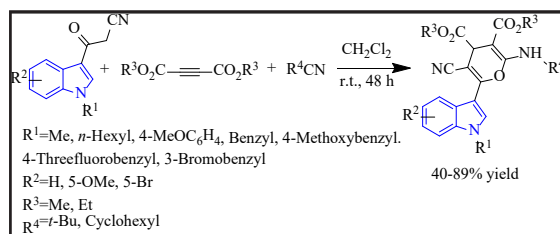


Scheme 22. Synthesis of hydroxy pyrimidines compounds.

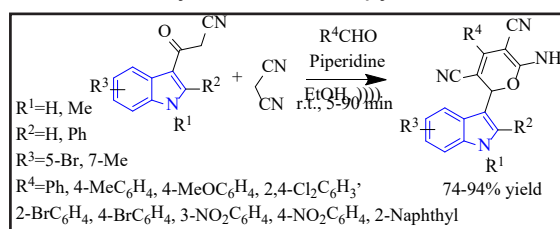
According to Gali et al., a range of indole integrated thiazolyl coumarins have been produced utilising a catalyst proportion of acetic acid in a reaction that involves indole variants, thiosemi-carbazides, and derivatives of chromen-2-ones (Scheme 23). [94] For the synthesis of analogues of 4H-pyran that have an indole scaffold, Song et al. demonstrated the [3+3] cyclization of analogues of cyanoacetyl-based indoles with DMAD & isocyanides (Scheme 24). (95) Chen and co-workers studied the effective preparation of substituted indole-pyran compounds using a one-pot mechanism of aldehydes, 3-cyanoacetyl indoles, and malononitrile with the addition of piperidine, which acts as a promotor. The reaction is carried out under ultrasonic irradiation at room temperature (Scheme 25). Thiamine hydrochloride, which is vitamin B<sub>1</sub> & CTAB were also used as promoters in this process, giving 92–94% products. (96)



Scheme 23. Synthesis of thiazolyl coumarins.



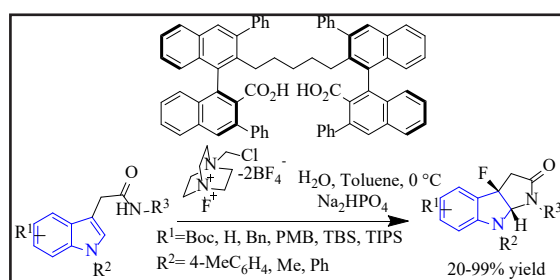
Scheme 24. Synthesis of 4-H-pyran derivative.



Scheme 25. Synthesis of substituted indole-pyran compounds.

### Phase transfer catalyst mediated synthesis

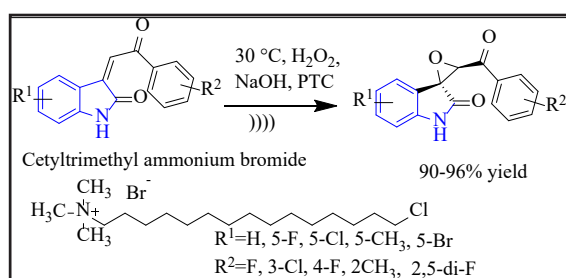
A different type of catalyst is a catalytic reaction with phase-transfer catalytic conditions. Ionic reactants are regularly soluble in an aqueous solution but insoluble in an organic liquid in the absence of a phase-transfer catalyst (PTC). The accelerator acts as a solvent, dissolving the ions in the organic solvent. Hiromichi et al. discovered fluorocyclization based indole analogues with the help of a dianionic phase-transfer catalyst. In this process, the author produces pyrroloindoline compounds, which are highly enantioselective under a modest synthesis method. (Scheme 26). (97)



Scheme 26. Synthesis of pyrroloindoline derivative.

The diastereoselective preparation of

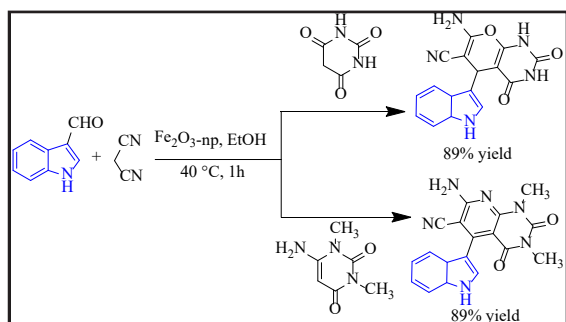
fluorine-containing [indole-3,2-oxirane] derivatives by using phase transfer catalyst (PTC) acetyl-trimethyl ammonium bromide was revealed by Dandia et al. The developed method was novel and eco-friendly for the manufacture of different indole-based heterocycles. The protocol involves aqueous ultrasonic irradiation for the epoxidation of indole-2-one analogues, which produce analogues of 3-benzoyl-2(1H)-ones (Scheme 27). (98)



Scheme 27. Synthesis of benzoyl-2(1H)-ones derivative.

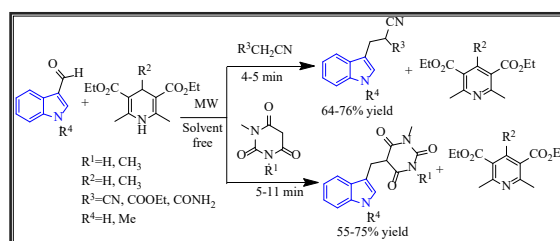
### Miscellaneous

M. Kidwai et al. unfolds the formation of pyrano[2,3-d] pyrimidines as well as the pyrido[2,3-d] pyrimidines by using magnetic particles ( $\text{Fe}_3\text{O}_4$ -NPs). The processes were carried out in ethanol using a 3-component one-pot process involving malononitrile, indole & barbituric acids as well as the 6-amino uracil analogues. (Scheme 28). (99)

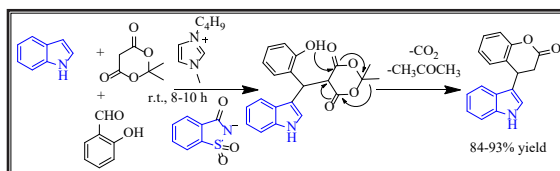


Scheme 28. Synthesis of pyrano[2,3-d] pyrimidines & analogues of pyrido[2,3-d] pyrimidines.

Baruah et al. described the formation of 3-alkylated indole analogues (Scheme 29). In a convection-driven 3-component reaction of alkyl nitriles, indole-3-aldehydes, as well as barbituric acids using DPH (1,4-dihydropyridines) analogues. (100) Atul et al. developed imidazolium saccharinate via multicomponent reaction between indole, salicylaldehyde and cyclic active methylene derivatives using ionic liquids. The study revealed that decarboxylation enhanced the properties of indoles and dihydrocoumarin, which give coumarin-based analogues of indole (Scheme 30). (101)



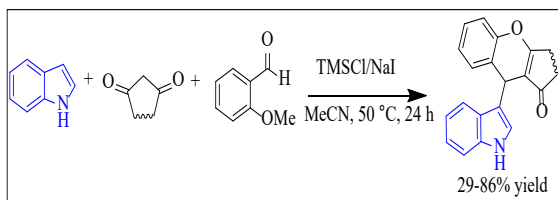
Scheme 29. Synthesis of alkylated indole derivative.



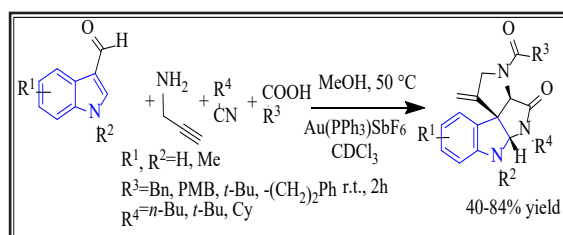
Scheme 30. Synthesis of imidazolium saccharinate.

Khalafi-Nezhad et al. demonstrated the utilisation of trimethylsilyl-chloride as a multipurpose catalyst for a one-pot, three-component reaction to produce analogues of xanthen-(9H)-ones from the reaction of indole and analogues of di-carbonyls. (Scheme 31). (102) The author developed a novel diastereoselective domino cyclization method using post-Ugi gold as the promotor for diastereoselective domino cyclization to synthesize variously substituted spiroindolines in Scheme 32. The Ugi reaction of propargylamine, acids, indole-3-aldehydes, or isocyanides yields a very high number of molecules that react with  $\text{Au}(\text{PPh}_3)_3\text{SbF}_6$  in chloroform ( $\text{CDCl}_3$ ) to form spiro-indolines in moderate yields. (103,104)



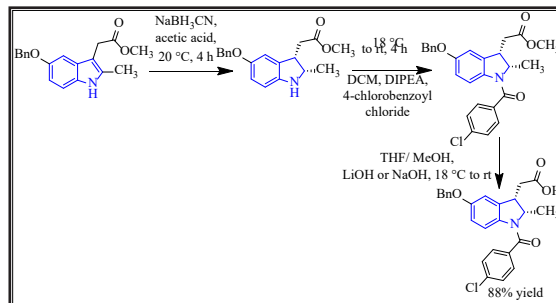


Scheme 31. Synthesis of xanthen-4-(9H)-ones derivative.

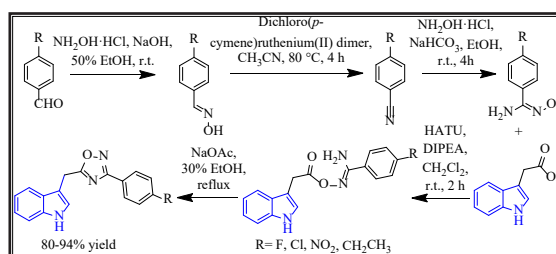


Scheme 32. Synthesis of derivative of spiroindolines.

The newly synthesized indole derivative, 1-(4-chlorobenzene)-5-hydroxy-2-methyl-3-indoleacetic acid, was shown to have insulin-sensitizing and glucose-lowering properties. Scheme 33 represents the seven-step synthesis of a product from para-nitrophenol. The final compound revealed the strongest hypoglycemic activity of any indole-3-butyric acid derivative. However, because of the presence of a 2,3-double bond, the amide bond of the final compound is easily hydrolyzed. (105) The 1,2,4-oxadiazole ring linked to the indole scaffold distinguishes phidians. They were first isolated from the aeolid opisthobranch mollusk *Phidiana militaris* in 2011, according to Gavagnin et al. (106). These indole compounds had strong cytotoxicity as well as neuroprotective properties as typical secondary metabolites. Furthermore, the findings indicated that they were both T-cell protein tyrosine phosphatase (TCPTP) and protein tyrosine phosphatase 1 B (PTP1B) inhibitors. Furthermore, structure-activity relationships (SAR) and molecular docking analyses of 40 different phidians analogues revealed that a 1,2,4-oxadiazole ring was required for PTP1B inhibitory activity. Scheme 34 (107) depicts the function-oriented synthesis of PTP1B inhibitory analogues.

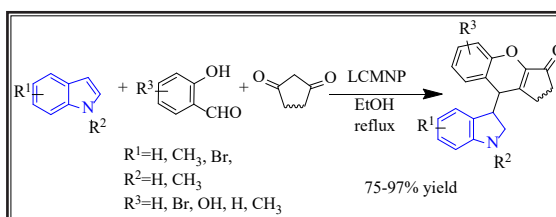


Scheme 33. Synthesis of derivative of indole-3-butyric acid.



Scheme 34. Synthesis of derivative of phidians.

Since many years, researchers have been studying the synthesis of 9-(1H-indol-3-yl) xanthen-4-(9H)-ones derivatives (Scheme 35), it is a class of multifunctional heterocyclic chemicals with an indole ring, and their inhibitory ac-



tivity on  $\alpha$ -glucosidase [108].

Scheme 35. Synthesis of 9-(1H-indol-3-yl) xanthen-4-(9H)-ones derivatives

## Conclusion

In medicinal chemistry and drug development, indole and its derivatives have proven to be excellent target molecules. They can be found in a broad range of organic sources,

and novel indole derivatives are produced on a regular basis. Because these scaffolds bind to a broad range of proteins, their production represents a possible route to new lead molecules. The pharmacological actions of indole scaffolds have been highlighted in this review. The remarkable biological and physiological activity of such indoles makes them potential candidates for microbe-borne diseases and other health problems like Alzheimer's disease. The indole is a very versatile nucleus in the pharmacological sector, as evidenced by the therapeutic potential of indole analogues. As a result, the information is expected to aid in the development of novel compounds with improved bioactive components, as well as novel synthetic methodologies.

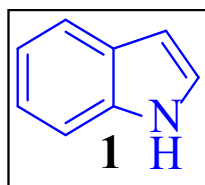


Fig 1 Structure of indole.

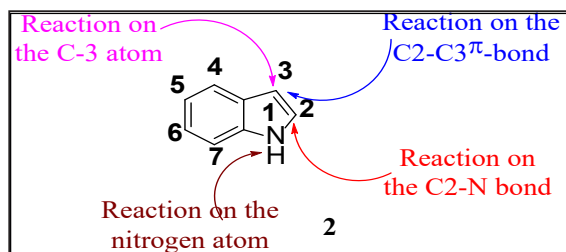


Fig 2. Active of carbon nitrogen in indole compound.

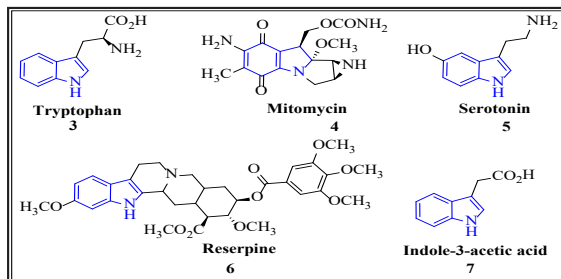


Fig 3. The structure of indole alkaloids.

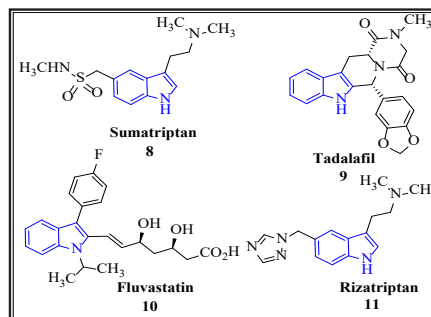


Fig 4. The structure of some pharmacological agents.

## Reference

- Evans, B. E., Rittle, K. E., Bock, M. G., Di Pardo, R. M., Freidinger, R. M., Whitter, W. L., Lundell, G. F., Veber, D. F., Anderson, P. S., Chang, R. S. L., Lotti, V. J., Cerino, D. J., Chen, T. B., Kling, P. J., Kunkel, K. A., Springer, J. P. and Hirshfield, J. (1988). Methods for Drug Discovery: Development of Potent, Selective, Orally Effective Cholecystokinin Antagonists. *J. Med. Chem.*, 31:2235-2246.
- Van Order, R. B., and Lindwall, H. G. (1942). Indole. In *Chem. Rev.*, 30:69-96.
- Horton, D. A., Bourne, G. T. and Smythe, M. L. (2003). The combinatorial synthesis of bicyclic privileged structures or privileged substructures. *Chem. Rev.*, 103:893-930.
- Sniady, A., Morreale, M. S., Wheeler, K. A. and Dembinski, R. (2008). Room-temperature electrophilic 5-endo-dig chlorocyclization of alk-3-yn-1-ones with the use of pool sanitizer: Synthesis of 3-chlorofurans and 5-chlorofuropyrimidine nucleosides. *European J. Org. Chem.*, 20:3449-3452.
- Cocuzza, A. J., Chidester, D. R., Culp, S., Fitzgerald, L. and Gilligan, P. (1999). Use of the suzuki reaction for the synthesis of aryl-substituted heterocycles as corticotropin-releasing hormone (CRH) antagonists, *Bioorganic & Med. Chem. Lett.*, 9:1063-1066.

6. Vitaku, E., Smith, D. T. and Njardarson, J. T. (2014). Analysis of the structural diversity, substitution patterns, and frequency of nitrogen heterocycles among U.S. FDA approved pharmaceuticals. *J. Med. Chem.*, 57:10257-10274.
7. Vitaglione, P. and Fogliano, V. (2004). Use of antioxidants to minimize the human health risk associated to mutagenic/carcinogenic heterocyclic amines in food. *J. Chromatography B: Analytical Technologies in the Biomedical and Life Sci.*, 802:189-199.
8. Abdel-Wahab, B. F., Awad, G. E. A. and Badria, F. A. (2011). Synthesis, antimicrobial, antioxidant, anti-hemolytic and cytotoxic evaluation of new imidazole-based heterocycles. *J. Med. Chem.*, 46:1505-1511.
9. Talati, J. D. and Gandhi, D. K. (1983). *N*-heterocyclic compounds as corrosion inhibitors for aluminium-copper alloy in hydrochloric acid. *Corr. Sci.*, 23:1315-1332.
10. Raja, P. B. and Sethuraman, M. G. (2008). Natural products as corrosion inhibitor for metals in corrosive media-A review. *Mat. Lett.*, 62:113-116.
11. Stead, C. V. (1982). Halogenated heterocycles in reactive dyes. *Dyes and pigments*, 3:161-171.
12. Li, G. and Donghui, Z. (2009). Cyclic poly( $\alpha$ -peptoid)s and their block copolymers from *N*-heterocyclic carbene-mediated ring-opening polymerizations of *N*-substituted *N*-carboxylanhydrides. *J. Am. Chem. Soc.*, 131:18072-18074.
13. Butuc, E. and Gherasim, G. M. (1984). Ordered heterocyclic copolymers. Polyamide-imides with S-triazine rings. *J. Poly. Sci.: Poly. Chem. Ed.*, 22:503-507.
14. Sunderhaus, J. D. and Martin, S. F. (2009). Applications of multicomponent reactions to the synthesis of diverse heterocyclic scaffolds. *Chem.-A Euro. J.*, 15:1300-1308.
15. Zhu, J. (2003). Recent developments in the isonitrile-based multicomponent synthesis of heterocycles. *Euro. J. Org. Chem.*, 7:1133-1144.
16. Jiang, B., Rajale, T., Wever, W., Tu, S. J. and Li, G. (2010). Multicomponent reactions for the synthesis of heterocycles. *Chem.-An Asian J.*, 5:2318-2335.
17. Ugi, I., Domling, A. and Werner, B. (2000). Since 1995 the new chemistry of multicomponent reactions and their libraries, including their heterocyclic chemistry. *J. Het. Chem.*, 37:647-658.
18. Kappe, C. O. (2000). Recent advances in the Biginelli dihydropyrimidine synthesis. New tricks from an old dog. *Acc. Chem. Res.*, 33:879-888.
19. Orru, R. V. A. and De Greef, M. (2003). Recent advances in solution-phase multicomponent methodology for the synthesis of heterocyclic compounds. *Syn.*, 10:1471-1499.
20. Ngouansavanh, T. and Zhu, J. (2006). Alcohols in Isonitrile-Based Multicomponent Reaction: Passerini Reaction of Alcohols in the Presence of *O*-Iodoxybenzoic Acid. *Angewandte Chemie*, 118:3575-3577.
21. Ishikura, M., Abe, T., Choshi, T. and Hibino, S. (2015). Simple indole alkaloids and those with a nonrearranged monoterpenoid unit. *Nat. Prod. Rep.*, 32:1389-1471.
22. Kinsman, A. C. and Kerr, M. A. (2003). The Total Synthesis of (+)-Hapalindole Q by an Organomediated Diels-Alder Reaction. *J. Amer. Chem. Soc.*, 125:14120-14125.
23. Chang-Fong, J., Rangisetty, J. B., Dukat, M., Setola, V., Raffay, T., Roth, B. and Glennon, R. A. (2004). 1,2,3,4-Tetrahydro-carbazoles as 5-HT<sub>6</sub> serotonin receptor

- ligands. *Bioorg. and Med. Chem. Lett.*, 14:1961-1964.
24. Brock, W. H. (2001). Baeyer (Johann Friedrich Wilhelm Adolf von.) (eLS)
25. Robinson, B., (1969). Recent studies on the Fischer indole synthesis. *Chem. rev.*, 69:227-250.
26. Robinson, B., (1963). The Fischer indole synthesis. *Chem. rev.*, 63:373-401.
27. Kumari, A. and Singh, R. K. (2019). Medicinal chemistry of indole derivatives: Current to future therapeutic prospectives. In *Bioorg. Chem.*, 89:103021.
28. Mohammad, A., Bhat, A. R., Hoi, K. K., Choi, I. and Athar, F. (2017). Synthesis, characterization and antibacterial screening of some novel 1,2,4-triazine derivatives. *Chin. Chem. Lett.*, 28:1559-1565.
29. Lepri, S., Buonerba, F., Goracci, L., Velilla, I., Ruzziconi, R., Schindler, B. D., Seo, S. M., Kaatz, G. W. and Cruciani, G. (2016). Indole Based Weapons to Fight Antibiotic Resistance: A Structure-Activity Relationship Study. *J. Med. Chem.*, 59:867-891.
30. Liu, Q. L., Chen, A. H., Tang, J. Y., Ma, Y. L., Jiang, Z. H., Liu, Y. P., Chen, G. Y., Fu, Y. H. and Xu, W. (2017). A new indole alkaloid with anti-inflammatory activity from *Nauclea officinalis*, *Nat. Prod. Res.*, 31:2107-2112.
31. Abadi, A. H., Hegazy, G. H. and El-Zaher, A. A. (2005). Synthesis of novel 4-substituted-7-trifluoromethylquinoline derivatives with nitric oxide releasing properties and their evaluation as analgesic and anti-inflammatory agents, *Bioorg. & Med. Chem.*, 13:5759-5765.
32. Giampieri, M., Balbi, A., Mazzei, M., La Colla, P., Ibba, C. and Loddo, R. (2009). Antiviral activity of indole derivatives. *Antiviral Res.*, 83:179-185.
33. Li, J. Y., Sun, X. F., Li, J. J., Yu, F., Zhang, Y., Huang, X. J. and Jiang, F. X. (2020). The antimalarial activity of indole alkaloids and hybrids. *Archiv Der Pharm.*, 353:2000131.
34. Mukhopadhyay, S., Handy, G. A., Funayama, S. and Cordell, G. A. (1981). Anticancer indole alkaloids of *Rhazya stricta*. *J. Nat. Prod.*, 44:696-700.
35. Dekker, W. H., Selling, H. A. and Overeem, J. C. (1975). Structure-Activity Relations of Some Antifungal Indoles. *J. Agri. and Food Chem.*, 23:785-791.
36. Desai, N. C., Somani, H., Trivedi, A., Bhatt, K., Nawale, L., Khedkar, V. M., Jha, P. C. and Sarkar, D. (2016). Synthesis, biological evaluation and molecular docking study of some novel indole and pyridine based 1,3,4-oxadiazole derivatives as potential antitubercular agents. *Bioorg. and Med. Chem. Lett.*, 26:1776-1783.
37. Estevão, M. S., Carvalho, L. C., Ribeiro, D., Couto, D., Freitas, M., Gomes, A., Ferreira, L. M., Fernandes, E. and Marques, M. M. B. (2010). Antioxidant activity of unexplored indole derivatives: Synthesis and screening. *Euro. J. Med. Chem.*, 45:4869-4878.
38. Dolle, R. E. and Nelson, K. H. (1999). Comprehensive survey of combinatorial library synthesis: 1998. *J. Com. Chem.*, 1:235-282.
39. Franzén, R. G. (2000). Recent advances in the preparation of heterocycles on solid support: A review of the literature. *J. Comb. Chem.*, 2:195-214.
40. Dolle, R. E. (2001). Comprehensive survey of combinatorial library synthesis: 2000. *J. Comb. Chem.*, 3:477-517.
41. Hanessian, S., McNaughton-Smith, G., Lombart, H. G. and Lubell, W. D. (1997). Design and synthesis of conformationally constrained amino acids as versatile

- scaffolds and peptide mimetics. *Tetrah.*, 53:12789-12854.
42. Paprocki, D., Madej, A., Koszelewski, D., Brodzka, A. and Ostaszewski, R. (2018). Multicomponent reactions accelerated by aqueous micelles. *Fron. in Chem.*, 6:1-21.
43. Ziarani, G. M., Hosseini, Nasab, N. and Lashgari, N. (2016). Synthesis of heterocyclic scaffolds through 6-aminouracil-involved multicomponent reactions. *RSC Adv.*, 6:38827-38848.
44. Ziarani, G. M., Moradi, R. and Lashgari, N. (2015). Asymmetric synthesis of chiral 3,3-disubstituted oxindoles using isatin as starting material. *Tetrah. Asymm.*, 26:517-541.
45. Ziarani, G. M., Hosseini Nasab, N. and Lashgari, N. (2016). Synthesis of heterocyclic scaffolds through 6-aminouracil-involved multicomponent reactions. *RSC Adv.*, 6:38827-38848.
46. Ziarani, G. M., Aleali, F. and Lashgari, N. (2016). Recent applications of barbituric acid in multicomponent reactions *RSC Adv.*, 6:50895-50922.
47. Ziarani, G. M., Gholamzadeh, P., Lashgari, N. and Hajiabbasia, P. (2013). Oxindole as starting material in organic synthesis. *Arkivoc: Online J. Org. Chem.*, 2013:470-535.
48. Ziarani, G. M., Lashgari, N., Azimian, F., Kruger, H. G. and Gholamzadeh, P. (2015). Ninhydrin in synthesis of heterocyclic compounds. *Arkivoc: Online J. Org. Chem.*, 2015:1-139.
49. Ahmadi, T., Ziarani, G. M., Gholamzadeh, P. and Mollabagher, H., (2017). Recent advances in asymmetric multicomponent reactions (AMCRs). *Tetrah. Asymm.*, 28:708-724.
50. Moradi, R., Ziarani, G. M. and Lashgari, N. (2017). Recent applications of isatin in the synthesis of organic compounds. *Arkivoc: Online J. Org. Chem.*, 2017:148-201.
51. Rahimifard, M., Ziarani, G. M. and Lashkariani, B. M. (2014). Application of guanidine and its salts in multicomponent reactions. *Tur. J. Chem.*, 38:345-371.
52. Ali, S., Zakir, S., Patel, M. and Farooqui, M. (2012). Synthesis of new a aminophosphonate system bearing Indazole moiety and their biological activity. *Euro. J. Med. Chem.*, 50:39-43.
53. Baumann, M., Baxendale, I. R., Ley, S. V. and Nikbin, N. (2011). An overview of the key routes to the bestselling 5-membered ring heterocyclic pharmaceuticals. *Beils. J. Org. Chem.*, 7:442-495.
54. Inman, M. and Moody, C. J. (2013). Indole synthesis-something old, something new. *Chem. Sci.*, 4:29-41.
55. Brown, G. D., Denning, D. W., Gow, N. A. R., Levitz, S. M., Netea, M. G. and White, T. C. (2012). Hidden killers: Human fungal infections. *Sci. Trans. Med.*, 4:165rv13.
56. Roberts, R. R., Hota, B., Ahmad, L., Scott, D., Foster, S. D., Abbasi, F., Schabowski, S., Kampe, L. M., Ciavarella, G., Supino, M., Naples, J., Cordell, R., Levy, S. B. and Weinstein, R. A. (2009). Hospital and societal costs of antimicrobial-resistant infections in a Chicago teaching hospital: implications for antibiotic stewardship. *Clin. Infect. Dis.*, 49:1175-1184.
57. Zhang, F. F., Gan, L. L. and Zhou, C. H. (2010). Synthesis, antibacterial and antifungal activities of some carbazole derivatives. *Bioorg. & Med. Chem. Lett.*, 20:1881-1884.
58. Liu, C., Bayer, A., Cosgrove, S. E., Daum, R. S., Fridkin, S. K., Gorwitz, R. J., Kaplan, S. L., Karchmer, A. W., Levine, D. P., Murray, B. E., Rybak, M. J., Talan, D. A. and Chambers, H. F. (2011). Clinical practice



- guidelines by the Infectious Diseases Society of America for the treatment of methicillin-resistant *Staphylococcus aureus* infections in adults and children. *Clin. Infect. Dis.*, 52:e18-e55.
59. Kaku, N., Morinaga, Y., Takeda, K., Kosai, K., Uno, N., Hasegawa, H., Miyazaki, T., Izumikawa, K., Mukae, H. and Yanagihara, K. (2016). Antimicrobial and immunomodulatory effects of tedizolid against methicillin-resistant *Staphylococcus aureus* in a murine model of hematogenous pulmonary infection. *Internat. J. Med. Microbio.*, 30:421-428.
60. O'Sullivan, D. A. and Lepkowski, W. (1990). Chemical science. *Chem. & Eng. News*, 8:42-61.
61. Berger, M., Gray, J. A. and Roth, B. L. (2009) The expanded biology of serotonin. *Ann. Rev. Med.*, 60:355-366.
62. Junior, C. V., Danuello, A., Bolzani, V. da, S., Barreiro, J. E. and Fraga, C. A. M. (2007). Molecular Hybridization: A Useful Tool in the Design of New Drug Prototypes. *Curr. Med. Chem.*, 14:1829-1852.
63. Shirinzadeh, H., Süzen, S., Altanlar, N., Westwell, A. D. (2018). Antimicrobial Activities of New Indole Derivatives Containing 1,2,4-Triazole, 1,3,4-Thiadiazole and Carbothioamide. *Tur. J. Pharm. Sci.*, 15:291-297.
64. Mane, Y. D., Sarnikar, Y. P., Surwase, S. M., Biradar, D. O., Gorepatil, P. B., Shinde, V. S. and Khade, B. C. (2017). Design, synthesis, and antimicrobial activity of novel 5-substituted indole-2-carboxamide derivatives. *Res. Chem. Interm.*, 43:1253-1275.
65. Schulze, B. and Schubert, U. S. (2014). Beyond click chemistry-supramolecular interactions of 1,2,3-triazoles. *Chem. Soc. Rev.* 43:2522-2571.
66. Küçükgülzel, G. and Çikla-Süzgün, P. (2015). Recent advances bioactive 1,2,4-triazole-3-thiones. *Euro. J. Med. Chem.*, 97:830-870.
67. Dilmaghani, K. A., Pur, F. N. and Nezhad, M. H. (2015) Synthesis and antibacterial evaluation of new thione substituted 1,2,4-triazole schiff bases as novel antimicrobial agents. *Iran. J. Pharm. Res.*, 14:693-699.
68. Sarkar, S., Pal, R. and Sen, A. K. (2013) Efficient synthesis of 3-benzyl-3-(indol-3-yl)-2-phenyl-2,3-dihydroisoindolinones derivatives via a simple and convenient MCR in aqueous micellar system. *Tetrah. Lett.*, 54:4273-4276.
69. Jennings, J. J., Bhatt, C. P. and Franz, A. K. (2016) Lanthanum(III)-Catalyzed Three-Component Reaction of Coumarin-3-carboxylates for the Synthesis of Indolylmalonamides and Analysis of Their Photophysical Properties. *J. Org. Chem.*, 81:6211-6222.
70. Li, J. J. (2003). Mannich reaction. *Name React.*, 2:246-247.
71. Zhang, E., Tian, H., Xu, S., Yu, X. and Xu, Q. (2013). Iron-catalyzed direct synthesis of imines from amines or alcohols and amines via aerobic oxidative reactions under air. *Org. Lett.*, 15 2704-2707.
72. Singh, V. K., Sharma, L. K. and Singh, R. K. P. (2016). Iron mediated one pot three component synthesis of 3-substituted indoles via aerobic iminium ion formation. *Tetrah. Lett.*, 57:407-410.
73. Shinde, V. V. and Jeong, Y. T. (2015). A green and convenient protocol for the synthesis of diarylmethanes via a one-pot, three-component reaction catalyzed by a novel silica tungstic acid (STA) under solvent-free conditions. *Comptes Rendus Chimie*, 18:449-455.

74. Chen, D. F., Zhao, F., Hu, Y., and Gong, L. Z. (2014). C-H functionalization/asymmetric michael addition cascade enabled by relay catalysis: Metal carbenoid used for C-C bond formation. *Angewandte Chemie-Int. Ed.*, 53:10763-10767.
75. Jiang, Y. H. and Yan, C. G. (2016). Three-Component Reaction for the Convenient Synthesis of Functionalized 3-{1-[2-(1*H*-Indol-3-yl)ethyl]-4,5,6,7-tetrahydro-1*H*-indol-3-yl}indolin-2-ones. *Syn.*, 48:3057-3064.
76. Poomathi, N., Muralidharan, D. and Perumal, P. T. (2013). Stannous chloride mediated one pot synthesis of functionalized indole-3-yl pyridines using 3-cyanoacetylindoles and 3-formylchromones. *Tetrah. Lett.*, 54:7091-7094.
77. Naureen, S., Chaudhry, F., Asif, N., Munawar, M. A., Ashraf, M., Nasim, F. H., Arshad, H. and Khan, M. A. (2015) Discovery of indole-based tetraarylimidazoles as potent inhibitors of urease with low antilipooxygenase activity. *Euro. J. Med. Chem.*, 102:464-470.
78. Naureen, S., Noreen, S., Nazeer, A., Ashraf, M., Alam, U., Munawar, M. A. and Khan, M. A. (2015) Triarylimidazoles-synthesis of 3-(4,5-diaryl-1*H*-imidazol-2-yl)-2-phenyl-1*H*-indole derivatives as potent  $\alpha$ -glucosidase inhibitors. *Med. Chem. Res.*, 24:1586-1595.
79. Bhattacharjee, S., Das, D. K. and Khan, A. T. (2014). Ammonium chloride-catalyzed three-component reaction for the synthesis of fused 4*H*-chromene derivatives in aqueous medium. *Syn.*, 46:73-80.
80. So, S. S. and Mattson, A. E. (2014). Stereoselective N-H insertion-arylation reactions of nitrodiazoesters. *Asian J. Org. Chem.*, 3:425-428.
81. Borah, P., Naidu, P. S., Majumder, S. and Bhuyan, P. J. (2014). Microwave-assisted one-pot multi-component reaction: synthesis of novel and highly functionalized 3-(pyranyl)- and 3-(dihydropyridinyl)indole derivatives. *Mol. Divers.*, 18:759-767.
82. Taheri, A., Lai, B., Yang, J., Zhang, J. and Gu, Y. (2016). Facile synthesis of densely substituted chroman derivatives through Brønsted acid ionic liquid catalyzed three-component reactions of aromatic aldehydes, 1,1-diarylethylenes and nucleophiles *Tetrah.*, 72:479-488.
83. Gordillo-Cruz, R. E., Gómez, A. R., Islas-Jácome, A., Cortes-García, C. J., Díaz-Cervantes, E., Robles, J. and Gámez-Montaña, R. (2013). Synthesis of 3-tetrazolylmethyl-azepino [4, 5-*b*]indol-4-ones in two reaction steps:(Ugi-azide/*N*-acylation/SN<sub>2</sub>)/free radical cyclization and docking studies to a 5-Ht 6 model. *Org. & Biomol. Chem.*, 11:6470-6476.
84. El-Sayed, N. S., Shirazi, A. N., El-Meligy, M. G., El-Ziaty, A. K., Rowley, D., Sun, J., Nagib, Z. A. and Parang, K. (2014). Synthesis of 4-aryl-6-indolylpyridine-3-carbonitriles and evaluation of their antiproliferative activity. *Tetrah. Lett.*, 55:1154-1158.
85. Liu, J. Y., Zhang, H., Feng, B. M., Jiang, B., Wang, S. L. and Tu, S. J. (2012). A multi-component synthetic strategy for two-carbon-tethered 1,3-oxathiole-indole pairs. *Org. & Biomol. Chem.*, 10:5036-5038.
86. Fatma, S., Singh, D., Mishra, P., Singh, P. K., Ankit, P., Singh, M. and Singh, J. (2013) Nucleophilic heterocyclic carbene promoted one pot multicomponent synthesis of new 6-(1*H*-indol-3-yl)-2-oxo-4-aryl-1,2,3,4-tetrahydropyrimidine-5-carbonitriles: an eco-compatible approach with PEG as a biodegradable medium. *RSC Adv.*, 3:22527-22531.
87. Viola, A., Ferrazzano, L., Martelli, G., Ancona, S., Gentilucci, L. and Tolomelli, A. (2014). An improved microwave assisted

- protocol for Yonemitsu-type trimolecular condensation. *Tetrah.* 70:6781-6788.
88. Wang, L., Huang, M., Zhu, X. and Wan, Y. (2013). Polyethylene glycol (PEG-200)-promoted sustainable one-pot three-component synthesis of 3-indole derivatives in water. *App. Cat. A: Gen.*, 454:160-163.
89. Mahmoodi, N. O. and Ghavidast, A. (2014). Synthesis of photochromic bis-1,3-diazabicyclo-[3.1.0]hex-3-ene derivatives having a bisindole linkage. *Chem. Het. Com.*, 49:1451-1457.
90. Gali, R., Banothu, J., Porika, M., Velpula, R., Bavantula, R. and Abbagani, S. (2014). Synthesis and *in vitro* cytotoxic activity of novel coumarinylimidazo[2,1-*b*]thiazole derivatives. *RSC Adv.*, 4:53812-53819.
91. Mahmoodi, N. O., Khalili, B., Rezaeianzade, O. and Ghavidast, A. (2016). One-pot multicomponent synthesis of indol-3-yl-hydrazinyl thiazoles as antimicrobial agents. *Res. Chem. Inter.*, 42:6531-6542.
92. Alford, J. S. and Davies, H. M. L. (2014). Mild aminoacylation of indoles and pyrroles through a three-component reaction with ynol ethers and sulfonyl azides. *J. Amer. Chem. Soc.*, 136:10266-10269.
93. Gupta, R., Jain, A., Madan, Y. and Menghani, E. (2014). A "One Pot," Environmentally Friendly, Multicomponent Synthesis of 2-Amino-5-cyano-4-[(2-aryl)-1*H*-indol-3-yl]-6-hydroxypyrimidines and Their Antimicrobial Activity. *J. Het. Chem.*, 51:1395-1403.
94. Gali, R., Banothu, J., Gondru, R., Bavantula, R., Velivela, Y. and Crooks, P. A. (2015). One-pot multicomponent synthesis of indole incorporated thiazolylcoumarins and their antibacterial, anticancer and DNA cleavage studies. *Bioorg. & Med. Chem. Lett.*, 25:106-112.
95. Song, P., Zhao, L. and Ji, S. (2014). Facile synthesis of 4*H*-pyran derivatives bearing indole skeleton via [3+3] cyclization of 3-indolyl-3-oxopropanenitriles with dialkyl acetylenedicarboxylates and isocyanides. *Chin. J. Chem.*, 32:381-386.
96. Zhu, S. L., Ji, S. J., Su, X. M., Sun, C. and Liu, Y. (2008). Facile and efficient synthesis of a new class of bis(3'-indolyl)pyridine derivatives via one-pot multicomponent reactions. *Tetrah. Lett.*, 49:1777-1781.
97. Egami, H., Hotta, R., Otsubo, M., Rouno, T., Niwa, T., Yamashita, K. and Hamashima, Y. (2020). Asymmetric Dearomatizing Fluoroamidation of Indole Derivatives with Dianionic Phase-Transfer Catalyst. *Org. Lett.*, 22:5656-5660.
98. Dandia, A., Singh, R. and Bhaskaran, S. (2011) Facile stereoselective synthesis of spiro[indole-oxiranes] by combination of phase transfer catalyst and ultrasound irradiation and their bioassay. *Ultra. Sonochem.*, 18:1113-1117.
99. Kidwai, M., Jain, A. and Bhardwaj, S. (2012). Magnetic nanoparticles catalyzed synthesis of diverse *N*-Heterocycles. *Mol. Div.*, 16:121-128.
100. Baruah, B., Naidu, P. S., Borah, P. and Bhuyan, P. J. (2012). Synthesis of 5-alkylated barbituric acids and 3-alkylated indoles via microwave-assisted three-component reactions in solvent-free conditions using Hantzsch 1,4-dihydropyridines as reducing agents. *Mol. Div.*, 16:291-298.
101. Kumar, A., Kumar, P., Tripathi, V. D. and Srivastava, S. (2012). A novel access to indole-3-substituted dihydrocoumarins in artificial sweetener saccharin based functional ionic liquids. *RSC Adv.*, 2:11641-11644.
102. Khalafi-Nezhad, A., Nourisefat, M. and Panahi, F. (2014). Trimethylsilyl iodide as a multifunctional agent in the one-pot synthesis of 9-(1*H*-Indol-3-yl)xanthen-4-

- (9*H*)-ones from *O*-methyl protected salicylaldehydes, indoles, and  $\beta$ -dicarbonyl compounds. *Syn.*, 46:2071-2078.
103. Kumar, A., Vachhani, D. D., Modha, S. G., Sharma, S. K., Parmar, V. S. and Van Der Eycken, E. V. (2013). Post-Ugi gold-catalyzed diastereoselective domino cyclization for the synthesis of diversely substituted spiroindolines. *Beils. J. Org. Chem.*, 9:2097-2102.
104. Modha, S. G., Kumar, A., Vachhani, D. D., Jacobs, J., Sharma, S. K., Parmar, V. S., Meervelt, L. V. and Van Der Eycken, E. V. (2012). A diversity-oriented approach to spiroindolines: post-ugi gold-catalyzed diastereoselective domino cyclization. *Angewandte Chemie-Inter. Ed.*, 51:9572-9575.
105. Fan, L., Wang, J., Ma, X., Xiao, W., Li, Z., Zhong, G. and Wu, H. (2015). Design, synthesis and biological evaluation of GY3-based derivatives for anti-type 2 diabetes activity. *Bioorg. & Med. Chem. Lett.*, 25:1500-1505.
106. Carbone, M., Li, Y., Irace, C., Mollo, E., Castelluccio, F., Di Pascale, A. and Gavnagnin, M. (2011). Structure and cytotoxicity of phidianidines A and B: first finding of 1,2,4-oxadiazole system in a marine natural product. *Org. Lett.*, 13:2516-2519.
107. Liu, J., Chen, Y., Li, J. Y., Luo, C., Li, J., Chen, K. X. and Guo, Y. W. (2018). Function-oriented synthesis of marine phidianidine derivatives as potential PTP1B inhibitors with specific selectivity. *Mar. Drugs.*, 16:97.
108. Nourisefat, M., Panahi, F., Nabipour, M., Heidari, S. and Khalafi-Nezhad, A. (2016). L-Cysteine-functionalized magnetic nanoparticles (LCMNP): as a magnetic reusable organocatalyst for one-pot synthesis of 9-(1*H*-indol-3-yl) xanthen-4-(9*H*)-ones. *J. Iran. Chem. Soc.*, 13:1853-1865.

#### Abbreviation

- 5-HT1D- 5-Hydroxytryptamine receptors
- DMF-Dimethylformamide
- DPH-1,4-dihydropyridines
- LXR- Liver x receptor
- NHC- *N*-heterocyclic carbene
- PEG- Polyethylene glycol
- PTC-Phase transfer catalyst
- PTP1B- Protein tyrosine phosphatase 1 B inhibitors
- PTS- Platinum monosulfide
- *p*-TsOH- *p*-toluene sulfonic Acid
- SAR- Structure activity relationship
- STA- Supported tungstic Acid
- TCPTP- T-cell protein tyrosine phosphatase
- TMSN<sub>3</sub>-Trimethylsilyl azide

## Differential Approach of Bioremediation by *Sclerotium rolfsii* Towards Textile Dye

Anthony Samuel<sup>1</sup>, Vasantha Veerappa Lakshmaiah<sup>1\*</sup>, Priyanjali Dias<sup>1</sup>,  
Praveen N<sup>1</sup>, Cannon Antony Fernandes<sup>1</sup>, Aatika Nizam<sup>2</sup>,  
Suresh Babu Naidu Krishna<sup>3\*</sup>

<sup>1</sup> Department of Life Sciences, CHRIST (Deemed to be University), Bengaluru-560029, India

<sup>2</sup> Department of Chemistry, CHRIST (Deemed to be University), Bengaluru-560029, India

<sup>3</sup> Department of Biomedical and Clinical Technology, Durban University of Technology,  
Durban-4000, South Africa

Corresponding author: vasantha.vl@christuniversity.in

### Abstract

Synthetic dyes are extensively used in various industries and are one of the major contaminants of industrial effluents. Dyes being xenobiotic, carcinogenic, and toxic there is need for their effective removal and detoxification to conserve water resources. Tremendous research has been carried out to identify potent microorganisms that facilitate bioremediation of these harmful dyes. A static batch culture has proved white rot fungi *Sclerotium rolfsii* as an efficient catalyst in bioremediation of textile dyes and to compare their efficiency in decolourisation of two different azo dyes. Studies revealed the organism employ different remedial approach to cationic dye (Malachite green) and anionic dyes (Rose Bengal). Decolourisation of malachite green was a gradual with degradation and bio-transformation to colourless, non-toxic by products while Decolourisation of rose Bengal was quick process of biosorption. *S.rolfsii* exhibited 89% of decolourisation of malachite green dyes at higher concentration of 900mg/L while 96% for rose Bengal at 900mg/L. The mechanism of dye decolourisation was proposed using the UV Vis spectrophotometry, FTIR, XRD, HPLC and SEM. Microbial toxicity studies confirmed the dye metabolites of degraded malachite green was less toxic compared to original dye. Com-

prehensively studies illustrate the sustained application of *S. rolfsii* as model organism for bioremediation of complex industrial effluents due to its differential bio remedial approach can potentially decolourise or remove various dyes.

**Keywords:** Biodegradation, Bioadsorption, *Sclerotium rolfsii*, Malachite green, Rose Bengal.

### Introduction

Dyes are extensively used in various sectors of industries like paper, printing, textile, pharmaceuticals, and food industries. The industrial effluents of these industries carry huge amounts of dyes and are mostly released into water bodies [27, 32]. Dyes present in water-bodies affect aquatic plants and animals. They hinder in the penetration of sunlight thereby affecting photosynthesis in plants. Ecosystems are interconnected and disturbance in aquatic ecosystem will affect overall integrity of biosphere. Dyes being recalcitrant in nature they tend to persist in environment. They are carcinogenic and teratogenic affecting human health. Across worldwide nearly 5-20% of dyes are released as part of industrial effluent to waterbodies leading to environmental issues.

Discharges of these dyes alters the phys-



io-chemical properties of water like pH, increases BOD and COD [23]. They intensely colour the water and imparts unpleasant odour. Removal of these dyes can be achieved by physio-chemical method like flocculation, adsorption, ionisation, oxidation, irradiation etc. These methods have certain limitations like they are not effective, expensive, produces secondary sludge whose disposal is a problem and produces toxic by-products [1]. A variety of microorganisms like bacteria, actinomycetes, fungi and yeast can be used in biodegradation and complete mineralisation of dyes [29, 33]. Bioremediation have received wide acceptance by public mainly because this technique eliminates waste completely and permanently, cost effective, less impact on environment and can be coupled with physical and chemical methods [17, 28].

White rot Fungi have proved to be most potent in bioremediation of dye compared to bacteria mainly due to its biomass and secretion of ligninolytic enzymes such as laccase, manganese peroxidase, and lignin peroxidase [4, 17, 30]. These enzymes play a vital role in detoxification of dyes and bleaching of woods [16, 36]. White-rot fungi, belonging to the basidiomycetes, are the only organisms capable of mineralizing lignin efficiently and thus can enzymatically degrade dyes [14]. In recent years many researches are carried out to exploit the use of white rot fungi in degradation of complex aromatic compounds. *Rhizopus arrhizus*, *Rhizopus oryzae*, *Penicillium sp.*, *Trichoderma harzianum* and *Haematonectria haematococca*, which have been used to remove dyes [7, 22, 35, 36].

Biosorption is another alternative method of bioremediation of dyes where dyes can be effectively removed from aqueous medium. Biosorption is a physiochemical process which occurs on the surface of microbial cell wall. This process includes electrostatic interaction, ion exchange, complexation, chelation and micro-precipitation [35]. The process is cheap, rapid and effective and microbial biomass obtained from industries like yeast slurry from brewing

industry or agricultural waste like barley husk, wood chips, fruit peel can be used as absorbents [3, 5, 19, 18, 34, 35, 37].

In recent years, there has been a growing interest in the field of screening of fungal strains that can produce these enzymes that can help in degradation of xenobiotics substances like textile dyes and petrochemicals [25]. *S. rolfsii* is a facultative parasite that survives in the soil primarily in the form of sclerotia, which are the source of inoculum and can remain viable for several years together [6, 10, 13, 32]. Of the major extracellular enzymes produced by this pathogenic fungus, laccase and lignin peroxidase are known to have a functional role in degrading toxic xenobiotic substances.

Literature reviews reveals unexplored potential of *Sclerotium rolfsii* in removal of Malachite green and Rose Bengal dyes. The objective of current research was to understand the differential mechanism employed by fungi to decolourize and detoxify the widely used textile dyes.

## Materials and Methods

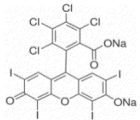
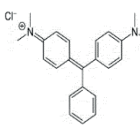
### Source of culture and chemicals

The fungal culture of *Sclerotium rolfsii* was obtained from Indian Institute of Horticulture Research, Bangalore. The acquired fungal sample was subcultured on Potato Dextrose Agar (PDA) medium and incubated at 26°C for 7~10 days till sclerotia were formed on mycelial mat, and served as the master culture. All chemicals like dyes and growth media components were purchased from Sigma Aldrich and Himedia.

### Dye decolourisation on solid media

To screening the ability of fungi to decolourise different dyes was performed as per Park's work with certain modifications [25]. Extensively grown mycelia of *S. rolfsii* were divided into 1 cm<sup>2</sup> pieces along with sclerotia and were placed on PDA media with 100 mgL<sup>-1</sup> concentration of selected dyes. Control and Test

Table 1: Dyes used in the studies

Names of Dyes	Structure	$\lambda$ max
Rose Bengal (Acid Red)		595 nm
Malachite Green (Basic Green)		680 nm

were maintained for each of the selected dyes. Control was not inoculated with fungi while the test media was inoculated. Both control and test plates were incubated at 26°C. This method was used to examine dye decolourization on agar media.

#### **Dye decolourisation in liquid media**

Malachite Green (Basic Green 4) and Rose Bengal (Acid Red 94) of concentration ranging from 100-900 mgL<sup>-1</sup> were prepared. Protocol for decolourisation in liquid media was analysed as per Lefebvre's work. Control samples were not inoculated while test samples were inoculated [15]. Cultures were incubated at static conditions at 26°C. Colour intensity of culture fluids were determined using UV-Vis Spectroscopy at 620 nm for Malachite Green (MG) and 595 nm for Rose Bengal (RB) at regular interval from fourth day to sixteenth day. The percentage of dye decolourisation was estimated.

#### **Extraction of dye metabolites for analysis**

Culture broth with malachite green after incubation period was subjected to solvent extraction using equal volume of ethyl acetate. Broth and ethyl acetate were mixed for 30 mins followed by the separation of organic layer which was subjected to rotatory evaporated to concentrate the dye intermediate metabolites. Which was used for HPLC analysis and toxicity studies.

#### **Spectroscopic analysis of degradation and biosorption studies**

The dye metabolites of malachite green after fungal Dye degradation were isolated for FTIR, HPLC analysis and for toxicity studies. To study the surface morphology, change on the fungal mycelium after adsorption of rose Bengal was subjected to XRD and SEM analysis

#### **Results and Discussion**

##### **Dye decolourisation on solid media**

*S. rolfsii* was grown on Potato Dextrose Agar (PDA) with 100 mgL<sup>-1</sup> of selected dyes, fungi grew as a smooth mycelial mat that spreads radially from its origin. It proceeded to grow on media in a radial manner up to the edge of the plate uniformly. Complete growth covering the media as uniform mycelial mat was observed on 5th day of inoculation. Test plate showed prominent dye decolourisation with Malachite Green and Rose Bengal on comparison with control.

##### **Dye degradation in liquid medium and effect of dye concentration**

To understand the effect of dye concentration on rate of decolourization Potato Dextrose Broth (PDB) medium with dye concentration ranging from 100-900 mgL<sup>-1</sup> was incubated at 26°C for a period of 16 days in a static mode. On day 4 Mycelia growth reached maximum forming a uniform mat on surface of the medium. Absorbance was read at 680 nm for MG and 595 nm for RB at interval of 4 days for 16 days. There was a progressive decolourization observed for MG, while abrupt fall and its persistence during incubation was observed for RB (Fig.4). This clearly indicated the mechanism of decolourization adopted by *S.rolfsii* was for basic dye (MG) and acidic dye (RB) were different.

##### **Studies of degradation of rose bengal**

In case of RB culture, the media had completely lost the colour and dye had adsorbed on mycelial mat. Absorbance studies of culture

media from day 4 to 16 showed negative values indicating complete absence of dye in medium. This explains that adsorption of dye is quick on mycelium and had removed the dye from culture media significantly on day 4 itself and thus absorbance readings value had dropped and persisted till end of incubation period as indicated in (fig.1).

Initially when *S. rolfsii* culture was set for decolourisation of RB the pH of the medium was maintained at 7 but as the fungal mycelium grew the pH of the medium dropped to 4.8 and had become acidic. The change in pH of the medium is due to release of chemicals like oxalic acid due to the metabolism of fungi [24]. This leads to protonation of the amino group on chitin cell wall of fungi [5]. Which led to enhanced bio-adsorption of anionic dye (RB) on the net positively charged mycelial mat.

The functional groups associated with fungal biomass also influence rate of dye adsorption. After 5 days of inoculation mycelial mat grew to maximum in static liquid culture with RB concentration ranging from 100-900 mgL<sup>-1</sup>. High biomass density and surface area increased the number of amino group availability for electrostatic attraction of anionic dye [2, 20, 34].

Absorbance spectrum obtained for RB decolourization for 700 mgL<sup>-1</sup> from day 5 to 16 showed big drop in the color intensity (Fig.1) proving *S.rolfii* as excellent organism for absorption of dye. Hence is promising microorganism for bioremediation of RB.

#### Studies of degradation of malachite green

The rate of decolourization of MG was studied using UV-Vis Spectroscopy. A gradual decrease in the absorbance values over incubation period for dye concentration ranging from 100 mgL<sup>-1</sup> to 900 mgL<sup>-1</sup> was recorded from day 5 to 16 days.

As per the (fig.1) *S. rolfsii* exhibited efficient degradation of Malachite Green with initial

concentration of 100 mgL<sup>-1</sup> reduced to 11.12 mgL<sup>-1</sup>. Similarly with the other concentrations: 300 mgL<sup>-1</sup> to 43.26 mgL<sup>-1</sup>, 500 mgL<sup>-1</sup> to 74.4 mgL<sup>-1</sup>, 700 mgL<sup>-1</sup> to 92.15 mgL<sup>-1</sup> and 900 mgL<sup>-1</sup> to 121.68 mgL<sup>-1</sup> on 16th day of inoculation. Gradual decrease in concentration of dye with time proves the ability of fungi to metabolise the dye at higher concentrations as well.

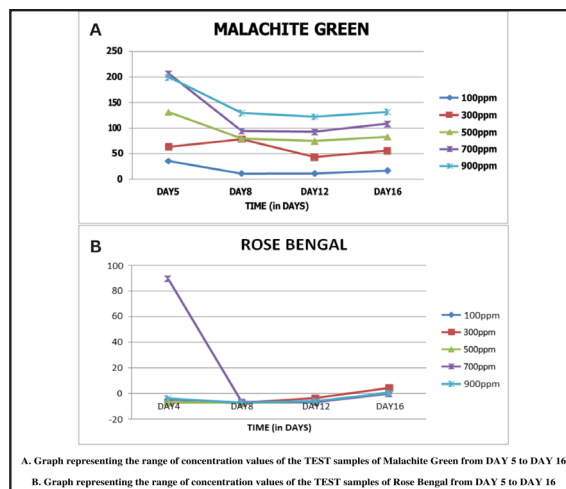


Figure 1. Degradation of Malachite green and Rose Bengal by *S. rolfsii*

Dye degradation ability of *S. rolfsii* is attributed to lignolytic enzymes like laccase (lac) and Manganese Peroxidase (MnP) which are extracellular and catalyse dye degradation process [17, 19]. Increase in biomass during the incubation period signifies increasing amounts of these extracellular enzymes production that facilitates effective dye degradation. *S.rolfii* produces acid stable extracellular laccase that catalyses the degradation of dye at low pH. The presence of dyes also acts as inducer for enzyme produced that catalysis dye degradation or transformation of dye. Additionally, the Production of MnP increased the dye degradation ability. *S.rolfii* exhibited tolerance and decolourisation at higher concentration of dye. This study shows that as the fungi was exposed to increasing concentration of dye they get acclimatized and degrade MG. The characteristic Absorbance spectrum of 700 mgL<sup>-1</sup> obtained

during the incubation period exhibited direct correlation between growth, incubation time and decolorization. As growth and incubation period increased the dye decolorization increased. The decrease in intensity of dye absorbance peak over time is attributed to enzymatic degradation of dye.

Percentage of dye degradation with increasing concentration of MG exhibited high potential of fungi to degrade upto 86% of 300 mgL<sup>-1</sup>, 700 mgL<sup>-1</sup> and 900 mgL<sup>-1</sup> respectively while 100 mgL<sup>-1</sup> was degraded upto 89% by end of the incubation period. This proves *S.rolfsii* as promising organism to degrade MG at higher concentration.

#### Fourier-transform infrared spectroscopy studies

FTIR were used to confirm dye degradation and presence of intermediate metabolites. Parental dye malachite green and its dye metabolite extracted from media were subjected to FTIR studies.

Interpretation of the FTIR spectrum of control indicated as Control in (Fig 2) for Malachite Green dye, we observed sharp peak at 1592 cm<sup>-1</sup>, corresponding to the C=N bond stretching. The sharp peak at 1509 cm<sup>-1</sup> relates to C-C stretching in aromatic ring. The sharp peak at 1229 cm<sup>-1</sup> agrees with the C-N aliphatic stretching. Peak at 1190 cm<sup>-1</sup> corresponds to C-N aromatic stretching. The sharp peak at 826 cm<sup>-1</sup> matches to C-H out of plane bending in aromatic ring. The weak peaks at 3036 cm<sup>-1</sup> and 2883 cm<sup>-1</sup> gives the C-H stretching in aromatic ring and alkanes respectively.

The IR spectrum of the test or the dye metabolites of malachite green after degradation represented in (Fig.2) and comparing it with control there was much difference giving us the knowledge that Malachite Green dye has degraded. There are new peaks formed at 3300 cm<sup>-1</sup> corresponding to O-H stretching indicating the formation of alcohols or carboxylic acids during degradation. The sharp peak observed

at 2921 cm<sup>-1</sup> relates to the N-H stretching of aromatic amines and strong peak at 1714 cm<sup>-1</sup> corresponds to C=O functional group due to aromatic ketones or aldehydes formed in the course of degradation. Peaks at 1235 cm<sup>-1</sup> corresponds to the C-N aromatic stretching and peak at 1097 cm<sup>-1</sup> corresponds to C-O stretching of alcohols. Peak at 800 cm<sup>-1</sup> gives information about the disubstituted benzene ring derivatives formed. This change in spectrum of test suggest dye degradation by *S. rolfsii*.

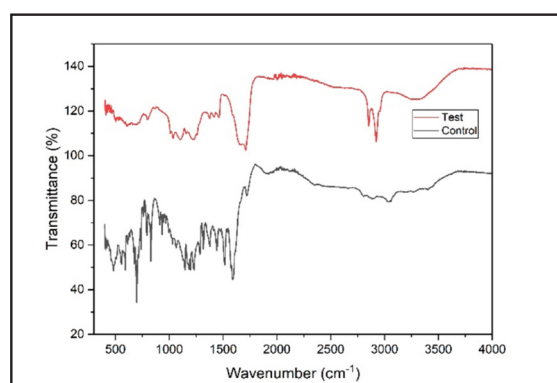


Figure 2. FTIR spectrum of Malachite Green dye after degradation (Test), Parental Dye (control)

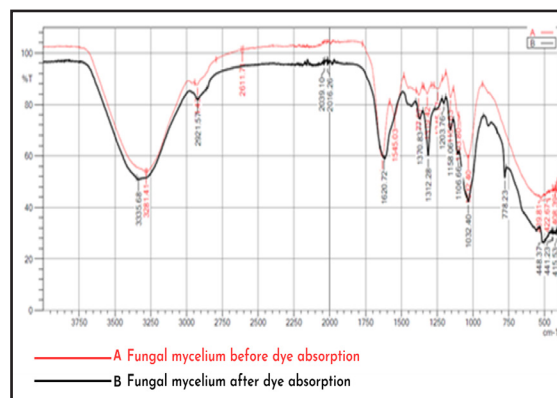


Figure 3. FTIR spectra of *Sclerotium.rolfsii* biomass before (A) and after dye sorption (B) of Rose Bengal dye

The spectrum of the *Sclerotium.rolfsii* biomass with and without dye loading were compared. The study revealed slight shifting of peaks (3281.41, 1633.57, 1545.03, 1319.42 and



1032.40  $\text{cm}^{-1}$ ) from their position with alteration in intensity and appearance of new peaks indicating the involvement of some functional group of the fungi in the biosorption of Rose Bengal dye on the surface of the fungal biomass.

#### XRD analysis of fungal mycelia

XRD pattern was analysed for Rose Bengal dye absorption on the mycelia of *S.rolfsii*. Both adsorbed and un-adsorbed mycelia was subjected to XRD analysis. Significant variation in the pattern of peaks was observed. The un-adsorbed fungal mycelial XRD pattern showed hollow peak indicating the non-crystalline and amorphous nature of fungal mycelia. After the adsorption of the dye to the fungal biomass showed few crystalline peaks at around 25.9, 29.2, and 35.8o of 2 theta values indicating that there was transformation in the nature of the fungal biomass due to adsorption of Rose Bengal dye. This change in fungal mycelial morphology from amorphous to crystalline structure confirms dye biosorption on mycelia.

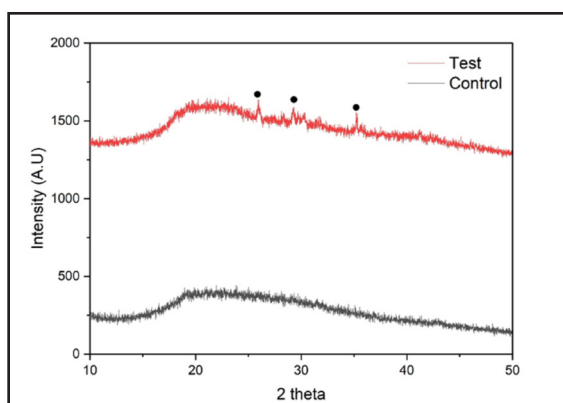


Figure 4: XRD pattern of *S. rolfsii* mycelium before and after adsorption of Rose Bengal

#### Scanning electron micrograph studies

Surface morphology change on the fungi after adsorption of rose Bengal was subjected to SEM analysis. Fungal mycelium acting as adsorbent clearly showed a distinct change in its morphological change. Mycelium surface was

uniform and smooth with deep pore and pockets as shown in (Figure 5A) before the adsorption of dye while after adsorption its surface is rough no pores and with fine particles on surface (Figure 5B). Similar results were reported when fungal biomass was used for the adsorption of Acid blue 161 [38] [39] [40]

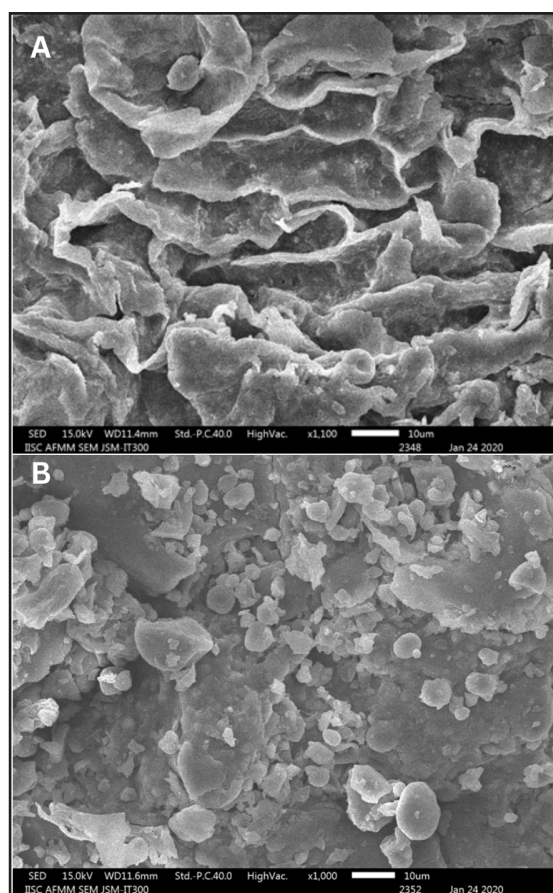


Figure 5: Micrograph of scanning electron 1000X (A- Fungal Biomass before dye adsorption, B- Fungal Biomass after dye adsorption)

#### HPLC analysis for malachite green degradation

The metabolites obtained before and after the malachite green dye degradation by *S. rolfsii* was concentrated and subjected to HPLC analysis at two different absorbance wavelengths of 680 nm and 280 nm. The absorption



spectra of the samples (control and test) are presented in (fig.6). The HPLC elution profile of the dye malachite green (Control) showed single sharp peaks at 680nm with retention time (RT) of 4.5minutes (Figure 6B). The elution profile obtained for the fungal treated samples significantly differed from the control in terms of height of the peak obtained and retention time at 680nm. The HPLC profile of sample treated with fungi *S. rolfsii* showed one peaks with retention time 4.3 with reduced height of peak and shift in retention time clearly indicating the degradation of dye (Fig. 6A). The UV absorption spectrum at 280 nm for dye metabolite obtained after 16 days of incubation showed no peak at 680 nm

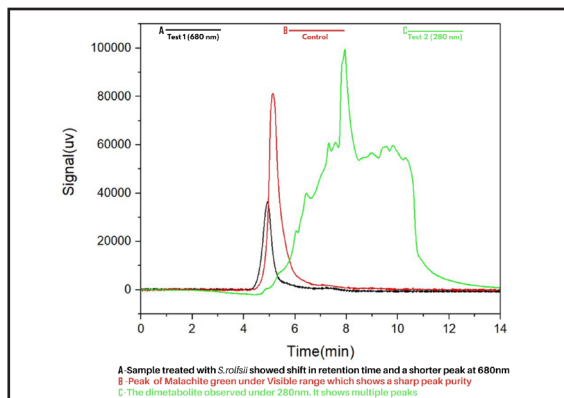


Figure 6: HPLC chromatogram of Malachite green and dye metabolites at 680nm and 280nm

but with multiple peaks at 280nm as shown in (Figure 6C). From these observations' microbial degradation and transformation of malachite green was confirmed.

#### **Microbial toxicity studies of malachite green and metabolic intermediates**

Toxicological effect of parental dye and their metabolites obtained after microbial degradation was studied. *Bacillus subtilis* was incubated with malachite green dye before and after dye degradation to ensure the degraded products are environmentally safe. A clear zone of inhibition was observed with parental Malachite Green indicating the toxic effect of azo dye while the dye metabolites showed no zone of inhibi-

tion. This proves the *S. rolfsii* had degraded the toxic dye to nontoxic metabolic intermediates. The products obtained after fungal dye degradation did not show any growth inhibition.

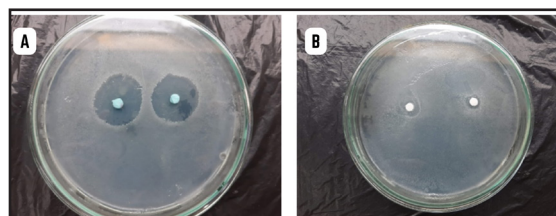


Figure 7. Toxicity study of dye before (A) and after (B) MG degradation

#### **Conclusion**

This study was done to explore the potential of *S. rolfsii* as promising microorganism for bioremediation of Malachite Green and Rose Bengal the most extensively used textile dyes which has not been studied. Static batch culture system with higher concentration of dyes ranging from 100-900 mgL<sup>-1</sup> were established to test degradation ability of the organism. Fungi exhibited excellent potential to degrade the dye at high concentration of 900 mgL<sup>-1</sup> with 89% of degradation. *S. rolfsii* follows two different mechanisms for removal of dye like bio-adsorption for Rose Bengal (anionic dye) and biodegradation for Malachite Green (Cationic dye). UV-Vis spectroscopy, XRD, FTIR and HPLC were the tools used to analyse the bioremediation of dyes. The degraded intermediate or transformed products were reported. Toxicity studies of degraded products exhibits no toxic effect on test microorganism. In this mycoremediation fungi employs two main mechanism of like biodegradation and biosorption of dyes and hence identifying such microorganisms with differential bioremediation approach will facilitate the dye decolourisation and detoxification of complex industrial effluents with various dyes. Fungi can be considered as best and reliable mediators of dye remediation.

#### **Conflict of interest**

Authors declare no conflict of interest

## References

1. Akar T, Ozkara E, Celik S, et al (2013) Chemical modification of a plant origin biomass using cationic surfactant ABDAC and the biosorptive decolorization of RR45 containing solutions. *Colloids and Surfaces B: Biointerfaces*. <https://doi.org/10.1016/j.colsurfb.2012.06.016>
2. Barr DP, Aust SD (1994) Mechanisms white rot fungi use to degrade pollutants. *Environmental Science and Technology*. <https://doi.org/10.1021/es00051a002>
3. Bayramoğlu G, Çelik G, Arica MY (2006) Biosorption of Reactive Blue 4 dye by native and treated fungus *Phanerochaete chrysosporium*: Batch and continuous flow system studies. *Journal of Hazardous Materials*. <https://doi.org/10.1016/j.jhazmat.2006.05.005>
4. Chander M, Arora DS (2007) Evaluation of some white-rot fungi for their potential to decolourise industrial dyes. *Dyes and Pigments*. <https://doi.org/10.1016/j.dyepig.2005.08.023>
5. Chen KC, Wu JY, Liou DJ, Hwang SCJ (2003) Decolorization of the textile dyes by newly isolated bacterial strains. *Journal of Biotechnology*. [https://doi.org/10.1016/S0168-1656\(02\)00303-6](https://doi.org/10.1016/S0168-1656(02)00303-6)
6. Chet I, Hüttermann A (1982) De novo synthesis of polyphenol oxidase (Laccase) during formation of sclerotia in *Sclerotium rolfsii*. *FEMS Microbiol Lett*. doi: 10.1111/j.1574-6968.1982.tb08664.x
7. Corso CR, Maganha De Almeida AC (2009) Bioremediation of dyes in textile effluents by *aspergillus oryzae*. In: *Microbial Ecology*
8. Fu Y, Viraraghavan T (2002) Removal of Congo Red from an aqueous solution by fungus *Aspergillus niger*. *Advances in Environmental Research*. [https://doi.org/10.1016/S1093-0191\(01\)00123-X](https://doi.org/10.1016/S1093-0191(01)00123-X)
9. Ghosh A, Dastidar MG, Sreekrishnan TR (2017) Bioremediation of chromium complex dyes and treatment of sludge generated during the process. *International Biodeterioration and Biodegradation* 119:448–460. <https://doi.org/10.1016/j.ibiod.2016.08.013>
10. Gübitz GM, Hayn M, Sommerauer M, Steiner W (1996) Mannan-degrading enzymes from *Sclerotium rolfsii*: Characterisation and synergism of two endo  $\beta$ -mannanases and a  $\beta$ -mannosidase. *Bioresource Technology*. [https://doi.org/10.1016/S0960-8524\(96\)00093-4](https://doi.org/10.1016/S0960-8524(96)00093-4)
11. Gopal S, Natesan S, Sudha M, et al (2014) Microbial degradation of Azo Dyes: A review
12. Ghosh A, Dastidar MG, Sreekrishnan TR (2017) Bioremediation of chromium complex dyes and treatment of sludge generated during the process. *Int Biodeterior Biodegrad*.
13. Haltrich D, Laussamayer B, Steiner W (1994) Xylanase formation by *Sclerotium rolfsii*: effect of growth substrates and development of a culture medium using statistically designed experiments. *Applied Microbiology and Biotechnology* 42:522–530. <https://doi.org/10.1007/BF00173915>
14. Husain Q (2010) Peroxidase mediated decolorization and remediation of wastewater containing industrial dyes: A review. *Reviews in Environmental Science and Biotechnology*
15. Jadhav JP, Govindwar SP (2006) Bio-transformation of malachite green by *Saccharomyces cerevisiae* MTCC 463.

- Yeast 23:315–323. <https://doi.org/10.1002/yea.1356>
16. Kalyani D, Dhiman SS, Kim H, et al (2012) Characterization of a novel laccase from the isolated *Coltricia perennis* and its application to detoxification of biomass. *Process Biochemistry*. <https://doi.org/10.1016/j.procbio.2012.01.013>
  17. Kaushik P, Malik A (2009) Fungal dye decolourization: Recent advances and future potential. *Environment International*
  18. Kumari K, Abraham TE (2007) Biosorption of anionic textile dyes by nonviable biomass of fungi and yeast. *Bioresource Technology*. <https://doi.org/10.1016/j.biortech.2006.07.030>
  19. Mohorčič M, Teodorovič S, Golob V, Friedrich J (2006) Fungal and enzymatic decolourisation of artificial textile dye baths. *Chemosphere*. <https://doi.org/10.1016/j.chemosphere.2005.09.063>
  20. Mungasavalli DP, Viraraghavan T, Jin YC (2007) Biosorption of chromium from aqueous solutions by pretreated *Aspergillus niger*: Batch and column studies. *Colloids and Surfaces A: Physicochemical and Engineering Aspects*. <https://doi.org/10.1016/j.colsurfa.2006.12.060>
  21. Nigam TRP, Marchant IMBR (2001) Microbial decolourisation and degradation of textile dyes. 81–87. <https://doi.org/10.1007/s002530000587>
  22. O'Mahony MM, Dobson ADW, Barnes JD, Singleton I (2006) The use of ozone in the remediation of polycyclic aromatic hydrocarbon contaminated soil. *Chemosphere* 63:307–314. <https://doi.org/10.1016/j.chemosphere.2005.07.018>
  23. Pandey A, Singh P & Iyengar L, Bacterial decolorization and degradation of azo dyes. *Int. Biodeterior, Biodegrad*, 59 (2007) 73-84
  24. Puvaneswari N, Muthukrishnan J, Gunasekaran P (2006) Toxicity assessment and microbial degradation of azo dyes. 44:618–626
  25. Pandey A, Singh P, Iyengar L (2007) Bacterial decolorization and degradation of azo dyes. *International Biodeterioration and Biodegradation* 59:73–84. <https://doi.org/10.1016/j.ibiod.2006.08.006>
  26. Je WP, Choi SY, Hwang HJ & Kim YB, Fungal mycoflora and mycotoxins in Korean polished rice destined for humans, *Int J Food Microbiol*, 103 (2005) 305-314
  27. Saravanakumar K, Kathiresan K (2014) Bioremoval of the synthetic dye malachite green by marine *Trichoderma* sp. *SpringerPlus*. <https://doi.org/10.1186/2193-1801-3-631>
  28. Singh RL, Singh PK, Singh RP (2015) Enzymatic decolorization and degradation of azo dyes - A review. *International Biodeterioration and Biodegradation* 104:21–31. <https://doi.org/10.1016/j.ibiod.2015.04.027>
  29. Saratale RG, Saratale GD, Chang JS, Govindwar SP (2011) Bacterial decolorization and degradation of azo dyes: A review. *Journal of the Taiwan Institute of Chemical Engineers* 42:138–157. <https://doi.org/10.1016/j.jtice.2010.06.006>
  30. Spadaro JT, Gold MH, Renganathan V (1992) Degradation of azo dyes by the lignin-degrading fungus *Phanerochaete chrysosporium*. *Applied and Environmental Microbiology* 58:2397–2401. <https://doi.org/10.1128/aem.58.8.2397-2401.1992>
  31. Srivastava S, Sinha R, Roy D (2004) Toxicological effects of malachite green. *Aquatic Toxicology*

32. Sadana JC, Patil R V. (1985) The purification and properties of cellobiose dehydrogenase from *Sclerotium rolfsii* and its role in cellulolysis. *Journal of General Microbiology* 131:1917–1923. <https://doi.org/10.1099/00221287-131-8-1917>
33. Stolz A (2001) Basic and applied aspects in the microbial degradation of azo dyes. *Applied Microbiology and Biotechnology* 56:69–80. <https://doi.org/10.1007/s002530100686>
34. Vijayaraghavan K and Yun Y (2008) Bacterial biosorbents and biosorption. *Biotechnology Advances*, pp 266-291.
35. Vijayaraghavan K, Lee MW, Yun YS (2008) A new approach to study the decolorization of complex reactive dye bath effluent by biosorption technique. *Bioresource Technology*. <https://doi.org/10.1016/j.biortech.2007.10.012>
36. Wong Y, Yu J (1999) Laccase-catalyzed decolorization of synthetic dyes. *Water Research* 33:3512–3520. [https://doi.org/10.1016/S0043-1354\(99\)00066-4](https://doi.org/10.1016/S0043-1354(99)00066-4)
37. Yesilada O, Cing S, Asma D (2002) Decolorisation of the textile dye Astrazon Red FBL by *Funalia trogii* pellets. *Bioresource Technology*. [https://doi.org/10.1016/S0960-8524\(01\)00117-1](https://doi.org/10.1016/S0960-8524(01)00117-1)
38. Johana Puchana-Rosero Mayerly, Lima Elder C, Ortiz-Monsalve Santiago, Mella Bianca, da costa Dimitrius, Poll Eduardo, Gutterres Mariliz (2017) Fungal biomass as biosorbent for the removal of Acid Blue 161 dye in aqueous solution. *Environmental Science and Pollution Research* 24: 4200–4209. <https://doi.org/10.1007/s11356-016-8153-4>
39. Ghariani Bouthaina, Hadrich Bilel, Ibtihel Louati, Mtibaa Rim, Daassi Dalel, Rodriguez-Couto Susana, Nasri Moncef, Mechichi Tahar (2019) Porous heat-treated fungal biomass: preparation, characterization and application for removal of textile dyes from aqueous solutions. *Journal of Porous materials* 26, 1475-1488. <https://doi.org/10.1007/s10934-019-00746-6>
40. Rusu Lăcrămioara, Grigoraș Cristina-Gabriela, Suceveanu Elena Mirela, Simion Andrei-Ionuț, Dediu Botezatu Andreea Veronica, Istrate Bogdan, Doroftei Ioan (2021) Eco-Friendly Biosorbents Based on Microbial Biomass and Natural Polymers: Synthesis, Characterization and Application for the Removal of Drugs and Dyes from Aqueous Solutions. *Materials* 14(17), 4810. <https://doi.org/10.3390/ma14174810>
41. Afibirin Zubair Nuha Amao, Ajao Abdulahi Taiwo, Adeyemo Elijah Olaolu, AD-ENIYI Omoyele Dele (2020) Biodegradation of Malachite Green by White-Rot Fungus, *Pleurotus Pulmarinus*. *Egyptian Academic Journal of Biological Sciences G. Microbiology* 12(1), 79-90. <https://doi.org/10.21608/EAJBSG.2020.96943>
42. Kim Thoa Le Thi, Thao Trinh Thi Phuong, Hung Nguyen Bao, Khoo Kuan Shiong, Quang Hoang Tan, Lan Tran Thuy, Hoang Vu Duc, Park Seung-Moon, Ooi Chien Wei, Show Pau Loke, Huy Nguyen Duc (2022) Biodegradation and Detoxification of Malachite Green Dye by Extracellular Laccase Expressed from *Fusarium oxysporum*. *Waste and Biomass Valorization* 13, 2511–2518. <https://doi.org/10.1007/s12649-022-01692-2>
43. Argumedo-Delira Rosalba, Gómez-Martínez Mario J, Uribe-Kaffure Ramiro (2021) *Trichoderma* Biomass as an Alternative for Removal of Congo Red and Malachite Green Industrial Dyes. *Applied Sciences* 11(1), 448. <https://doi.org/10.3390/app11010448>

44. Backes Emanuelli, Kato Camila G, V. da Silva Tamires B, Uber Thaís M, Pasquarelli Daniela L, Bracht Adelar, Peralta Rosane M (2022) Production of fungal laccase on pineapple waste and application in detoxification of malachite green. *Journal of Environmental Science and Health, Part B* 57(2), 90-101.
45. Pathy Abhijeet, Krishnamoorthy Nageshwari, Chang Scott X, Paramasivan Balasubramanian (2022) Malachite green removal using algal biochar and its composites with kombucha SCOBY: An integrated biosorption and phycoremediation approach. *Surfaces and Interfaces* 30, 101880. <https://doi.org/10.1016/j.surfin.2022.101880>



## Antimicrobial Study of Chitosan-Based Crosslinked Hydrogel Against *Staphylococcus aureus*, *Porphyromonas gingivalis*, *Pseudomonas aeruginosa*, and *Streptococcus mutans*

Arvind. S. Parmar,<sup>1</sup> Aakash. S. Panwar,<sup>2</sup>

<sup>1</sup>Institute of Pharmaceutical Science, SAGE University Indore, Madhya Pradesh, India.

<sup>2</sup>Institute of Pharmaceutical Science, SAGE University Indore, Madhya Pradesh, India.

\*Corresponding author: arvind07py@gmail.com

### Abstract

Gingivitis is a pathogenic disorder caused by the growth of bacterial flora inside the gum cavity, also known as the gingival cavity. The formation of hard plaque is initiated by the deposition of a biofilm of microbes on the surface of teeth at the age of gums. These plaques, when developed, turn into tarter and are difficult to remove. These hard structures formed around the teeth caused severe damage to soft tissue and affected teeth, eventually causing permanent tooth loss. Gingivitis in an advanced stage, called periodontitis, causes permanent damage to the gum and teeth. Periodontal disease is caused by the bacteria *Staphylococcus aureus*, *Porphyromonas gingivalis*, *Pseudomonas aeruginosa*, and *Streptococcus mutans*. The aim of the investigation is to study how well chitosan-based crosslinked hydrogels containing Chlorhexidine, Metronidazole, and Lignocaine hydrochloride inhibit the growth of selected bacteria isolated from oral microbial flora such as *Staphylococcus aureus*, *Porphyromonas Gingivalis*, *Pseudomonas Aeruginosa*, and *Streptococcus Mutans* in-vitro. Chitosan-based cross-linked hydrogel 2 % combined with all the active ingredients prepared and tested for antibacterial activity in SCAN-Laboratory Indrepuri, Bhopal.

Bacterial samples were taken from freshly extracted teeth provided by District Hospital Raise in Madhya Pradesh, India, and then preserved in a saline solution. Isolate and culture each bacterium colony separately before performing an identification test for each of them. The hydrogel was then diluted at 25%, 50%, 75%, and 100% concentrations up to 10 power -9 to perform the antibacterial activity. All isolated bacteria colonies were separately cultured and introduced to a paper disc etched with antimicrobial gel. The media were then incubated in the incubator, and the (Zoi) Zone of inhibition was checked for the gel's effectiveness. The mean diameter of the zone of inhibition against all isolated bacterial colonies was noticed to be in the 10-33 mm range, indicating the presence of strong anti-bacterial activity. A considerable qualitative difference ( $p = 0.000$ ) was found between the inhibitory effects of each concentration of hydrogel on the bacteria *Staphylococcus aureus*, *Porphyromonas gingivalis*, *Pseudomonas aeruginosa*, and *Streptococcus mutans*. Because of the largest diameter of the inhibition zone, the most effective antibacterial activity was found in 2% chitosan-based hydrogels.

Keywords: Gingivitis, Antimicrobial, Metronidazole, Crosslinked Hydrogel, Periodontitis.

## Introduction

According to a World Health Organization survey, nearly 10-15% of the global population suffers from dental problems, specifically periodontitis. Periodontitis is a pathogenic infection that damages the teeth's supporting tissues and thus can lead to permanent tooth loss. (1). The cause of periodontal disease is an increase in the population of pathogenic disease-causing agents in the oral cavity debris of microorganisms deposit over the surface of teeth and form a thick layer known as excessive biofilm deposition will indeed be plaque (2). The formation of biofilm, which can be exacerbated by poor dental hygiene and leads to plaque formation, is one of the major causes of the disease. Plaque buildup around teeth irritates surrounding tissues and, if left untreated, destroys tooth attachments (3). The general host response influenced by subgingival bacterial growth and the severity of infection left unnoticed exacerbates the symptoms of infection. Furthermore, if the pathogen grows rapidly, the host will simultaneously increase the pathogenic response and destroy the periodontium. (4). The disease is more severe and degenerative, affecting soft tissue around the teeth such as gingiva, ligaments, cementum, and supporting bones; in advanced stages, it may cause permanent loss. Pathogenic colonies proliferate quickly and deposit their dead remains on the upper surface of teeth, forming a permanent layer called biofilm and many additional layers collectively known as calculus. The disease concept is based on some considerations that may cause the disease to persist and proliferate, such as a susceptible host, an excess of pathogenic microbes due to poor hygiene, and the absence of beneficial bacteria. The elaborated growth of Gram-negative and mobile bacteria increases the prognosis. [5,6] Pathogens of various types are associated with the disease and are the main factor in its pathogenesis. Porphyromonas Gingivalis, Bacteroides forsythias, Treponema denticola, Prevotella intermedia, Fusobacterium nucleatum, and Eubacterium sp. are among the

bacteria responsible for chronic periodontitis. However, microaerophile bacteria such as Actinomyces mycomitans, Campylobacter rectus, and Eikenella corrodens cause chronic periodontitis (7 8). Functional groups on Chitosan tend to bind negatively charged groups on the cell wall of bacteria, affecting the physiology and permeability of the cell wall. They also interact with DNA, limiting replication and resulting in cell death (9). Metronidazole has broad antimicrobial activity against protozoan infections as well as anaerobic bacteria. Metronidazole was first used to treat trichomoniasis before its broad antimicrobial activity was discovered in 1950. Metronidazole is now a widely used periodontal disease treatment (10). Metronidazole is a highly effective drug for reducing the deposition of dead cells in periodontal pockets, removing calculus, and scaling. It can effectively limit anaerobic bacteria growth (11) Because of a three-dimensional network of polymer chains formed by physical or chemical interaction between functional groups, the hydrogel of the crosslinked polymer has a tendency to adsorb and hold a large amount of water more than natural polymer. Hydrogel has numerous benefits and improved properties. Tissue engineering, biosensors, regenerative agents, and improving adhesion properties are just a few of the applications. Chlorhexidine is antiseptic and disinfectant in nature and is also used as a cleaning agent for the oral cavity in low concentrations. Chlorhexidine destroys bacteria's cell walls by binding negatively charged phosphate groups, disrupts cellular integrity, and interacts with cytoplasm, resulting in cell death. Because biofilm reforms on a regular basis, surgical methods for removing calculus are less effective; however, nonsurgical methods such as antimicrobial therapy are quite effective because it provides active ingredients at the site and effectively inhibit microbe growth. Local drug delivery is advantageous because it delivers to the infected site, but it is also gaining popularity because it avoids many of the drawbacks of systemic applications (12,13) It has the possibility of causing hypersensitivity reactions, gastrointestinal intoler-

ance, and bacterial resistance. The goal of the research is to establish a more precise delivery system for delivering drugs to local tissues and maintaining their concentration in order to provide more effective results while overcoming the limitations of existing systemic approaches (14). To accomplish this, a crosslinked hydrogel containing a drug combination was created. The polymeric base was chosen to extend the time spent in the oral cavity. Oral cavity has many limitations due to the high flow of saliva. The approach is to develop a gel with natural polymer crosslinking to overcome the limitation. To some extent, hydrogel protects against factors such as pH and Enzyme and prevents drug exposure with biological content. By releasing the drug at a predetermined rate, you can extend the drug's residence time at the site of application and allow it to absorb for a longer period of time (15). The goal of this research is to create a more precise delivery system for controlled release to local tissues while maintaining concentration, resulting in more effective results while overcoming the limitations of current systemic approaches. A crosslinked hydrogel containing a drug combination was created to accomplish this. The polymeric base was selected to increase the amount of time spent in the oral cavity. Because of the high flow of saliva, the oral cavity has many limitations. To overcome the limitation, the approach is to create a gel with natural polymer cross-linking. Chitosan is a natural mucoadhesive polysaccharide derived from various sources. Chitosan is a natural mucoadhesive polysaccharide derived from various sources. Chitosan, Polyacrylamide, Polyvinyl alcohol, Polyethylene glycol, and Alginate are some examples of natural and synthetic polymers used to make hydrogel (16). Hydrogels are insoluble in water and have a high affinity to absorb water within the matrix (17). Polymer macromolecules interact and form a crosslinking network between polymeric chains. The reaction between polymeric chains is initiated by crosslinking agents, forming a network of water-repelling molecules. A chemical reaction in which natural or synthetic polymeric monomers

react to form copolymers or homopolymers (18). As a result, the complex structure retains a significant amount of water or biological fluid; high water content sustainably increases bioadhesive by increasing the contact angle between the mucus layer and molecules. It improves hydrogels' similarity to soft tissue and makes them more biocompatible, bioadhesive, and nonirritant, allowing its diverse applications to deliver drugs more precisely at the site of application (19).

## **Materials and Methods**

### ***Isolation and identification of organisms from extracted human tooth***

#### ***Collection of sample***

A fresh tooth sample was donated by District Hospital Raize in Madhya Pradesh, India, and stored in saline solution. The sample was then immersed in sterile saline and allowed to incubate for 24 hours.

#### ***Preparation of serial dilutions***

1 ml of the gel was diluted in 9 ml of nutrient broth to make a standard sample. Subsequently, serial dilutions were done to create crosslinked hydrogel at concentrations of 25%, 50%, 75%, and 100% up to 10 power 9 to perform the antibacterial activity.

#### ***Spread Plate technique***

With a sterile pipet or metallic loop, bacteria suspended in a solution are poured over prepared media. A sufficient number of bacteria spread across the surface of the culture media allows them to grow (20). The technique is stable and reliable, and it is aligned with the SOP to avoid contamination.

1. Preparation of samples to achieve a suitable concentration of the bacterial solution; the sample was serially diluted.
2. Agar plates are prepared by pouring sterile agar solution into Petri - dishes and continuing to allow it to solidify.

3. By pipetting out 0.1 ml diluted solution from a series of dilutions, a sterile glass spreader or pipet is used to spread the sample on the surface of prepared agar plates.
  4. Incubate prepared plates by placing the Petri dish in a moderate-temperature incubator for a duration that allows the bacterial colony to grow.
  5. Incubate the plate at 37 °C for 24 hours.
  6. Count the bacterial colonies that have grown on the surface of the agar plates after the incubation period.
  7. The CFU value of the sample will be given in CFU/ml of the prepared sample if the CFU value is calculated using the Dilution factor and the colony count.
3. Strew the inoculating loop across a quarter of the plate quickly, softly, and back and forth.
  4. Spread it in a pentagon shape on the opposite side of the agar plate quadrant.

### **Identification of microorganisms**

#### **Gram staining**

Microbiologists use this tool to identify and classify bacterial species. It is widely used in medical microbiology to diagnose bacterial infections and determine the best antibiotic treatment. It is the first test commonly used to diagnose any bacteria using methylene blue or crystal violet as a primary stain, followed by safranin. (21). Gram-positive bacteria retain crystal violet and appear purple after decolorization. In contrast, Gram-negative bacteria retain safranin instead of crystal violet due to a thick cell wall and appear pink under a microscope.

#### **Preparation of a slide smear**

- Apply a drop of culture suspension to the glass slide using the inoculation loop.
- Examine the slide under a microscope. If a bacterial colony appears, move a small amount of the suspension to the next slide for further examination.
- If culture is visible on the loop, it indicates that a large amount of culture was taken; it will disappear over 15mm diameter; if more than one culture is taken for the examination, a thin coating using the loop must be made; some slides can have up to four tiny stains.
- Keep the slide over a spirit lamp or in the oven to dry quickly and form a smear. Keep the slide moving to avoid overheating. Heating will bind the cells to the slide and prevent them from draining while washing.
- For staining, crystal violet stain is applied over a fixed smear of a culture. After a while, pour water over the slide and gently wash it to remove any extra stain. This will remove

#### **Streak plate technique**

It is a technique for separating and purifying bacterial colonies from a mixed culture. Select the separate wells in an agar plate, then collect the sample after successive dilutions of a mixture of bacterial colonies. The inoculum dilutes in successive sections of a plate until only one bacterial cell remains, with no other cells in the few MM area surrounding the cell. It enables each cell to culture independently, and the pure colony can grow in a specific area. Pure colonies can now be isolated by selecting isolated colony walls and re-striking them in different culture media to select individual colonies for further examination.

The method is based on the idea that a single bacteria can multiply multiple times and form a colony of uniform cells. The precise technique for obtaining pure bacteria culture has a wide range of applications in fields such as diagnosis, identification, characterization, and genetics.

1. Sterilize the inoculation loop with a spirit lamp or Bunsen burner and allow it to cool.
2. Divide the agar media on a plate into four equal sections and streak a single colony in each.



any traces of stains and bacteria that may have remained on the slide.

- To fix the color, an iodine solution is applied over the smear. After that, the slide is rinsed under running water to remove the iodine solution. To absorb excess water from a slide, tissue paper is used.
- Solvent treatment is the process of removing the color from a smear by using ethanol and acetone solution as a decolorizing agent. After some time, the slide is rinsed again with distilled water. To avoid over-decolorizing, we must stop adding decolorizing agents once the smear has stopped changing color. After soaking in water, the smear is treated with a fuchsine solution for 50-60 seconds before being washed with clean water, excess water removed with a tissue paper slide, and air dried.

### **Characteristic Identification**

**S. Aureas** can be identified and isolated using the MSA (Mannitol Salt Agar) test. MSA contains a high concentration of sodium chloride (7.5% NaCl), which inhibits bacterial growth. Only Halophile bacteria can withstand such high salinity levels. Mannitol and sugar alcohol are both added to culture media as ingredients. Bacteria ferment mannitol to produce acid, lowering the pH and turning phenol red. The color change from red to yellow indicates the presence of bacteria. In a high salt medium, other halophile bacteria may also survive to distinguish *S aureus* from them. Mannitol was added to the culture because staphylococcus and other halophile bacteria are incapable of fermenting it, resulting in a pH drop. Characteristic Yellow The color of the medium indicates the presence of *S. aureus*. Another method for confirming the presence of *S. Aureas* is the Coagulase test, in which bacteria produce the enzyme coagulase, which causes blood collected from humans to clot quickly. If *S. Aureas* is present in the sample, it will coagulate the blood; otherwise, it will remain liquified. Snyder test for *S. Mutans* The microbes collected from the

teeth's surface are transferred to a special agar medium called Snyder agar media. The medium contains a high concentration of glucose and is acidic in pH. *S. Mutans*, unlike other bacteria, can grow in acidic environments, which is why they are referred to as acidophilus. If bacteria are present in a sample, they will multiply and form successive colonies, which may be translucent or slightly yellow in color. *P. Aeruginous* Pyocyanin production test: bacteria are known to produce blue-green pigment, which is thought to be a characteristic feature. A variety of factors influence bacterial pyocyanin production, including environmental and oxygen availability in addition to other nutrients. Pigments act as electron donors in the absence of oxygen, allowing bacteria to use oxygen more efficiently. Pigment also plays a role in virulence damage tissue and inflammation during biofilm formation. Blood microbe culture Pigments are commonly seen on agar plates as small, black, dark brown spots that resemble fried eggs. This is because of pyocyanin. Under a microscope, it appears to be a comma-shaped rod. Because the bacteria are immobile, nonfunctional flagella tufts appear. Under a microscope, *P. Gingivalis* appears as a curved or comma-shaped rod with a polar tuft of flagella. However, the bacterium is not motile in its natural environment, and the flagella are not functional.

### **Biochemical test**

#### **IMViC Test**

The IMViC test is a series of four biochemical tests used to differentiate between different groups of bacteria, specifically Enterobacteriaceae. A series of four tests, each with its own characteristics used to identify different types of bacteria based on their metabolic characteristics. Different Enterobacteriaceae family species have different metabolic properties; they can identify easily on the basis of these tests. The test is named after the first letters of each of the four tests, which are the Indole test, Methyl Red test, Voges Proskauer test, and Citrate Utilization Test. The test is used to



distinguish between bacterial colonies that are closely related and may have similar metabolic properties. The Indole test is positive if bacteria break down the amino acid tryptophan to produce indole, the Methyl red test is positive if bacteria ferment glucose to produce acidic by-products, the Voges-Proskauer test is positive if cells can produce acetone during glucose fermentation, and the citrate test is positive if cells use citrate as a carbon source (22-23).

### **Indole test**

**Principle:** Some bacteria have the ability to convert the amino acid tryptophan to indole due to the presence of an enzyme; the presence of indole can be confirmed using Ehrlich's or Kovac's reagents. It will generate a red precipitate, which will appear as a ring in the alcoholic layer.

**Steps:** Transfer the bacteria suspension to a water and peptone solution containing the amino acid tryptophan and culture the mixture overnight in an incubation chamber at 37 degrees Celsius. Add a few drops of Kovac's reagent to the mixture the next day. After being inoculated in peptone water, which contains the amino acid tryptophan, the bacteria are cultured overnight at 37°C. After incubation, Kovac's reagent is added. Kovac's reagent is composed of para-dimethyl amino benzaldehyde, isoamyl alcohol, and concentrated hydrochloric acid. The reagent detects the presence of indole in anaerobic conditions by forming a red or pink ring at the surface.

### **Methyl red (MR) test**

**Principle:** The methyl red test assesses an organism's ability to metabolize glucose into an acidic byproduct. Because some bacteria have a high capacity for producing acid byproducts, the pH of the system may be affected, reducing the system's ability to maintain a buffer. Methyl red is a pH indicator that turns red when a strong acid is present in a system.

**Procedure:** The test must be carried out on a bacterial culture that has been grown for 48 hours at 37 degrees Celsius in a culture containing glucose. Following the completion of the incubation period, some media is transferred to a separate tube containing methyl red indicator. If the bacteria produce enough acidic byproduct, the mixture will immediately turn red. The positive test result aids in the differentiation of the bacterial colonies in the sample. When a few drops of Methyl red indicator are added, the red color indicates the presence of bacteria, while the yellow color indicates the absence of bacteria.

### **Voges proskauer (VP) test**

**Principle:** The Voges-Proskauer (VP) test relies on bacteria's ability to convert glucose into (butylene glycol) acetoin for identification. Some Enterobacteriaceae members, such as *E. coli* and Salmonella, are pathogenic to humans. The test employs two indicators. Alpha-naphthol and Potassium Hydroxide (KOH) When added to the culture in the presence of excess air, both reagents will react with the acetoin (Butylene Glycol), and the diacetyl will react with the guanidine components of peptone due to the presence of naphthol. Alpha-naphthol is a catalyst and color intensifier that produces a red color. The presence of color indicates that the cell is producing acetoin. The yellow color indicates the absence of bacteria.

**Procedure:** The colony of unknown bacteria transferred to the culture media after 48 hours of incubation in culture media containing glucose phosphate broth at 37°C, 0.6 ccs of Alpha naphthol added to the diluted sample taken from the plate, and gently shake the test tube, then transfer 0.2 ml of 40% KOH solution drop by drop while continuous stirring. Keep the test tube aside for about 15 minutes. The appearance of red color will confirm the presence of bacteria in the negative tube. Negative results are indicated by no or slightly low color.

### **Citrate utilization test**

Principle: Citrate utilization testing identifies microorganisms based on their proclivity to consume citrate as a carbon source and produce energy. Some Enterobacteriaceae pathogens are commonly harmful to humans. The experiment continues by inoculating microorganisms on summon citrate agar. Other nutrients and indicators are also introduced into the culture. In an acidic medium, indicators such as bromothymol blue change color from green to blue. If a cell consumes citrate, it will produce a large amount of citrate lyase, which breaks citrate down into pyruvate and other alkaline products, causing the ph to rise and the indicator to turn blue from green. If it does not turn blue, it means that the microorganism is not present. Microbes that can use the citrate Klebsiella Pneumonia and Enterobacterium Aerogenes include *Escherichia Coli* and Salmonella Typhi.

### **Antimicrobial activity of a prepared hydrogel on isolated microorganisms**

The ability of a substance to kill pathogenic bacteria is referred to as antimicrobial activity. Microbe-killing agents can be synthetic or natural, disrupting the cell wall or interfering with the metabolic pathway. The nature of the microbe or the agent used heavily influences the effectiveness of an antimicrobial agent. Different concentrations of 25 mg/ml, 50 mg/ml, 75 mg/ml, and 100 mg/ml were used to test the antimicrobial effect of the prepared hydrogel agar well method.

### **Preparation of media**

The gel's antimicrobial activity was tested using agar well diffusion at three different concentrations 25 mg/ml, 50 mg/ml, 75 mg/ml, and 100 mg/ml. The culture of bacteria and fungus requires the use of specific growth media formulations for cloning, plasmid DNA synthesis, and protein production. A Nutrient agar medium was made by combining nutrient broth, agar, and distilled water, and it was used to cultivate the bacterial culture. Nutrient broth con-

tains peptone, sodium chloride, yeast extract, vitamins, and carbohydrates, all of which are required for bacterial growth. Agar is used as a solidifying agent (24).

### **Sterilization**

The killing of harmful microorganisms from the surface of any object is referred to as sterilization. It plays an important role in preventing the growth of microorganisms that we do not want. There are several methods for killing microbes, including physical methods such as heat, filtration, and radiation. Another method is chemical, which employs disinfectant chemicals. Some common examples include alcohol, bleach, ethylene oxide, hydrogen peroxide, glutaraldehyde, and formaldehyde solutions. Following that, the prepared media undergoes sterilization. The media were autoclaved for 15-20 minutes at 121°C. (25)

### **Inoculation of microbial culture**

Aseptically placed media in a Petri dish up to 90mm high. Allow the media to settle for a while. The media was then spread evenly in clean cotton plates before being placed in the incubation chamber.

### **Sample preparation**

In a test tube, a measured amount of prepared hydrogel was placed, followed by the preparation of a standard sample and dilution up to a certain level. The standard sample was used to make samples with concentrations of 25, 50, 75, and 100 mg/ml. Fill each well half-way with the diluted sample.

### **In-Vitro antimicrobial activity**

Chitosan was used as the base for the cross-linked hydrogel, which was then tested for antimicrobial properties. Four different strains of bacteria were used to test the hydrogel's activity *S. Aureus*, *P. Gingivalis*, *P. Aeruginosa*, and *S. Mutans* were among them. At Raisen District Hospital, all microorganisms were collected from the patient's freshly extracted tooth, and

isolation and antimicrobial studies were performed (5) at the SCAN laboratory in Indrapuri, Bhopal, Madhya Pradesh, India. The agar well diffusion method is commonly used to investigate the antimicrobial properties of gels. Wells were prepared on agar media plates and filled with a suitable amount of diluted gel solution. Each bacterial strain was placed on a separate agar plate. Following that, the antimicrobial gel was applied to the cultured colonies to see if it could inhibit the growth of bacteria. Following that, the zone of inhibition was measured in millimeters (26).

**Incubation**

After the plate has been colonized with bacterial colonies, a gel of varying concentrations is applied, and the plate is kept in an incubation chamber at 37°C under aerobic conditions for about 24 hours. After incubation, the plates were examined for the zone of inhibition. When bacterial colonies come into contact with an antimicrobial substance that kills microbes, the inhibition zone forms, and it grows with increasing concentration which is expressed in millimeters (27).

**Results and Discussion**



Figure 1: Tooth sample for isolation of bacteria



Figure 2: Serial Dilutions of the Tooth Sample

Table 1. Determination of Colony Count

Sr. No.	Dilutions	Colony Count	Dilution Factor	Average
1.	10-5	233	105	3.841X 10-8 Cfu/ml
2.	10-6	189	106	
3.	10-7	94	107	



Figure 3: Image of Spread Plate Technique

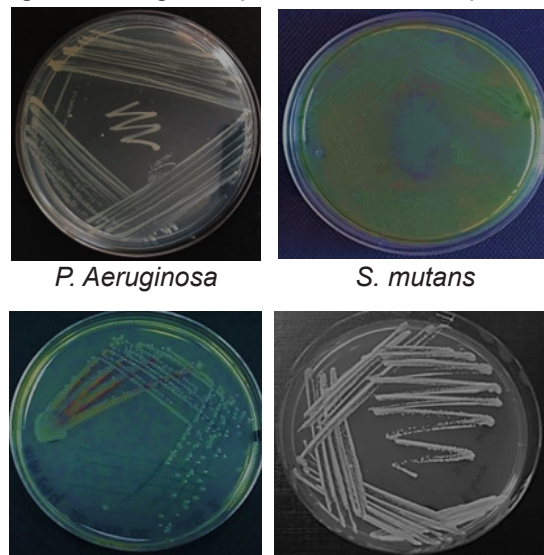


Figure 4: Image of Pentagonal Striking



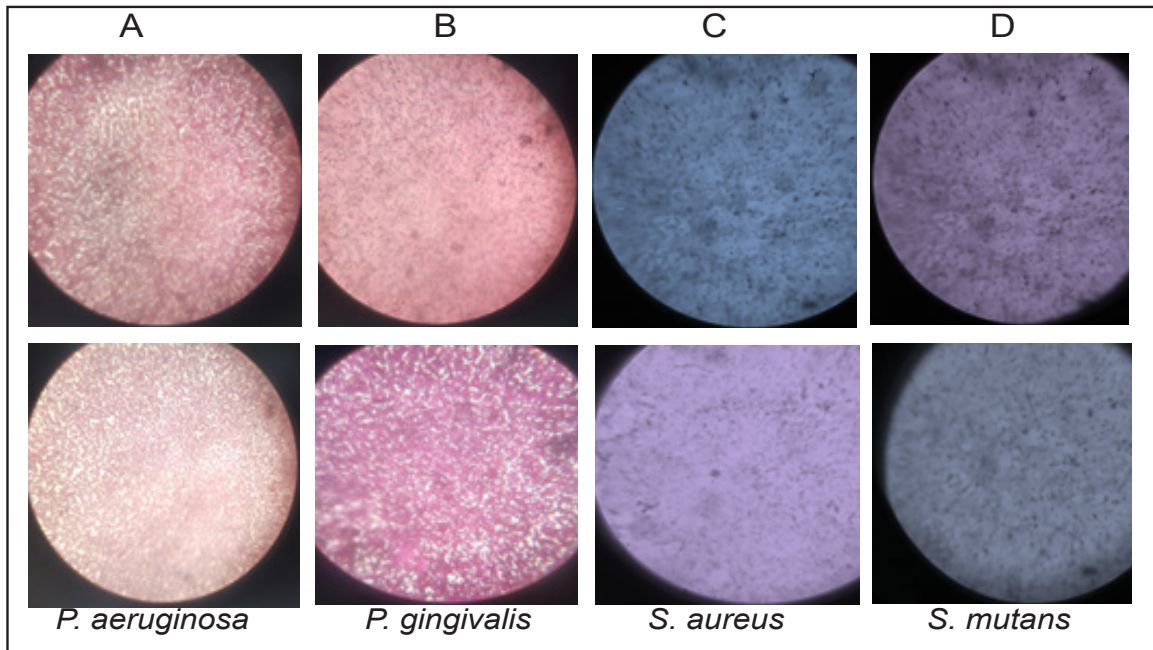


Fig. 5 Image of Gram Staining 100x

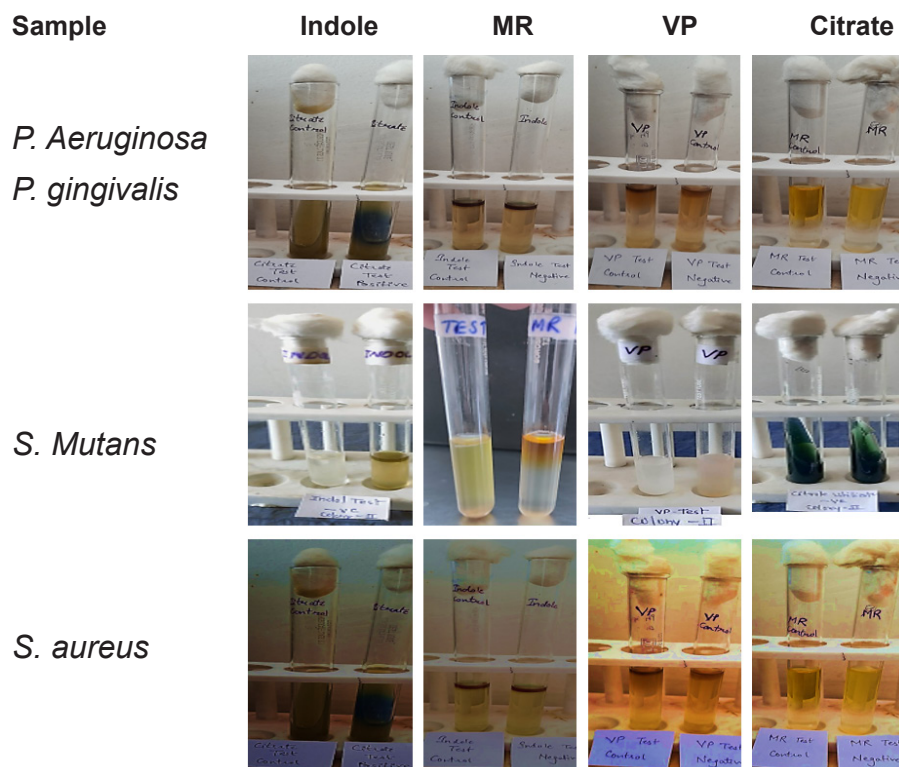
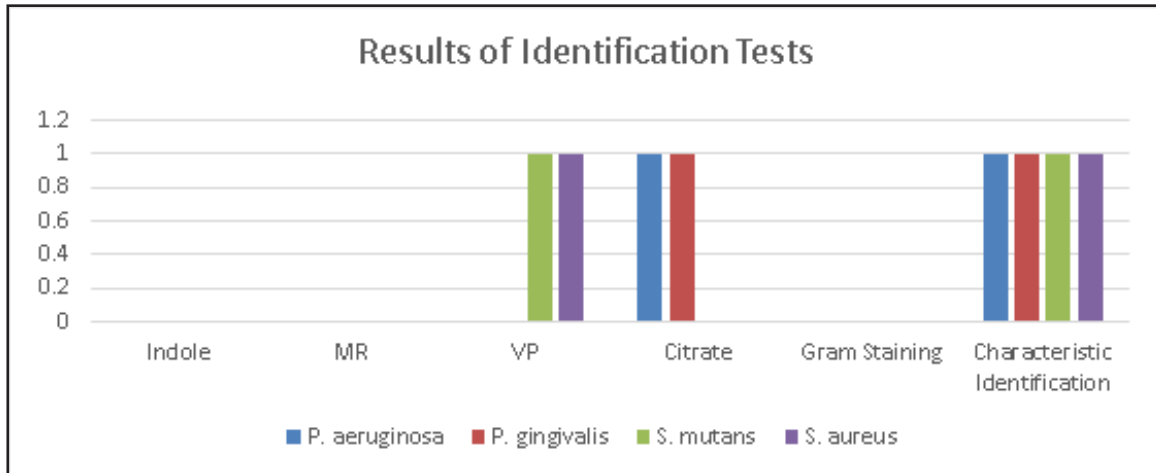


Fig. 6 Results of IMViC Tests for all the Isolated Colonies



Graph 1. Microorganism Identification Test

Table 2: Results of Identification Tests of *P. Aeruginosa* and *P. Gingivalis* Organism

Sample	Indole	MR	VP	Citrate	Gram Staining	Characteristic Identification
<i>P. Aeruginosa</i>	-ve	-ve	-ve	+ve	-ve	+ve
<i>P. Gingivalis</i>	-ve	-ve	-ve	+ve	-ve	+ve

Table 3: Results of Identification Tests of *S. Mutans*, *S. Aureus* Organism

Sample	Indole	MR	VP	Citrate	Gram staining	Characteristic Identification
<i>S. Mutans</i>	-ve	-ve	+ve	-ve	+ve	+ve
<i>S. Aureus</i>	-ve	-ve	+ve	-ve	+ve	+ve

Several laboratory methods such as the Spread plate Technique, Streak Plate Technique, Gram Staining, Characteristic Identification, and IMVIC Test were used during the study to isolate and identify the presence of *S. Aureus*, *P. Gingivalis*, *P. Aeruginosa*, and *S. Mutans* in a sample (Indole test, Methyl Red test, Voges Proskauer test, and Citrate Utilization Test). One common method for identifying *Staphylococcus aureus*, for example, is to perform a gram staining and then culture the bacteria on a selective media, such as Mannitol Salt Agar (MSA). *Staphylococcus Aureus* colonies will appear as yellow colonies on MSA due to their ability to ferment mannitol. Further tests, such as the coagulase test, can be used to confirm the identity of *S. Aureus*. *P. Gingivalis* is distinguished by its dis-

tinct colony morphology, which consists of black or brown pigmentation on blood agar. *P. Aeruginosa* is distinguished by its blue-green color on agar plates and fruity odor. *P. Gingivalis* looks like a curved or comma-shaped rod with a polar flagella tuft. However, in its natural environment, the bacterium is not motile, and the flagella are not functional. Snyder agar media is a *Streptococcus mutans*-specific agar medium. The medium has a high concentration of glucose and a low pH. *S. Mutans*, unlike other bacteria, can grow in acidic environments, hence the name acidophilus. If bacteria are present in a sample, they will multiply and form successive colonies on blood agar, which may be translucent or slightly yellow in color (28).



Microbe culture in blood Pigments appears on agar plates as small, black, dark brown spots that resemble fried eggs. This is due to pyocyanin. Microbe culture in blood pigments appears on agar plates as small, black, dark brown spots that resemble fried eggs. This is due to pyocyanin. Once the colonies have been identified, an antimicrobial study can be performed to test the bacteria's susceptibility to various antimicrobial agents. This can be accomplished through a variety of methods such as disc diffusion, broth dilution, or agar dilution.

The MIC (Minimum Inhibitory Concen-

tration) value recorded is the lowest concentration of the assayed antimicrobial agent that prevents observable growth of the microorganism tested, and it is often given in g/mL or mg/L. The gel produces positive results and successfully inhibits microbe growth. The zone of inhibition is measured using a ruler, calipers, or a template. Its dimensions are given in millimeters and are frequently rounded to the nearest millimeter. The diameter of the disc is also mentioned. These measurements are made with the naked eye without using any tools. The prepared gel was applied to each microorganism colony individually (29, 30).

Table 4: Zone of Inhibition Through Gel

Sr. No.	Isolated Organism	Zone of Inhibition		
		25 mg/ml (mm)	50mg/ml (mm)	100mg/ml (mm)
1.	<i>P. Aeruginosa</i>	14±0.47	21±0.5	25±0.47
2.	<i>S. Mutans</i>	10±0.94	12±0.47	17±0.47
3.	<i>P. Gingivalis</i>	11±0.94	19±0.5	29±0.47
4.	<i>S. Aureas</i>	13±0.94	24±0.5	33±0.47

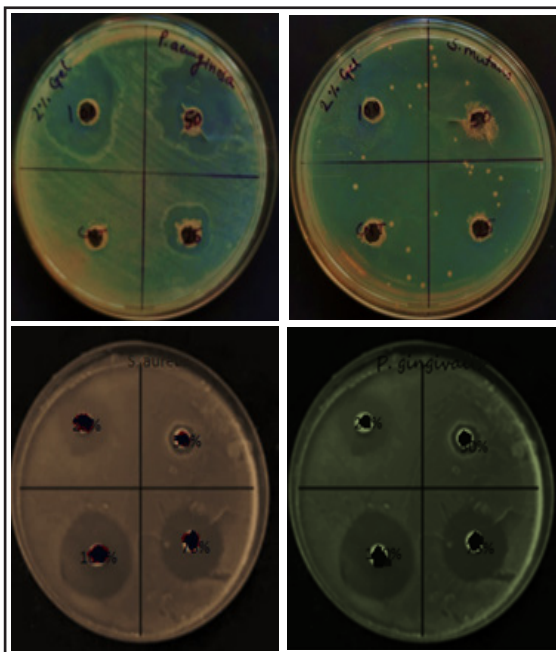


Figure 7: Antimicrobial Activity of 2% hydrogel

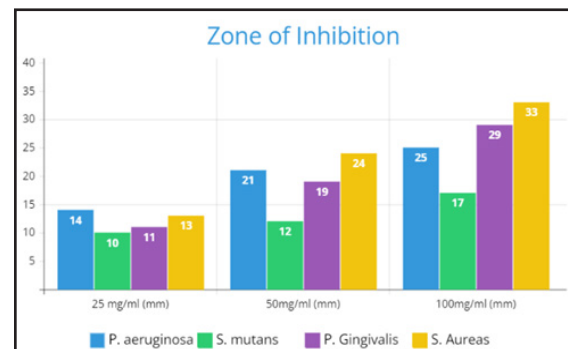


Figure 8: Zone of inhibition

## Discussion

Based on their metabolic characteristics, the IMViC test may be used to distinguish between several types of bacteria belonging to the Enterobacteriaceae family. In order to distinguish between bacterial colonies that are closely related, each test offers a special property. To offer a more complete identification of the bacteria under examination, the findings of each test

might be merged. If bacteria can convert tryptophan to indole, the Indole test is positive. A crimson or pink ring will appear on the surface when indole is present. Suppose the bacteria create acidic byproducts from the fermentation of glucose, causing a drop in pH and the appearance of a red color when methyl red indicator is added. In that case, the methyl red test is positive. If the fermentation of glucose by the bacteria produces acetoin, which reacts with alpha-naphthol and potassium hydroxide to give a red color, the Voges-Proskauer test is positive. If the bacteria can use citrate as a carbon source, raising the pH and changing the color of the sample from green to blue, therefore the Citrate Utilization Test is positive.

The results of the study indicated that the prepared hydrogel had significant antimicrobial activity against all four tested microorganisms. The zone of inhibition increased with increasing concentration of the hydrogel. The highest zone of inhibition was observed at a concentration of 100 mg/ml, indicating that higher concentrations of the hydrogel were more effective in inhibiting bacterial growth. The study also revealed that the hydrogel was more effective against gram-positive bacteria (*S. aureus* and *S. mutans*) than gram-negative bacteria (*P. gingivalis* and *P. aeruginosa*). This is likely due to differences in the cell wall structure of gram-negative and gram-positive bacteria, making it easier for the hydrogel to penetrate and disrupt the cell wall of gram-positive bacteria. Overall, the study suggests that the prepared hydrogel has potential as an effective antimicrobial agent against pathogenic microorganisms. Further studies are needed to evaluate the safety and efficacy of the hydrogel in clinical settings.

### Conclusion

Gram staining revealed Gram-negative *P. Aeruginosa* and *P. Gingivalis* in the first and second isolates, and Gram-positive *S. Mutans* and *S. Aureus* cocci in the third and fourth isolates. Since the IMVIC test confirms the absence of the Enterobacteriaceae family, which

is not found in the oral cavity but is found in the GI tract, all tests are negative. Finally, a characteristic identification test was performed to isolate and confirm the presence of all four strands for further investigation. The results of the tests show that *P. aeruginosa*, *S. mutans*, and *S. aureus* were obtained and isolated from the tooth sample. *S. aureus* was cultured in MSA (Mannitol salt agar) media, and the bacteria's presence was confirmed by a change in the color of the media from red to yellow due to the bacteria's ability to reduce acidity through metabolism. When *S. mutans* is cultured in Snyder agar media with a high concentration of glucose, its tendency to metabolize the glucose raises the pH and decreases acidity, turning the medium yellow. *P. aeruginosa* culture in agar media, where its ability to produce pyocyanin, a blue color pigment, turns the media blue. In agar media, *P. Gingivalis* produces pyocyanin, which causes brown or black spots that resemble fried eggs. Because of its comma rod shape and nonmotile flagella tuft, a microscopic examination of the bacteria will confirm its presence. *S. Mutans* is a Gram-positive bacterium with a thick cell wall and the gentian violet pigment. The cell wall's peptidoglycan (murein) and teichoic acids provide stiffness and structure by preventing protoplast osmotic lysis. The gel yields positive results, indicating that it can be used to inhibit microbes. Different concentrations of antimicrobial hydrogel were introduced into each isolated colony and the zone of inhibition was checked after incubation. The results of the preceding study show that the formulated hydrogel has a good antimicrobial effect. The area of the inhibition zone increased with increasing concentration, demonstrating the effectiveness of the gel at low and high concentrations. The prepared gel is capable of killing pathogenic bacteria. Further research into the approach's compatibility in oral mucosa for the treatment of gingivitis and periodontitis could be beneficial.

### References

1. Cohen R, Mariotti A, Rethman M (2001). Glossary of Periodontal Terms. 4th ed.,

- Chicago: American Academy of Periodontology; p. 40.
- Socransky SS, Haffajee AD (1992). The bacterial etiology of destructive periodontal diseases: current concepts. *J Periodontol*;63 (4s):322–331. DOI: 10.1902/jop.1992.63.4s.322.
  - Da Rocha Júnior HA, Silva C, Santiago F (2015). Local drug delivery systems in the treatment of periodontitis: a literature review. *J Int Acad Periodontol*;17(3):82–90.
  - Greenstein G. (2006) Local drug delivery in the treatment of periodontal diseases: assessing the clinical significance of the results. *J Periodontol*;77(4):565–578. DOI: 10.1902/jop.2006.050140.
  - Kesic L. (2008) Microbial etiology of periodontal disease – mini review. *Medicine and biology*; 15(1):1-6.
  - Daniluk T. (2006) Aerobic and anaerobic bacteria in subgingival and supragingival plaques of adult patients with periodontal disease. *Advances in medical sciences*; 51(1).
  - Dumitrescu AL. (2009) Etiology and pathogenesis of periodontal disease. 1 st edition, springer.
  - Aurer A, Plancak D. (2004) Antimicrobial treatment of periodontal diseases. *Acta Stomatol Croat*; 38(1).
  - Nagy A, Harrison A, Sabbani S, Munson RS, Dutta PK, Jr, Waldman WJ. (2011) *Int J Nanomedicine*; 6:1833. [PMC free article] [PubMed] [Google Scholar]
  - Sato S. (2008) Metronidazole-containing Gel for the Treatment of Periodontitis: an In vivo Evaluation. *Periodontics, Braz Oral Res.*; 22(2):145-50.
  - Toskic-Radojicic M. (2005) Effects of topical application of Metronidazole-containing mucoadhesive lipogel in periodontal pockets. *Vojnosanit Pregl*; 62(7-8):565-568.
  - Aurer A, Plancak D. (2004) Antimicrobial treatment of periodontal diseases. *Acta Stomatol Croat*; 38(1).
  - Carranza Fermin A, Takei Henry H. (2011) The Treatment Plan. In Carranza's clinical periodontology. 11th edition, St. Louis, saunders-Elsevier; 384.
  - Sato S. (2008) Metronidazole-containing Gel for the Treatment of Periodontitis: An In vivo Evaluation. *Periodontics, Braz Oral Res.*; 22(2):145-50.
  - Ray M. (2010) Development and characterization of chitosan based polymeric hydrogel membranes. *Designed monomers & polymers*; 13(3):193-206, (14).
  - Hong Y. (2007) Covalently crosslinked chitosan hydrogel: properties of in vitro degradation and chondrocyte encapsulation. *Acta Biomaterialia*; 3:23-3.
  - Nguyen KT, West JL. (2002) Photopolymerizable hydrogels for tissue engineering applications. *Biomaterial*; 23:4307-4314.
  - Chung HK, Park TG. (2009) Self-assembled and nanostructured hydrogels for drug delivery and tissue engineering. *NanoToday*;4(5):429–437.
  - Lee J, Cuddihy MJ, Kotov NA. (2008) Three-dimensional cell culture matrices: state of the art. *Tissue Eng Part B*;14(1):61–86.
  - Ishak W.M.F.W., Jamek, S., Jalanni, N.A. and Jamaludin, N.F.M. (2011) Isolation and identification of bacteria from activated sludge and compost municipal solid waste

- treatment system. International Conference on Biology, Environment, and Chemistry. 24: 450-454.
21. Aneja, K.R. (2003) Experiments in Microbiology, Plant Pathology, and Biotechnology. New Age International (P) Limited: New Delhi, 4.607.
  22. Collins, C.H., Lyne, P.M. and Grange, J.M. 1989. Microbiological Methods (6th ed), Butterworth, London.
  23. Pacarynuk, L.A. and Danyk, H.C. (2004) Biochemical Tests. In: Principles of Microbiology, Laboratory Manual, Spring, TX, USA, p. 28-34.
  24. Gaurav Tiwari, Garima Singh, Ravi Shekhar, Ruchi Tiwari. (2022) Development and qualitative evaluation of periodontal gel containing an antibacterial agent for periodontal disease. Research Journal of Pharmacy and Technology.; 15(11):5225-1. doi: 10.52711/0974-360X.2022.00880
  25. Anjana S, Beena P, Shahana S, Namitha Navas, Sam Cherian Mathew, Salikh Salim, Elesy Abraham. (2021) Formulation and Evaluation of Intrapacket Dental Film of Antibacterial agent for Periodontitis. Research J Pharm and Tech.;14(5):2750-6. DOI: 10.52711/0974-360X.2021.00485.
  26. Victoria O. Fasiku (2021) Chitosan-Based Hydrogel for the Dual Delivery of Antimicrobial Agents Against Bacterial Methicillin-Resistant *Staphylococcus aureus* Biofilm-Infected Wounds; 6(34): 21994–22010. Published online 2021 Aug 19. doi: 10.1021/acsomega.1c02547
  27. Yihung Lee (2023) “Advances of multifunctional hydrogels for periodontal disease Smart Materials in Medicine” Volume 4, Pages 460-467 <https://doi.org/10.1016/j.smaim.2023.02.001>
  28. Francesca Paola Nocera (2022) “A Preliminary Study on Antimicrobial Susceptibility of *Staphylococcus* spp. and *Enterococcus* spp. Grown on Mannitol Salt Agar in European Wild Boar (*Sus scrofa*) Hunted in Campania Region—Italy” *Animals*, 12(1), 85; <https://doi.org/10.3390/ani12010085>
  29. Lawrence S. (2021) “The Minimum Inhibitory Concentration of Antibiotics: Methods, Interpretation, Clinical Relevance” *Pathogens*.; 10(2): 165. doi: 10.3390/pathogens10020165
  30. Holder IA, Boyce ST, (1994) Agar well diffusion assay testing of bacterial susceptibility to various antimicrobials in concentrations non-toxic for human cells in culture. *Burns.*, 20: 426-9.